The LLAMAComm Path Loss Model

Bruce McGuffin
MIT Lincoln Laboratory

DRAFT Report

Version 1.0
LLAMAComm Version 2.18

This material is based upon work supported by the Defense Advanced Research Projects Agency under Air Force Contract No. FA8702-15-D-0001. Any opinions, findings, conclusions or recommendations expressed in this material are those of the author(s) and do not necessarily reflect the views of the Defense Advanced Research Projects Agency.

Introduction

Equation Chapter (Next) Section 1

This report describes propagation models used by the LLAMAComm simulation package to predict long-term propagation losses such as shadowing and range loss. Short term losses such as fading are not included in this report. The models described here can be viewed as finding fading model parameters for a given setting, range, altitude etc. Examples of fading parameters supplied are median path loss, fading standard deviation, the Rice fading K-factor, delay spread, and correlation between fading losses from two locations to a common end point.

The LLAMAComm simulation is intended to work over a very wide range of system parameters, as summarized in Table 1. It also operates in an assortment of settings, including urban, suburban and rural settings. There are also model components for indoor propagation, and through-wall losses for links with both indoor and outdoor nodes. Note not all combinations of parameters are supported. Sets of parameters describing links that wont close with realistic transmit power are excluded, for example, very long ranges from low antennas in an urban setting.

Table 1: Llamacomm propagation model operating range

Frequency:	10 MHz - 6 GHz
Range:	10 m - 10 km
Antenna Height:	0 m - 10,000 m
Environment:	Urban, Dense Suburban, Rural
Locations:	Indoors, Outdoors

There are some restrictions on the model's applicability. Although the frequency range listed in Table 1 goes down to 10 MHz, this model does not included skywave propagation, a common propagation mode below 30 MHz, sometimes appearing at higher frequencies. Propagation differences for different signal polarizations are only dealt with superficially, by changing the ground reflection parameter when the ground-bounce path is explicitly calculated. Otherwise polarization effects are ignored.

Most of the propagation models used were obtained from the published literature as indicated in the references provided. In a few cases new models were derived from published measurement data collected from multiple references. Different models have been tied together to cover a wider range of parameter values than most single models cover. In some cases ad hoc techniques were used to smooth transitions between models. In a few cases models have been with parameters outside the range of values at which data used to derive the model was collected. In those cases it is believed the model can be reasonably extended based on comparison of extend results with well known propagation trends as parameters vary, and with limited measurement data. However, the user should be aware that these ad hoc techniques and model extensions have not been thoroughly tested.

The model developed here is largely statistical in nature, derived by fitting curves to measurements taken in multiple locations. This approach is certainly quicker and easier than other approaches, such as measuring propagation loss or explicitly modeling the physics of RF propagation over a particular link. Physical models, or better yet measured data provide superior results when radio performance at a known location is desired. But when it becomes necessary to predict performance of mobile radios, or widespread fixed networks, the statistical model is more useful. To give a simple example, measuring or deriving propagation loss from the street into one building is the best way to predict building penetration losses at that building. But the wide variation in building shape, layout, construction and building materials results in a wide variation in measured building penetration losses between buildings. A single building measurement is less informative about how a link will fare in general than a statistical model is.

A Note on terminology: many of the models used were developed for the cellular industry, and have an advantaged node called the base station (BS), and a disadvantaged or less advantaged node referred to as the mobile station (MS). At times this terminology will be used here for consistency with the literature. In general, there is no particular significance to which node is called BS and which MS, except that the models may have different height restrictions for the two node types.

1 Main Program

Equation Chapter (Next) Section 1

1.1 Program interface

The main pathloss program returns the following values to describe performance of a single point-to-point radio link, all in dB:

1. mean shadowing loss
2. shadowing standard deviation
3. external noise figure for a single point-to-point radio link

In order to estimate these parameters the program must be provided with three structures, one describing each node of the link, and one describing the environment in which the link operates. Node parameters of interest are:

1. Node location, a three-vector of node position. The first two dimensions are horizontal location relative to an arbitrary reference point, and the third dimension is height above mean ground level, in meters
2. Node frequency, the link center frequency, in MHz[1].
3. Polarization, currently only horizontal and vertical are supported[2]
4. Exterior wall material, currently supported values are 'none' (for outdoor nodes) and 'concrete'
5. For indoor node, the shortest distance from that node to an exterior building wall, in meters
6. For indoor node, the number of interior walls between that node and the nearest exterior wall
7. For indoor node communication with outdoor node that is within line-of-sight distance of building, angle of LOS path with building face[3] (see LOS building penetration model below)

Environmental parameters of interest are:

1. Environmental descriptor, either 'urban', 'suburban', or 'rural'
2. Mean roof height above ground level, in meters. Typical values are 3-4 meters per building floor, plus 3-4 meters for sloping roofs.
3. Line-of-sight distance, the assumed link distance below which propagation is line-of-sight, and above which it is not

---

[1] Although frequency is a node characteristic, obviously both nodes must operate at the same frequency. The pathloss program assumes the frequency specified for the receive node correctly describes the link.
[2] When used, polarization is taken from the value supplied for the transmit node, and the receiver is assumed to have the same polarization. i.e., cross-polarization is not currently supported.
[3] Although this parameter is in fact determined by the position of both nodes and the building face orientation, It is treated as a parameter of the indoor node.

1.2 Model Selection

The main program consists of a large decision tree that looks at the provided node and environment parameters, and selects one or more subroutines to calculate the output variables. Figure 1 illustrates the decision process. The first decision point is based on the environment, assumed to be the same for both nodes. Choices are urban, suburban, and rural. The second decision point is determined by whether both nodes are outdoors, one node is indoors, or both nodes are indoors. The third decision is based on node heights, either absolute, or relative to average roof height for some settings, and finally a decisions base on link range and frequency. The illustrated example shows the chain of decisions mode for a link in an urban environment, when both nodes are outdoors, the lower terminal is below mean roof height, the higher terminal is between roof height and 200 meters, ground range is greater than 1 km, and the frequency is between 150 MHz and 1.5 GHz. For this particular set of parameters the Okumura-Hata model (Sec. xx) is used to find median path loss, and the Okumura-Sigma model (Sec. xx) provides an estimate of the path loss standard deviation about the median value. Individual models are described in Chapter 3.

Figures in the next two sub-sections show the frequency and range decision regions for urban propagation models with different terminal heights. The number in each decision region corresponds to a row of Table 2, listing the models used. The second column of Table 2 lists the models used to estimate median range loss. When multiple models are listed their losses add. Column three lists the short-term mean path standard deviation about the median. When multiple models are listed, the standard deviations are combined as the root-sum-of-squares (RSS).

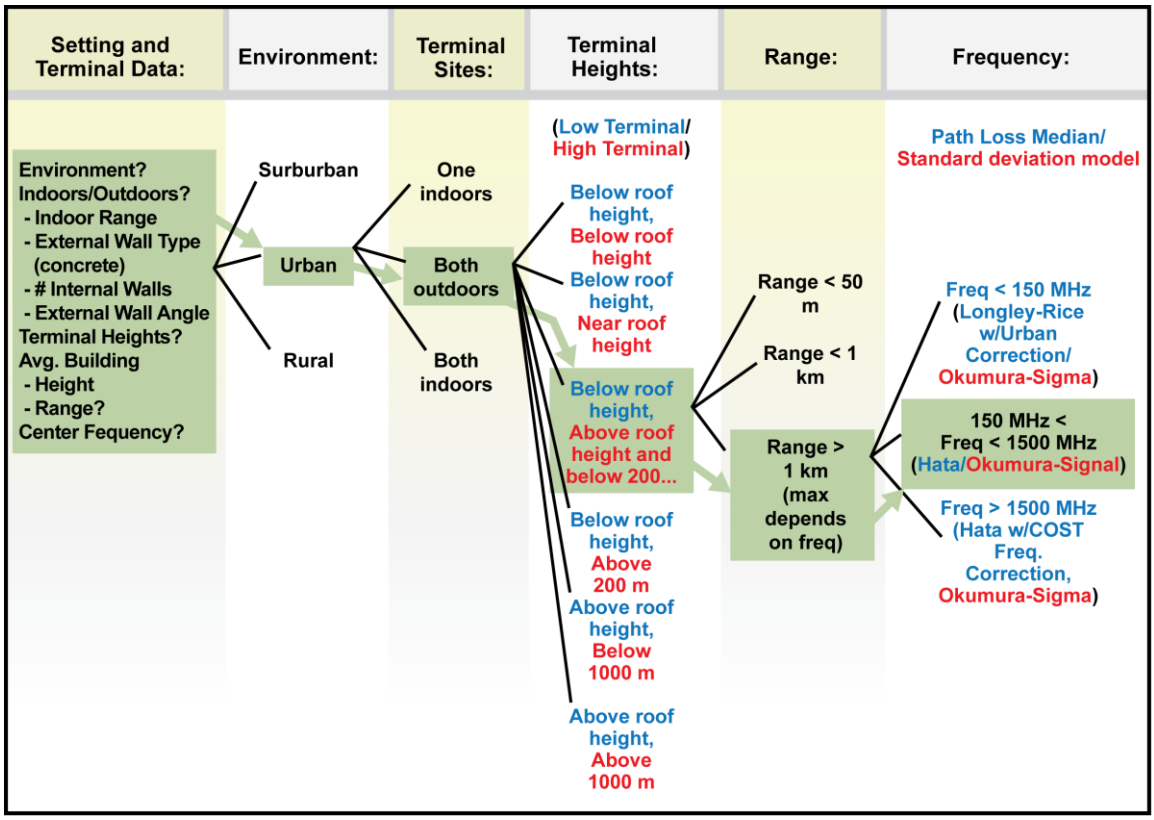

Figure 1) Example of Llamacom model selection process.

Table 1. Median Pathloss and Standard Deviation Models Corresponding to Each Region of Figures 2, 4, 5, 7, 8, 9, 10 and 12.

Region	Median Pathloss Model	Pathloss Standard Deviation
1	mean two-path	no long-term variation
2	Walfish-Ikegami	Okumura
3	Walfish-Ikegami with correction to match Longley-Rice at 1 km	Okumura
4a	< 150 MHz: Longley-Rice with urban correction 150 – 1500 MHz: Hata > 1500 MHz: Hata with COST corrections	Okumura
4b	< 150 MHz: Longley-Rice with suburban correction 150 – 1500 MHz: Hata > 1500 MHz: Hata with COST corrections	Okumura
5	Interpolate in high-node height between lower and upper models	Okumura
6	Applicable model from low-node to pseudo-node at 200 m height or 20 km range, line-of-sight from pseudo-node to high-node	Applicable standard deviation from low-node to pseudo-node
7	Longley-Rice	Longley-Rice
8	cabot	cabot
9	Applicable model from low-node to pseudo-node at 1000 m height or 2000 km range, line-of-sight from pseudo-node to high-node	Applicable standard deviation from low-node to pseudo-node
10	Cost-231 LOS building penetration model	4 dB
11	COST-231 NLOS building penetration plus Walfish-Ikegami from reference node to outdoor node	Okumura + 4 dB
12	COST-231 NLOS building penetration plus Walfish-Ikegami from reference node to outdoor node, with correction to match Longley-Rice at 1 km	Okumura + 4 dB
13a	COST-231 NLOS building penetration plus reference node to outdoor node loss: < 150 MHz: Longley-Rice with urban correction 150 – 1500 MHz: Hata > 1500 MHz: Hata with COST corrections	Okumura + 4 dB
13b	COST-231 NLOS building penetration plus reference-node to outdoor-node loss: < 150 MHz: Longley-Rice with suburban correction 150 – 1500 MHz: Hata > 1500 MHz: Hata with COST corrections	Okumura + 4 dB

14	COST-231 NLOS building penetration plus reference-node to outdoor-node loss by Interpolating in outdoor-node height between lower and upper models	Okumura + 4 dB
15	COST-231 NLOS building penetration plus Applicable model from reference-node to pseudo-node at 200 m height or 20 km range, line-of-sight from pseudo-node to high-node	Applicable standard deviation from low-node to pseudo-node + 4 dB
16	Indoor propagation	Indoor propagation
17	COST-231 NLOS building penetration at each node, plus Walfish-Ikegami between reference-nodes	Okumura + 5.7 dB
18	Line-of-sight	no long-term variation
19	Cost-231 LOS building penetration model through two walls (min 1 dB penetration loss)	4 dB
20	Cost-231 LOS building penetration model through two walls (min 1 dB penetration loss) with LOS range term modified to cabot range loss	Cabot + 4 dB
21	COST-231 NLOS building penetration model through two walls, Longley-Rice from reference noide to outdoor node	Longley-Rice + 4 dB
22	COST-231 NLOS building penetration model through two walls, Longley-Rice between reference nodes	Longley-Rice + 5.7 dB
23	COST-231 NLOS building penetration model through two walls, cabot between reference nodes	Cabot + 5.7 dB

1.2.1 Urban and Suburban Propagation Models

Models for the urban and suburban environments assume buildings are the main obstructions to line-of-sight (LOS) propagation. Similar models are used for each environment, frequently differing only by parameter values..

Figures 2Figure 1 and 4 cover outdoor models, when the lower of the two nodes is above or below average roof height, respectively. Figure 3 is an example of pathloss versus range and frequency for a link with parameters in the range of Figure 2. Figure 5 covers propagation with one node indoors and one outdoors, and Figure 6 is an example of pathloss for a link from Figure 5. Figure 7 covers propagation with both nodes indoors. Figures 8-10 and 12 correspond to Figures 2, 4, 5, and 7 but for suburban propagation.

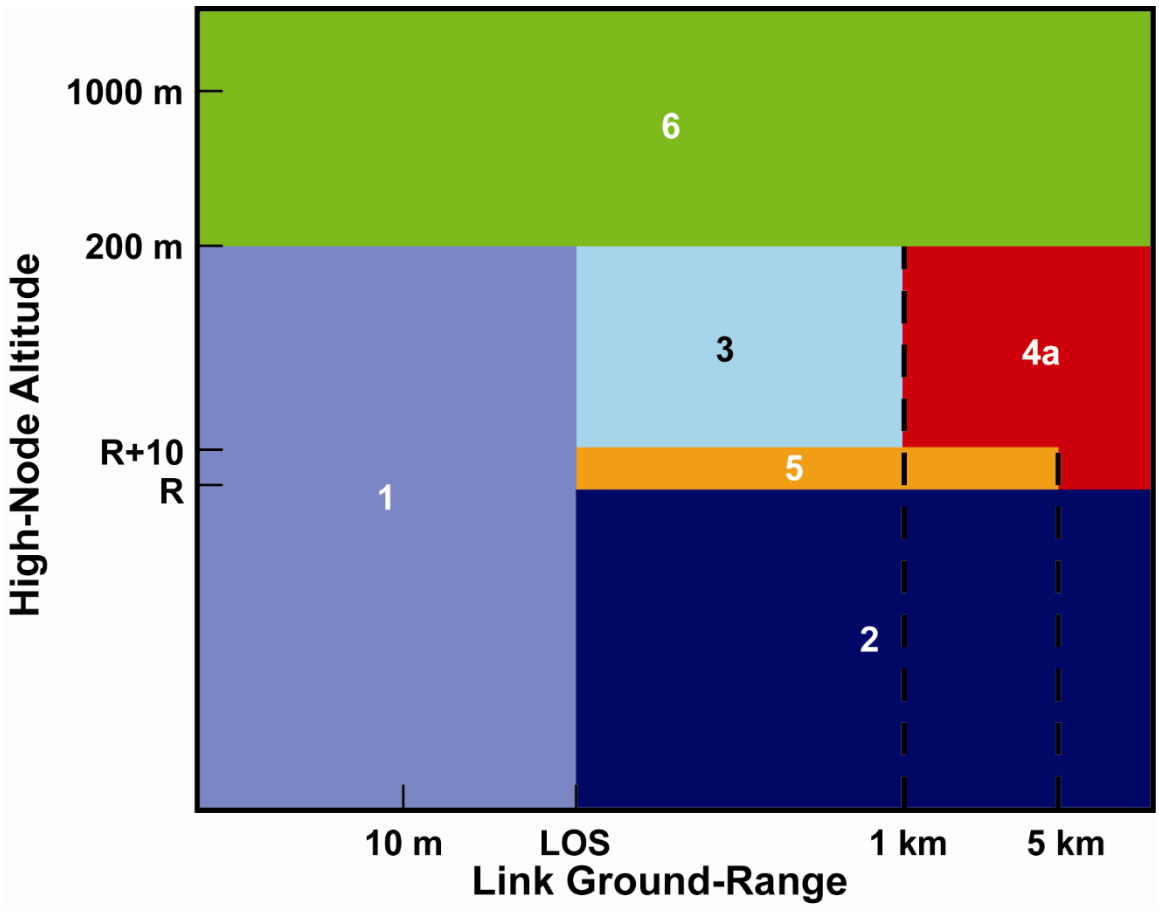

Figure 1) Pathloss model selection for two outdoor nodes in an urban environment, with the low node below roof height. High node a may be above or below average building height, R. LOS is ground range below which link is line-of-sight.

In all cases, some height boundaries are given relative to the specified parameter average roof height, and there is a range boundary at the specified parameter LOS (line-of-sight), which is the assumed range below which outdoor links experience line-of-sight propagation.

In the LOS region, the mean pathloss is calculated for shorter paths using the two-path model (a LOS path plus a ground-bounce path), at longer path lengths, defined as those with a relative delay between paths exceeding $\pi/2$ radians, median pathloss is the linear mean of the two-path loss, i.e., not including the effect of deep fades when the two paths are out-of-phase. This model is consistent with measurements in an urban environment, showing that when there is complicated multipath fading on LOS channels the mean follows the two-path model, while the fading is Rayleigh [Hampton].

At longer ranges, with the both nodes outdoors but below roof height, the COST-231 Walfish-Ikegami model is used with the 'urban' or 'suburban' environment setting. When the higher node is above roof height, and ranges are longer, typically exceeding

one km, a model is selected based on frequency. The model selected may be Longley-Rice with urban or suburban corrections, Hata, or Hata with the COST extension, depending on frequency.

In order to provide smooth transitions between models, propagation loss in some regions is modified slightly. When the low node is below roof height, the upper node is between roof height plus 10 m and 200 m, and range between LOS and 1 km, a correction factor is added to the mean range loss so that there is not a discontinuity at 1 km. Special care is also taken for the transition at roof height. The models for links with one node above roof height typically assume the high antenna is well above roof height, and perform poorly if it is not [Lowe?]. To compensate for that mismatch, and provide a smooth transition between the two models, a transition region was defined between average roof height, and average roof height plus 10 m. At ranges below 5 km, loss in this region is interpolated between the two sets of models.

Figure 3 is a plot of median pathloss as a function of range and frequency in an urban outdoor setting, with node heights 2 m and 30 m. The average building height is 18 m, and models were selected according to Figure 2.

Note that although LLamacom will provide results for the urban setting with both nodes below roof height and range exceeding 5 km, the model used here is based on measurements out to no more than 5 km, and is not expected to be accurate at greater ranges. However, this is such a severe propagation environment that this set of parameters is unlikely to be used. Models with one node above roof height extend to at least 20 km, and in some cases longer.

When the low node is below roof height, and the high node is above 200 m, a slightly different approach is taken. In general, the models suitable for one very low node are not matched to the case of one very high node. In this case, a pseudo-node is defined at the limit of the models used, as illustrated in Figure TBD. As shown, the pseudo-node is on the LOS path connecting the two physical nodes, at an altitude of 200 m if the resulting low-node to pseudo-node range does not exceed 20 km, and otherwise at 20 km range. The appropriate model is then used for low-node to pseudo-node propagation, and additional loss from the pseudo-node to high-node is modeled as LOS.

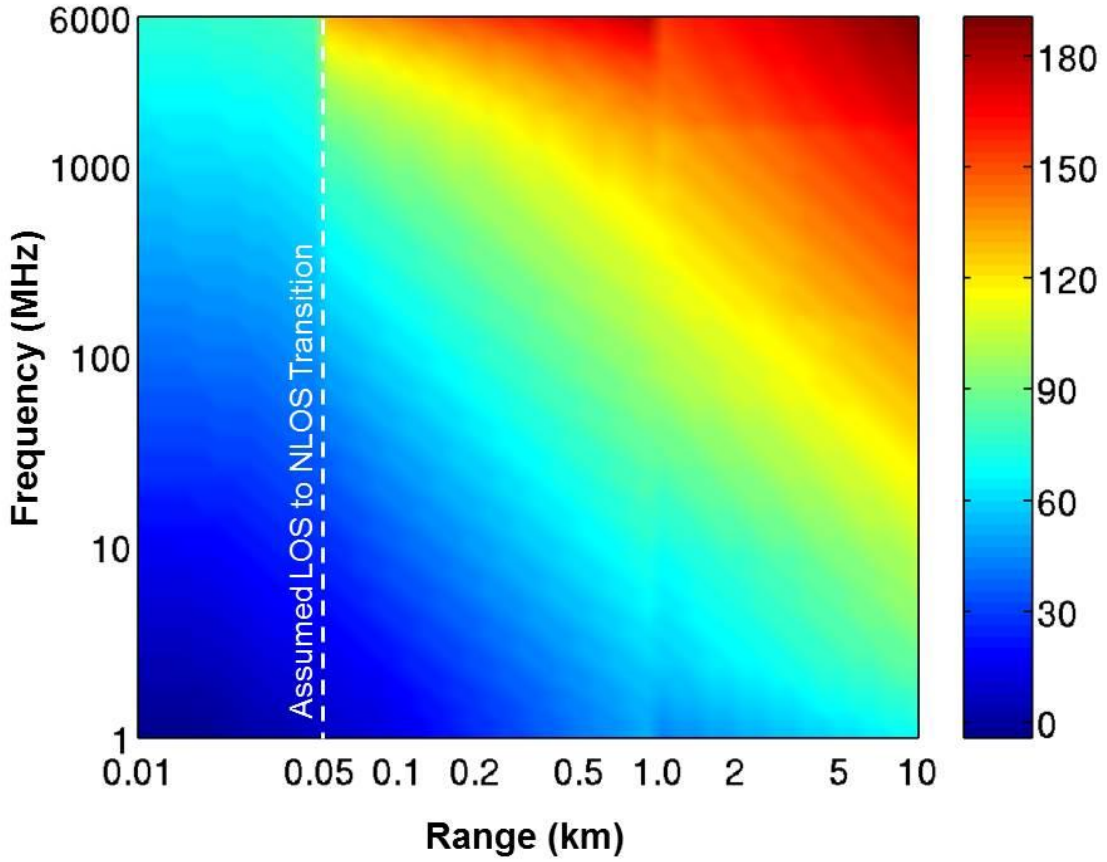

Figure 3). Urban outdoor link median pathloss (dB), low node height 2 m, high node height 30 m, average building height 18 m, line-of-sight range 50 m.

In the case or two nodes above roof height, the Longley-Rice model is used wherever applicable. This model is applicable for ranges of 1 km or greater, and high-node altitudes up to 1000 m. In an urban setting the Longley-Rice urban correction is used. A similar correction was found for suburban settings, as described in Section zz. For shorter ranges (<1 km), pathloss is interpolated in range between LOS propagation at 10 m, and the Longley-Rice model at 1 km (a graph would be nice). For altitudes above 1000 m, the pseudo-node approach is used, now with the pseudo-node maximum altitude 1000 m, and maximum range 1000 km (check this).

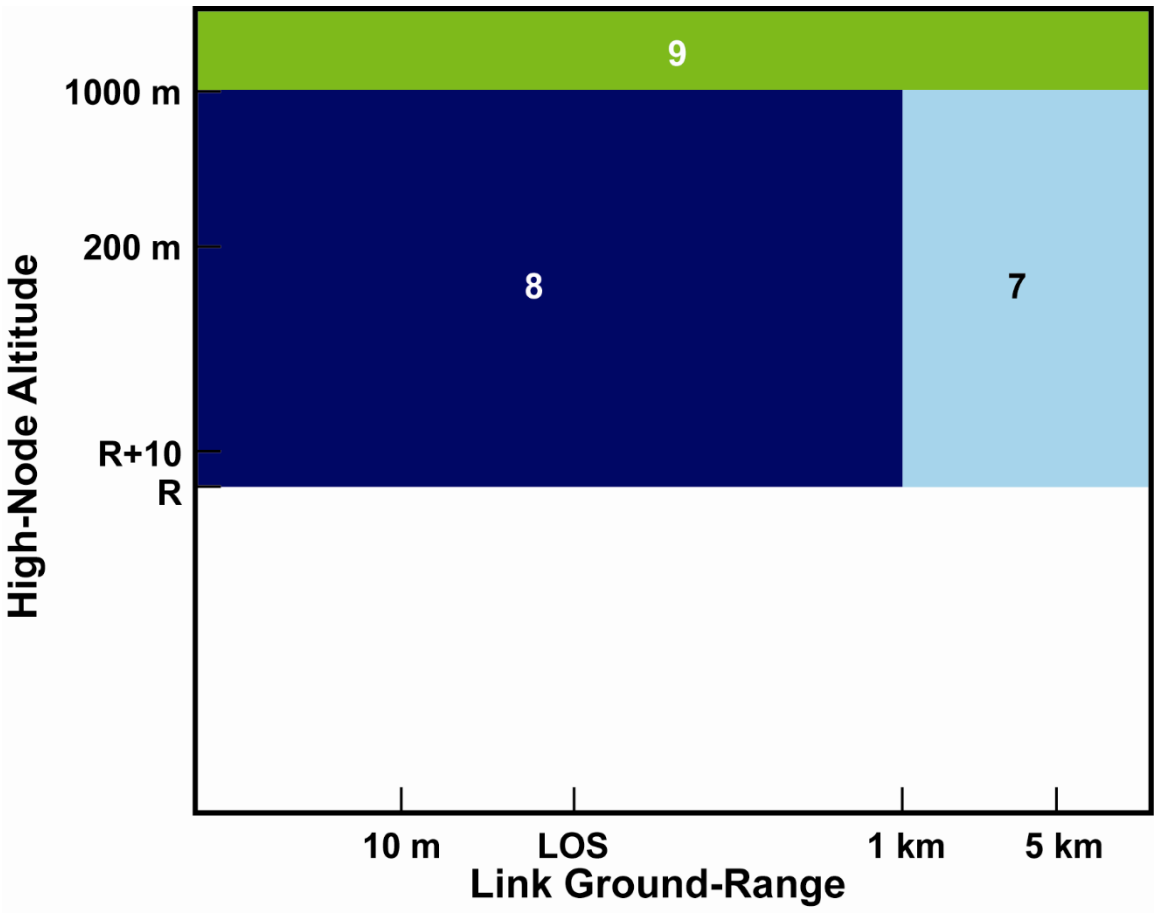

Figure 4) Pathloss model selection for two outdoor nodes in an urban environment, with the low node above roof height. R is average building height. LOS is ground range below which link is line-of-sight.

In all cases, the shadowing loss standard deviation is found using results from [Okumura] as described in Section 4, except that in the LOS regime there is no shadowing, and consequently the standard deviation is 0 dB.

The urban or suburban case with one node indoors is similar to the outdoor case, except that at LOS range the two-path model is replaced by the COST-231 LOS building penetration model. In this case, line-of-sight means that the outdoor node has an unobstructed path to the building at the point where the exterior building wall is closest to the indoor node. For greater ranges, building penetration loss is provided by the COST-231 non-LOS (NLOS) model, which is designed for use in conjunction with outdoor models. The outdoor model estimates propagation loss between the outdoor node and a point 2 m high, located just outside the building, where the exterior wall is closes to the indoor node. The COST-231 building penetration models were develop for frequencies 900 MHz and 1.8 GHz, they have been extended to other frequencies as described in Section 7. Building penetration is assumed to add another 4 dB to the shadowing standard

deviation. When two loss terms are combined, as here, the combined shadowing loss standard deviation is the rss of individual terms, i.e, $s = \sqrt{s_1^2 + s_2^2}$.

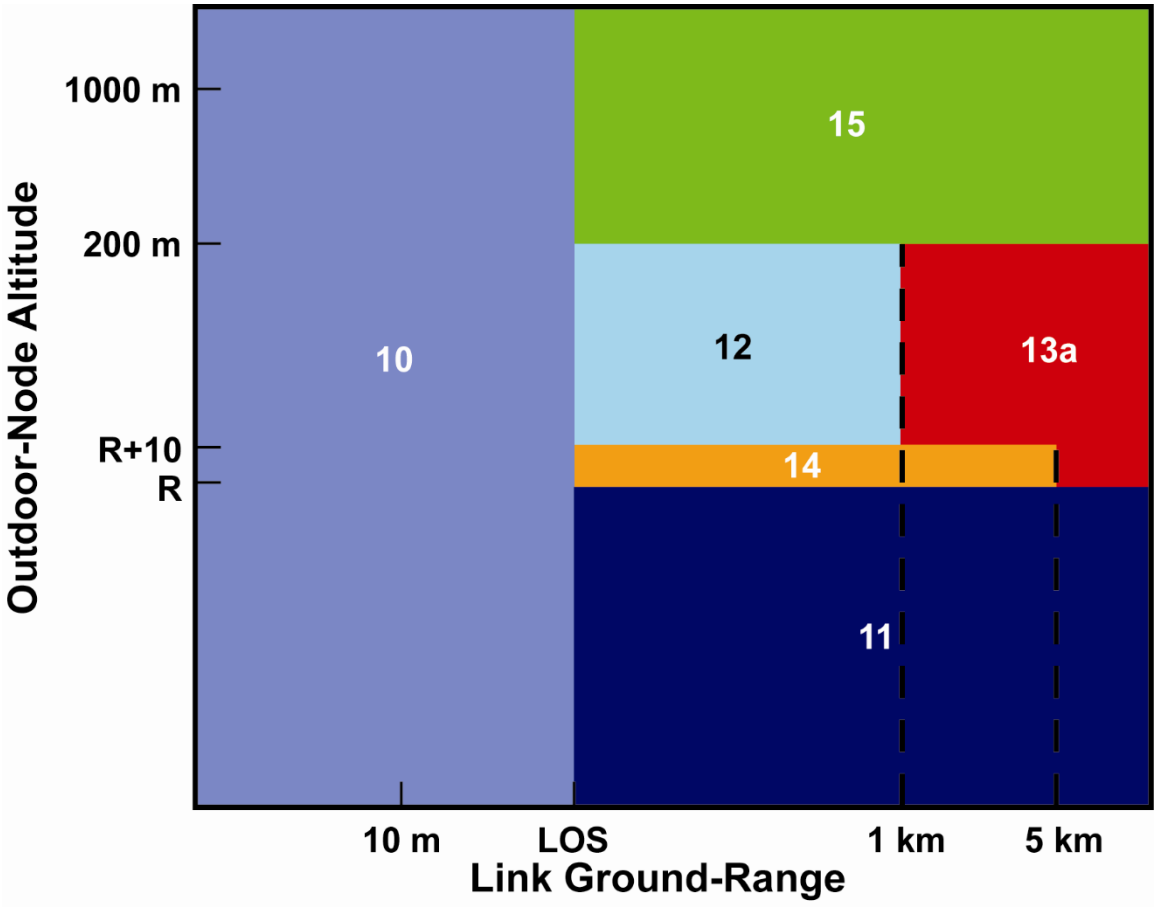

Figure 5) Pathloss model selection for one outdoor node and one indoor node in an urban environment. R is average building height. LOS is ground range below which link is line-of-sight.

Figure 6 shows median pathloss for an urban link with one node indoors and the other above roof height. The interior node is assumed to be 10 m from an exterior concrete wall with one intervening interior wall.

When both nodes are indoors, the Llamacomm model assumes that if urban link range is less than LOS, or the suburban link range is less than 10 m, both nodes are in the same building, and using the indoor model described in Section8. Currently, parameters used by the indoor propagation model assume masonry interior walls (e.g, concrete or cinder block) , and results are expected to be poor in other types of buildings, particularly wood frame buildings, as are typical in many North American suburbs. What about plasterboard on metal studs? It is assumed that if total link range is less than zz m, the transmitter and receiver are in the same room. Otherwise loss is found assuming they are

in different rooms. If specified transmitter and receiver height differ by more than 2 m, it is assumed they are one different floors of the building, the selection of 2 m height

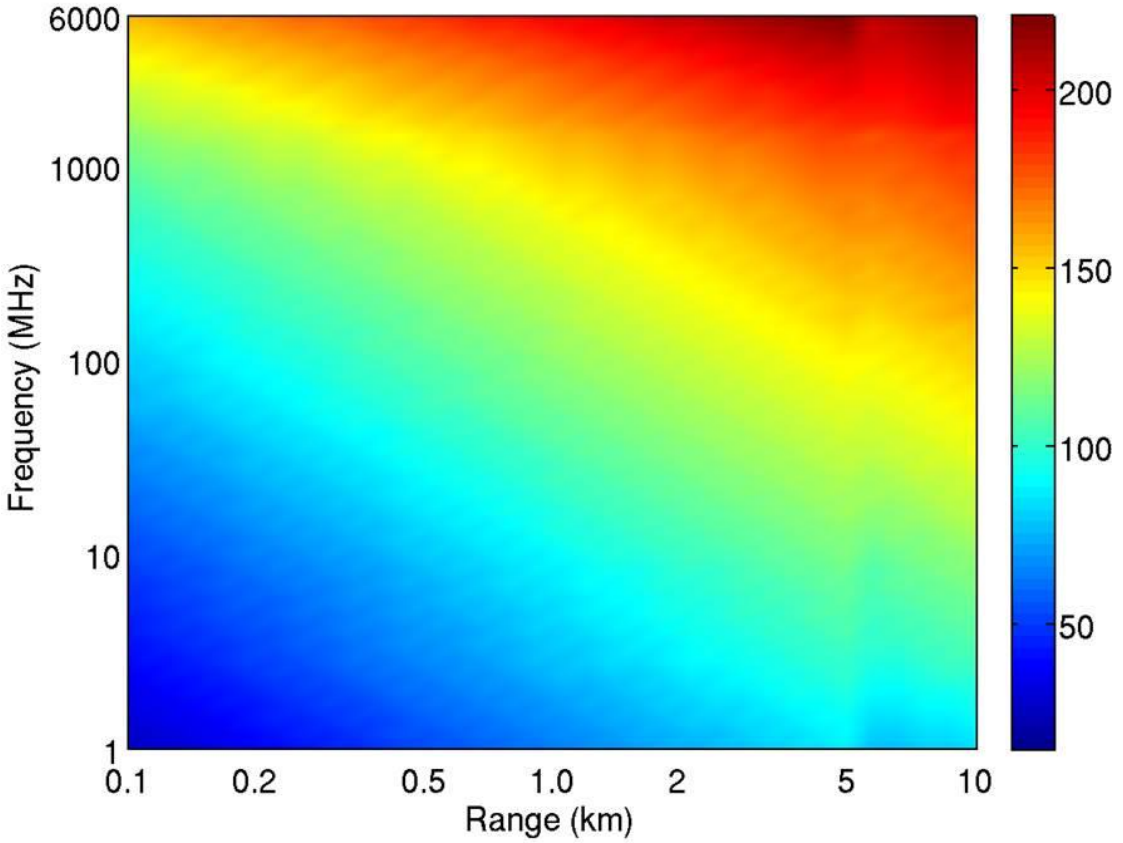

Figure 6) Urban indoor to outdoor link median pathloss (dB), low node height 2 m, high node height 23 m, average building height 18 m, low node is indoors, 10 m from exterior concrete wall with 1 intervening interior wall.

difference as the threshold reflects the belief that nodes are unlikely to be placed right at either floor or ceiling height. When link range is longer than the LOS distance nodes are assumed to be in different buildings, and the NLOS building penetration model is used for each node, with the appropriate outdoor model between buildings. In this case building penetration adds 5.7 dB to the outdoor shadowing standard deviation (4 dB for each building).

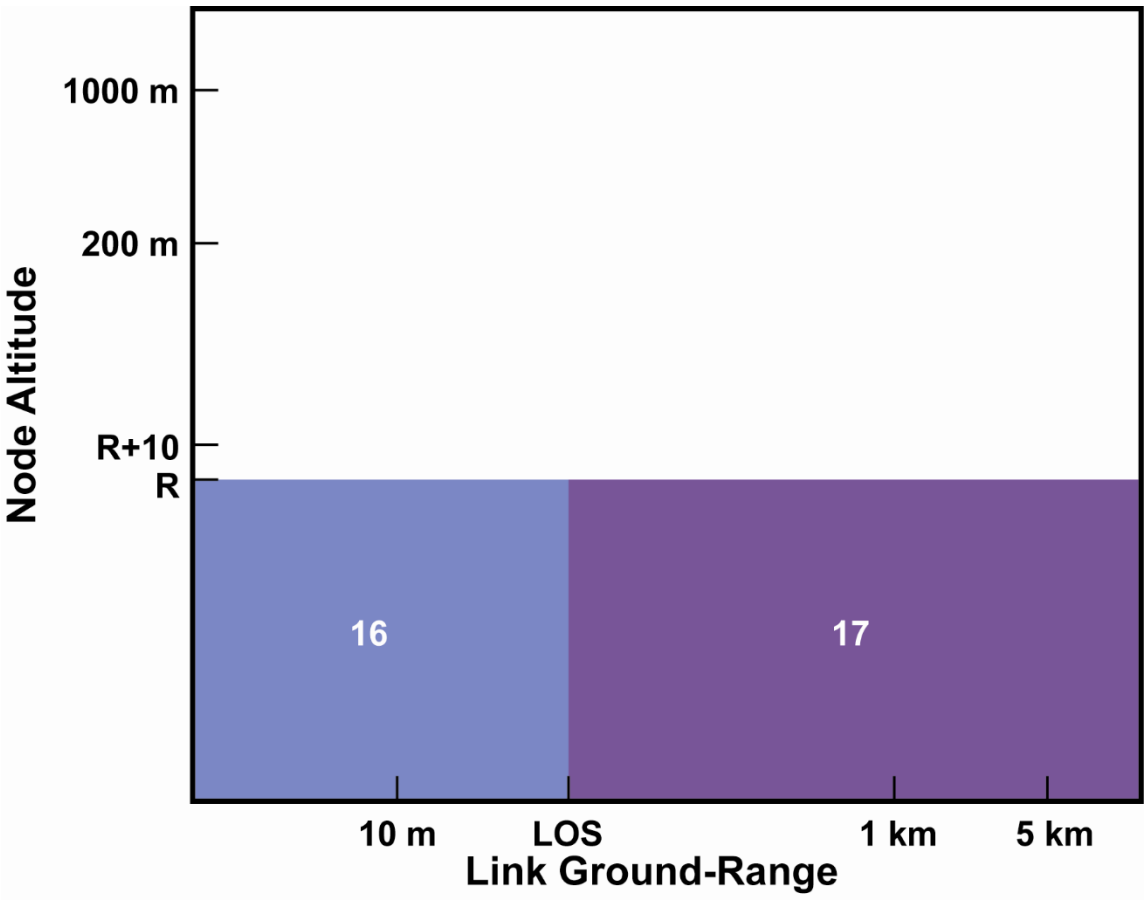

Figure 7) Pathlos model selection for two indoor nodes in an urban environment. R is average building height. LOS is ground range below which link is line-of-sight.

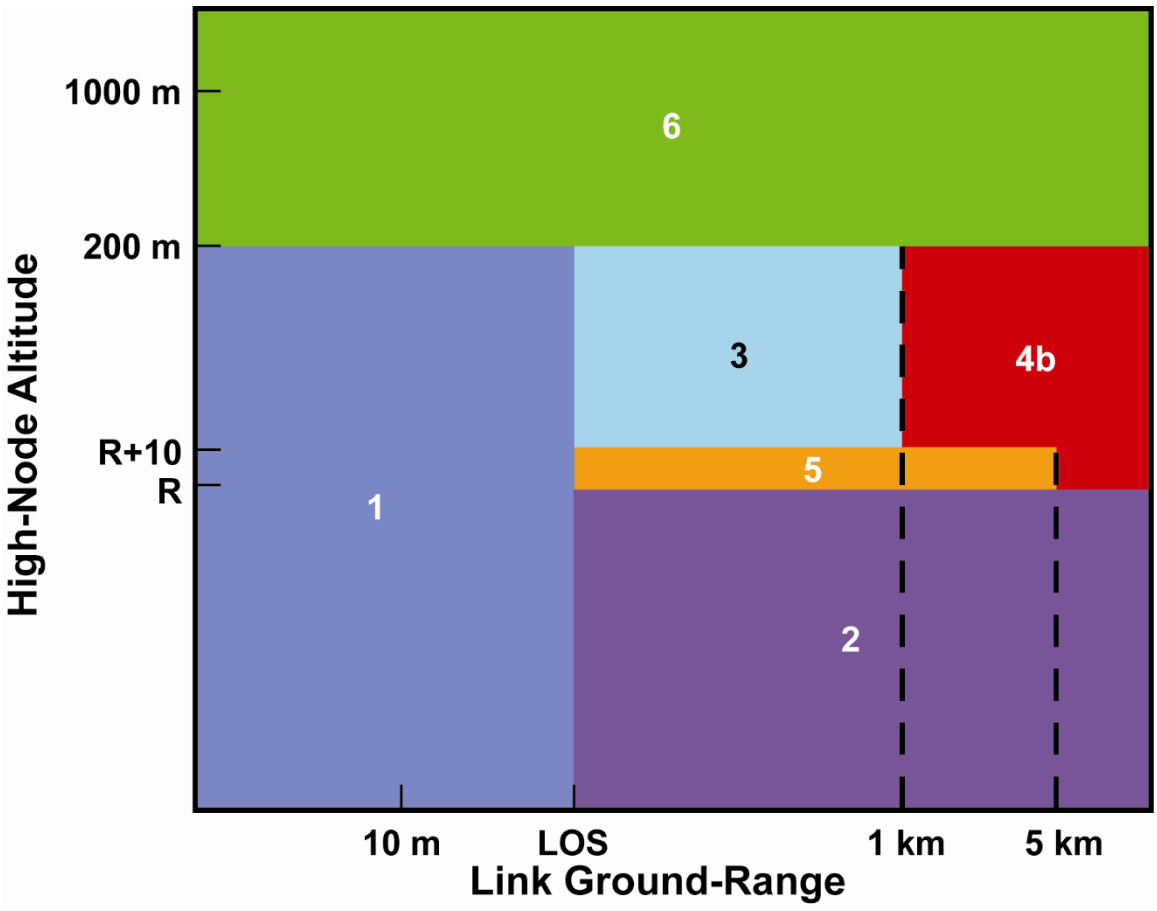

Figure 8) Suburban, both outdoors, low node below roof height

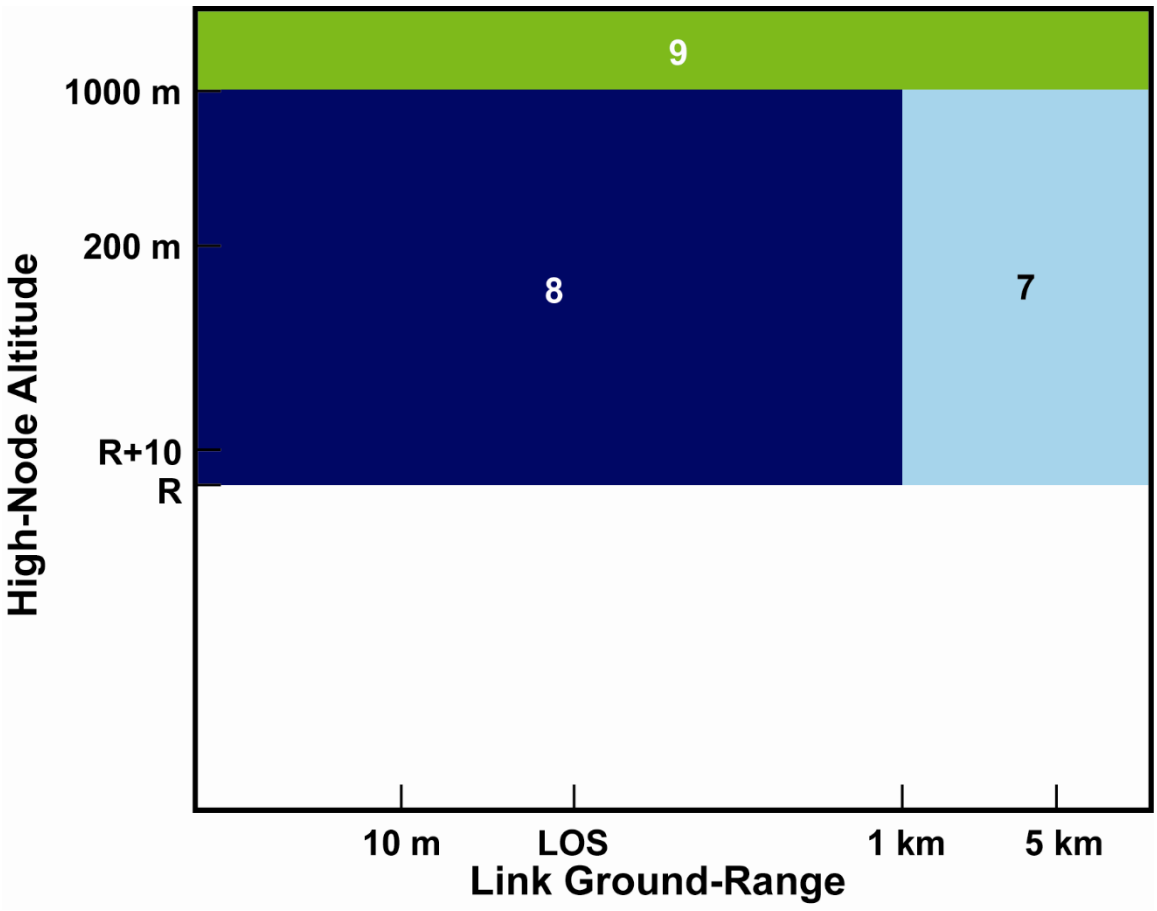

Figure 9) Suburban, both outdoors, low node above roof height

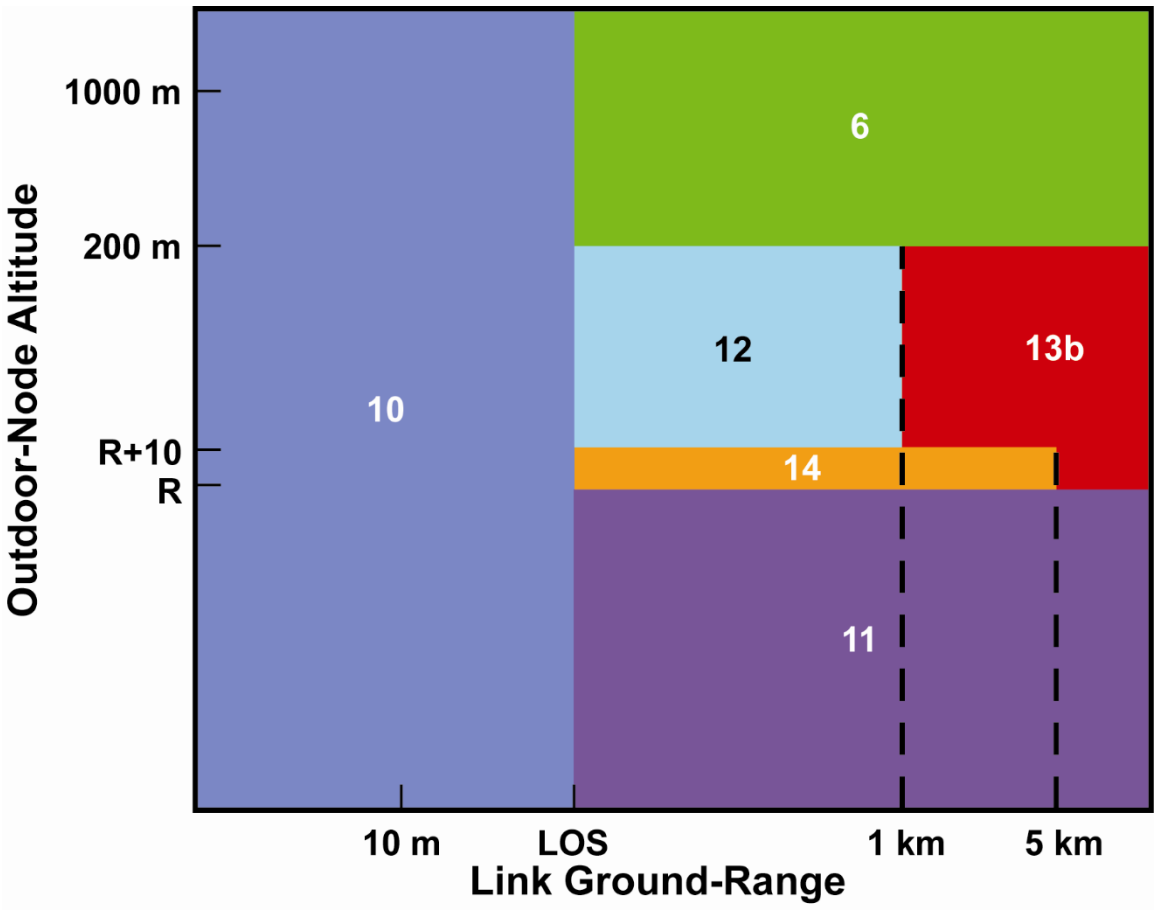

Figure 10) Suburban, one node indoors

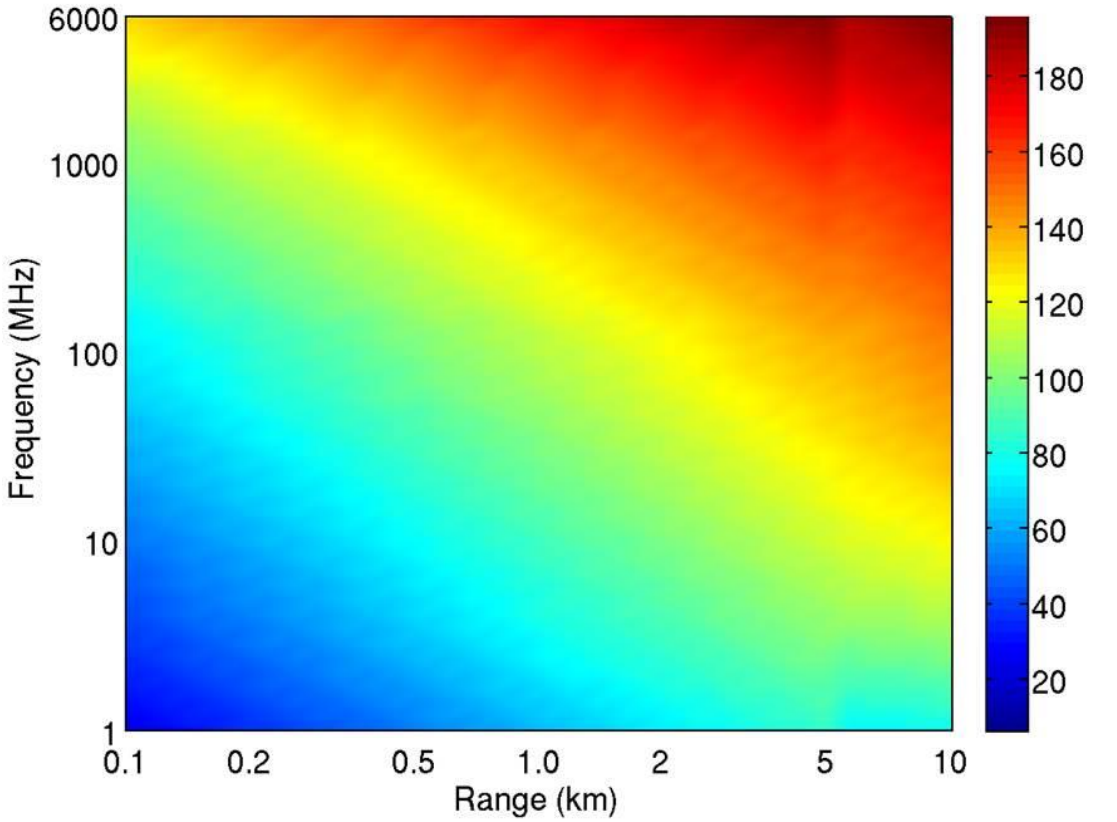

Figure 2-11) Suburban indoor to outdoor link median pathloss (dB), low node height 2 m, high node height 15 m, average building height 10 m, low node is indoors, 3 m from exterior concrete wall.

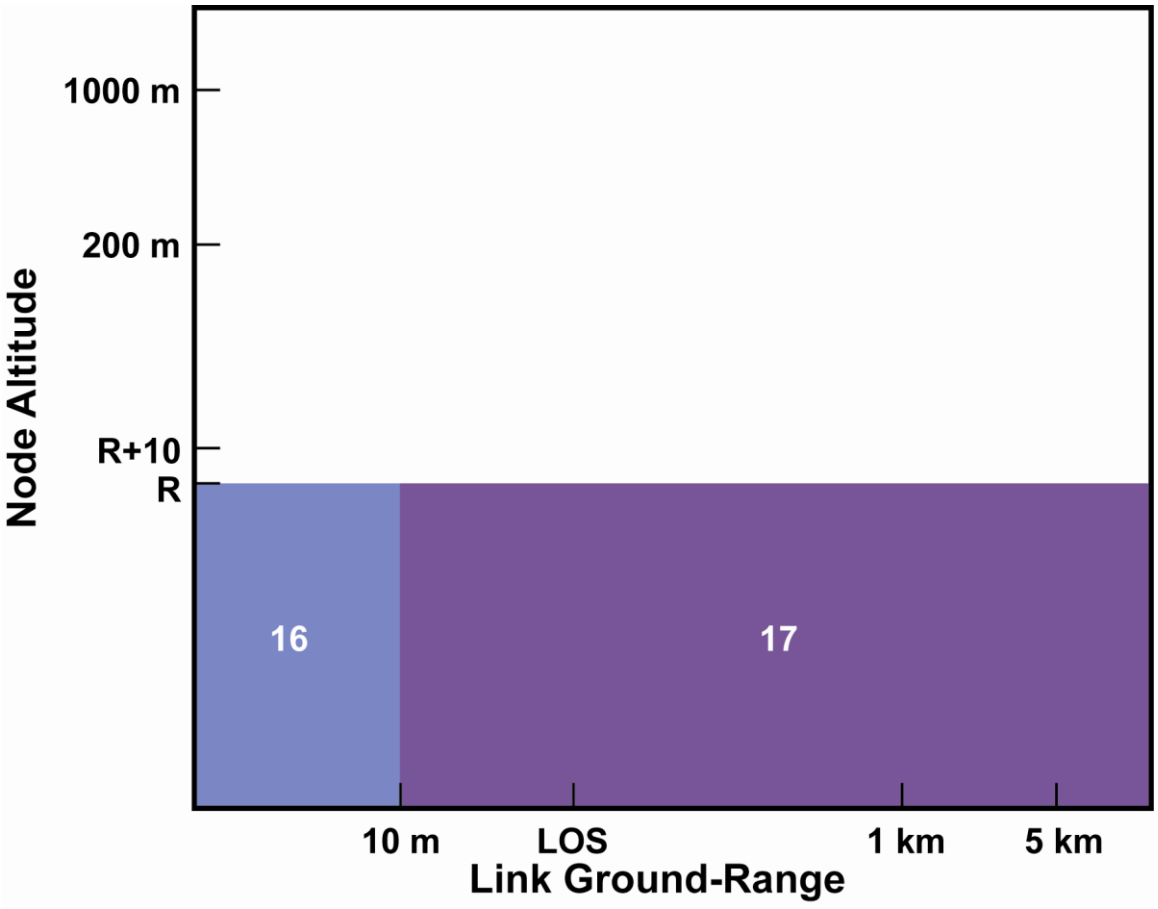

Figure 12) Suburban, both nodes indoors

1.2.2 Rural Propagation Models

The rural propagation models assume that buildings are sparsely distributed, and are not major cause of propagation loss. The main cause of excess propagation loss is obstruction by geographical features, e.g. hills. Consequently, the Longley-Rice propagation model is used in all cases to model the range component of loss, with suitable adaptations to cover ranges below 1 km, and node heights above 1000 m.

Decision regions for rural propagation with two outdoor nodes is illustrated in Figure 13. propagation is modeled as LOS at ranges below 10 m, and using the Longley-Rice model for ranges beyond 1 km, and node heights below 1000 m. Between 10 m and 1 km, loss is interpolated between LOS and Longley-Rice using

$$L = L_{10m} + \left(\log_{10} r - \log_{10} r_{10m}\right)\frac{L_{1km} - L_{10m}}{\log_{10} r_{1km} - \log_{10} r_{10m}} \quad (2.1)$$

Where L, L_{10m} and L_{1km} are loss in dB at the current range, 10 m range, and 1 km range respectively. r, r_{10m} and r_{1km} are slant range at the current ground range, 10 m ground range, and 1 km ground range respectively. The difference between slant range and ground range may be significant in a few scenarios where one node is at a significantly different height than the other, and was retained throughout for consistency.

For high-node height above 1000 m, a pseudo-node is defined at 1000 m altitude, or 1000 km range, as shown in Figure TBD. The low-altitude model is used to the pseudo-node, and LOS propagation from the pseudo-node to the high-node.

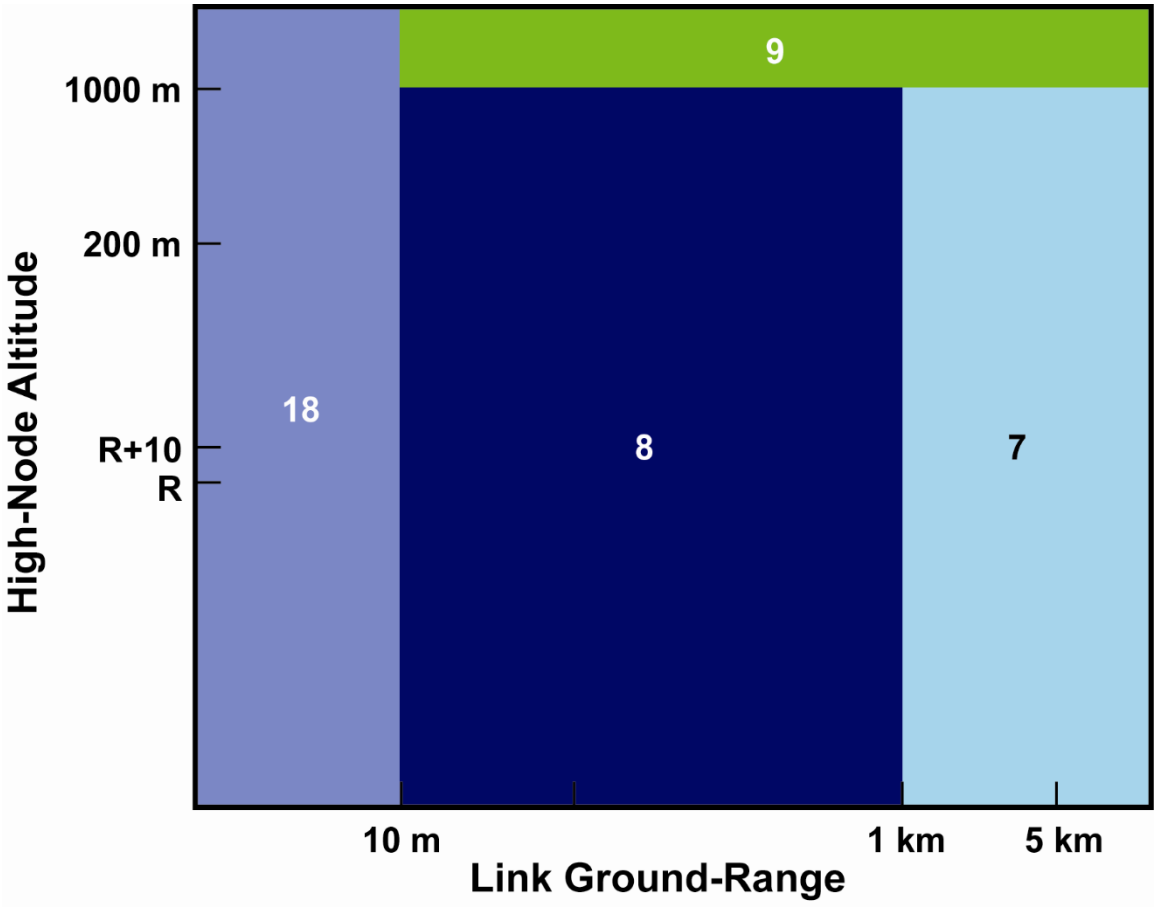

Figure 13) Pathlos model selection for two outdoor nodes in a rural environment.

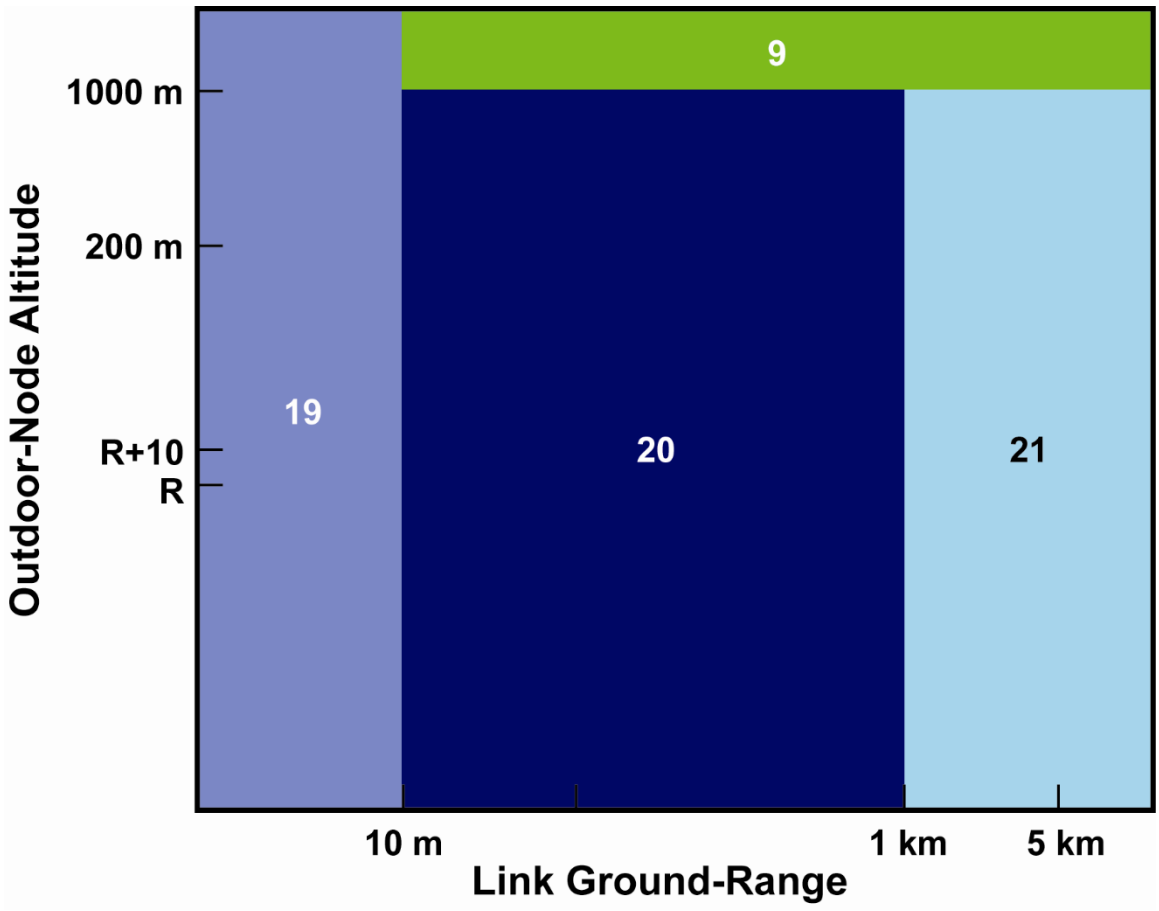

Figure 14) Path-loss model selection for one outdoor and one indoor node in a rural environment.

Decision regions for rural propagation with one node indoors is shown in Figure 14. The COST-231 LOS building penetration model with frequency extension is used, under the assumption that power penetrates through two building walls, one at the specified wall angle, and one at 90° minus the specified angle. The total power loss for propagation through two walls is found as

$$L_B = \min\left(1, 10\log_{10}\left(10^{-L(\phi)/10} + 10^{-L(90-\phi)/10}\right)\right) \quad dB, \tag{2.2}$$

i.e., power through each wall is summed in the linear domain with the restriction that resulting loss may not fall below 1 dB. As defined by COST-231, LOS building penetration model assumes outdoor range losses are found as LOS loss. Here, the model has been modified so the outdoor losses between 10 m and 1 km are found by interpolating between LOS loss at 10 m, and the Longley-Rice loss at 1 km. This was done because the COST-231 LOS building penetration model is based on data taken in urban environments, where outdoor LOS propagation paths were less than zz m.

For longer outdoor ranges, the COST-231 NLOS building penetration model was used, in conjunction with the Longley-Rice range loss model. The building penetration loss produced by this model was reduced 3 dB, reflecting an assumption that significant amounts of power are coming through two walls. As before, total building penetration loss is restricted to exceed 1 dB.

Figure 15 is a plot of rural median propagation loss versus range and frequency, for a link with one indoor node, which is assumed to be 3 m from two exterior concrete walls.

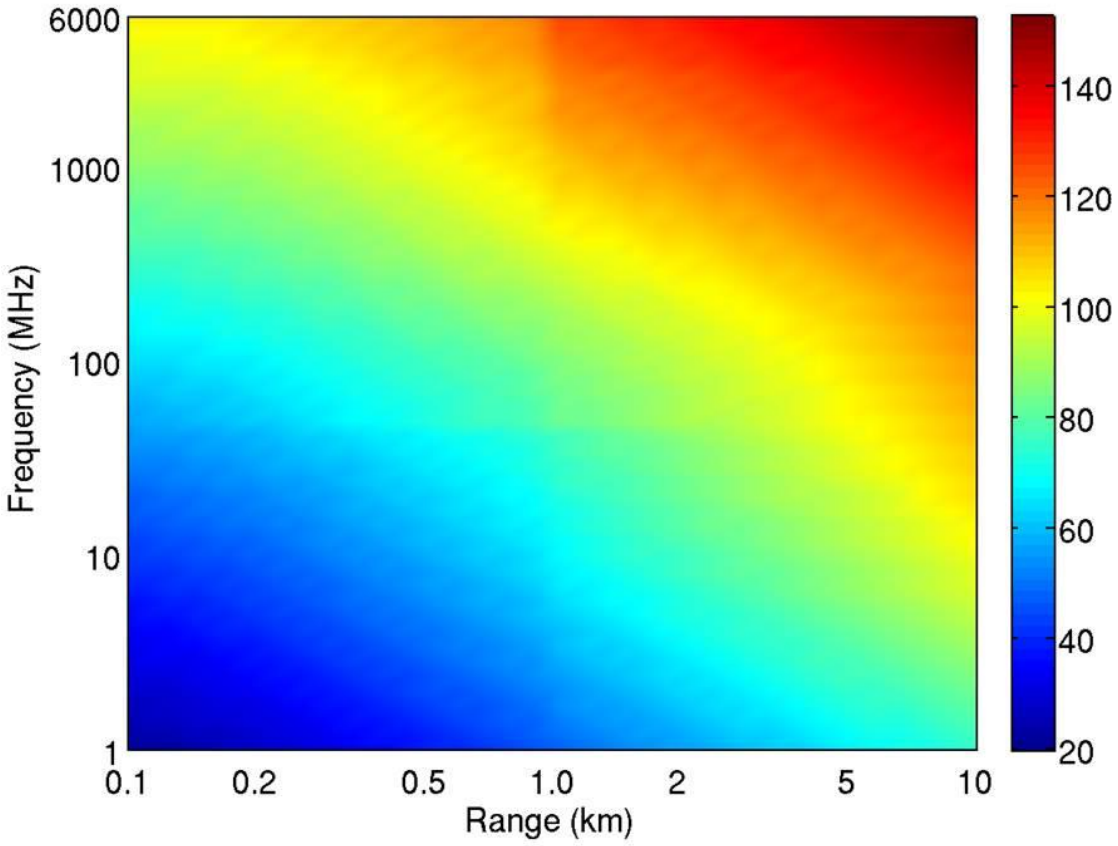

Figure 15) Rural indoor to outdoor link median pathloss (dB), low node height 1 m, high node height 100 m, low node is indoors, 3 m from two exterior concrete walls.

When the outdoor node altitude exceeds 1000 m, a pseudo-node is defined at 1000 m or 1000 km, with the appropriate exterior model used between the building and the pseudo-node, and LOS propagation from the pseudo-node to the high-node.

Decision regions when both nodes are indoors are shown in . When both nodes are indoors and range is less than 10 m, the indoor propagation model is used. Due to the lack of available data on indoor propagation in masonry (concrete, cinder blocks) residences, the same parameters are used as for office buildings with masonry interior walls. The same distance thresholds are used as in the urban/suburban models, i.e., total range < xx me means both nodes are in the same room, height difference > 2 m height

difference then nodes are one different floors. For longer ranges, each building penetration term us found using the COST-231 NLOS building penetration model, assuming penetration through two walls, as above. The exterior loss is calculated between to outdoor nodes a 2 m height, just outside the buildings, using the Longley-Rice model for ranges exceeding 1 km, and interpolating between LOS and Longley-Rice for ranges between 10 m and 1 km.

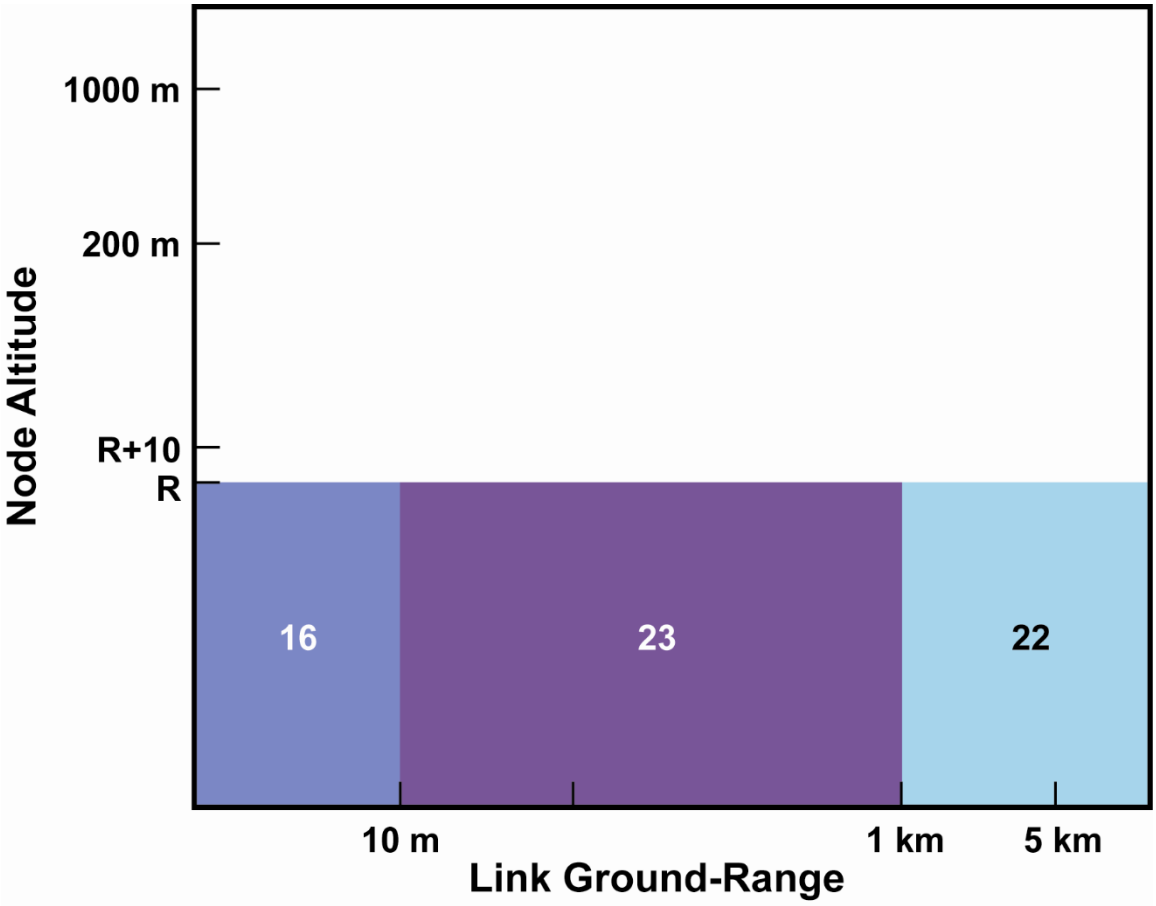

Figure 16) rural, both indoors

The outdoor loss standard deviation is that calculated by the Longley-Rice model, plus 4 dB for each indoor node, combined using RSS.

1.3 Model Applicability

In many cases, models are used in parameter regions outside their original range. Where this occurs, it was verified that model behavior in that region was plausible, and if models exist on either side of the range over which a model was extended, attempts were made to

find a model extension that did not produce large discontinuities where it joined up with another model. Ultimately, only the acquisition of more data in the previously uncovered ranges will verify the applicability of models used in such cases.

2 The Rice K-Factor

Equation Chapter (Next) Section 1

Other parameters are also important for modeling propagation loss and communications link performance, one important parameter is the Rice K-factor, defined as ratio of specular signal power to diffuse signal power.

2.1 Outdoor Paths

K-factor is random variable, apparently log-normal [Greenstein,Soma]. In general median value and variance are functions of range, antenna height, environment. Median K-factor can be characterized as a function of excess range loss [Soma].

$$K_{med} = 16.3 - 0.239\left(L_{med} - L_{LOS}\right) \quad \text{dB} \tag{3.1}$$

where

- L_{med} is median path loss including shadowing, but averaged over fading, in dB L_{LOS} is the line-of-sight loss for the given link range, in dB This equation is based on results taken at 2.5 GHz, mixed suburban, low-density urban (San Jose, CA), and "lightly hilly terrain". Most measurements in winter. Transmitter height 20 m, Rx height 3 m. 0.2 to 7 km range.

This approach is attractive because excess propagation loss models are avialable for a wide range of conditions and frequencies, implicitly includes antenna height, environment, frequency etc. through their effect on excess propagation loss. How do we know it is applicable under all conditions? Get consistent results in [Glazunov] at 1.88 GHz in urban and suburban environments (Stockholm).

Figure 17 shows a comparison of the median Rice K-factor estimate from eq. (3.1) using different propagation models [Hata,Walfisch,Longley] at 1.8 GHz in an urban setting to estimate excess propagation loss with models that fit the measured K-factor directly to link range in a similar environment [Soma,Greenstein]. Agreement is reasonable, and the method of estimating K-factor from excess propagation loss has the advantage that propagation loss models are already available for a wider range of parameters and settings.

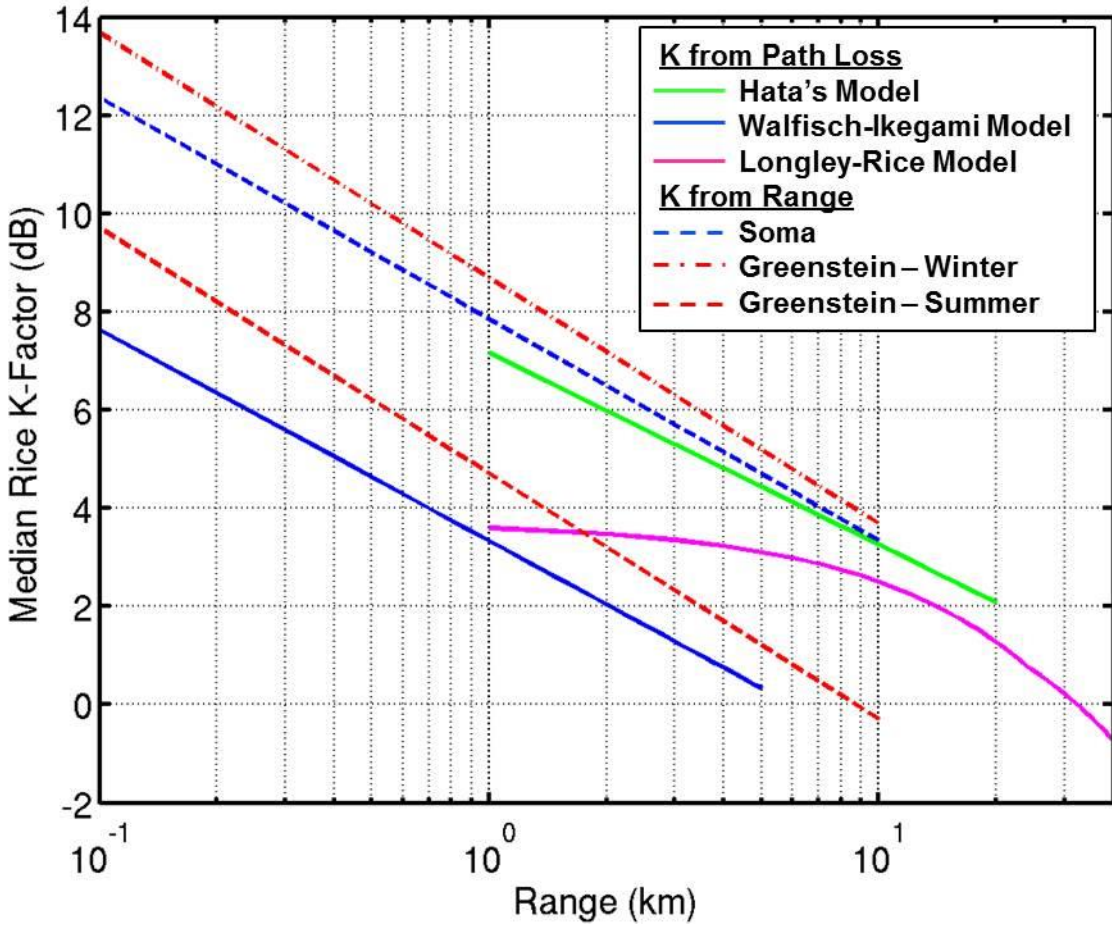

Figure 17) A comparison of Rice K-factor estimates at 1.8 GHz. Solid lines show Soma's approximation from excess path loss using different path loss models in an Urban setting with average building height 18 m, and terminal heights 2 and 20 m. Dashed lines show Rice K-factor estimates based on a direct fit of measured data to link range [Soma,Greenstein].

Antenna gain is also important [Greenstein]. Antenna gain is not a factor in excess propagation loss, and must be explicitly modeled, but Soma only shows results for high gain antennas, 12 and 17 dBi. In [IEEE802.16] a model for K-factor is presented that includes antenna beamwidth

$$k = C\left(\frac{B}{17}\right)^{-0.62} \tag{3.2}$$

where

- k is the linear-domain representation of the K-factor ($k=10^{K/10}$)
- C represents dependence on all other factors
- B is antenna beamwidth, in degrees

Often antennas are specified in terms of gain at peak-of-beam, relative to an isotropic antenna. An approximate conversion from antenna gain to beamwidth is accomplished by

assuming the antenna beam is an ideal function with constant gain in a cone centered on the beam peak, and no gain elsewhere. Consider a sphere of radius R centered on the antenna.. The area on the surface of the sphere subtended by the ideal antenna beam is $A = \pi p^2$ [CRC], where p is the length of a straight line from the beam edge on the surface of the sphere to beam-center, also on the sphere. Using the law of cosines, $p^2 = 2R^2(1-\cos(B/2))$. The total sphere surface area is $4\pi R^2$, and if beamwidth $B \leq 180°$ (antenna directivity ≥ 3 dB) the ratio of total sphere surface area to the area subtended by the ideal antenna beam approximates antenna gain.

$$G = 10\log_{10}\left(\frac{2}{1-\cos(B/2)}\right) \quad \text{dB} \tag{3.3}$$

The same result can be found when B>180° (directivity<3 dB), by a slightly different derivation. This expression can be inverted to get an approximate beamwidth from antenna gain

$$B = 2\cos^{-1}\left(1-2/10^{G/10}\right) \quad \text{degrees} \tag{3.4}$$

The transmitter and receiver antenna gains used in [Soma] are 12 and 17 dB, for approximate beamwidths 58° and 32°. Using eq. (3.2), the K-factors with 12 and 17 dB terminal antenna gains can be calculated, then a correction term for antennas with different gains can be formed by taking the ratios of eq. (3.5) for the antennas simulated to that for the antennas used by Soma. This term is added to the median K-factor previously calculated. For transmit and receive antennas with beamwidths B_1 and B_2, the correction factor used is

$$\Delta K_{BW} = -0.62\log_{10}\left(\frac{B_1 B_2}{1890}\right) \tag{3.5}$$

The Llamacomm simulation gets antenna beamwidth to use in this correction term by finding the peak antenna gain from the user-provided antenna function and converting it to beamwidth as in eq. (3.3). For example, a link between two half-wavelength dipoles (peak gain = 2.1 dB) has assumed beamwidth 207° at both nodes, reducing the link K-factor by 8.4 dB. Figure 18 is a plot of the Rice K-factor correction for antenna beamwidth using this procedure.

The log-normally distributed K-factor is generated by adding a zero-mean gaussian random value to the median value in dB. Standard deviation does not depend on beamwidth [Greenstein] and appears to be on the range 7 to 8 dB [Soma,Greenstein]. A value of 8 dB was used by Llamacomm for outdoor propagation.

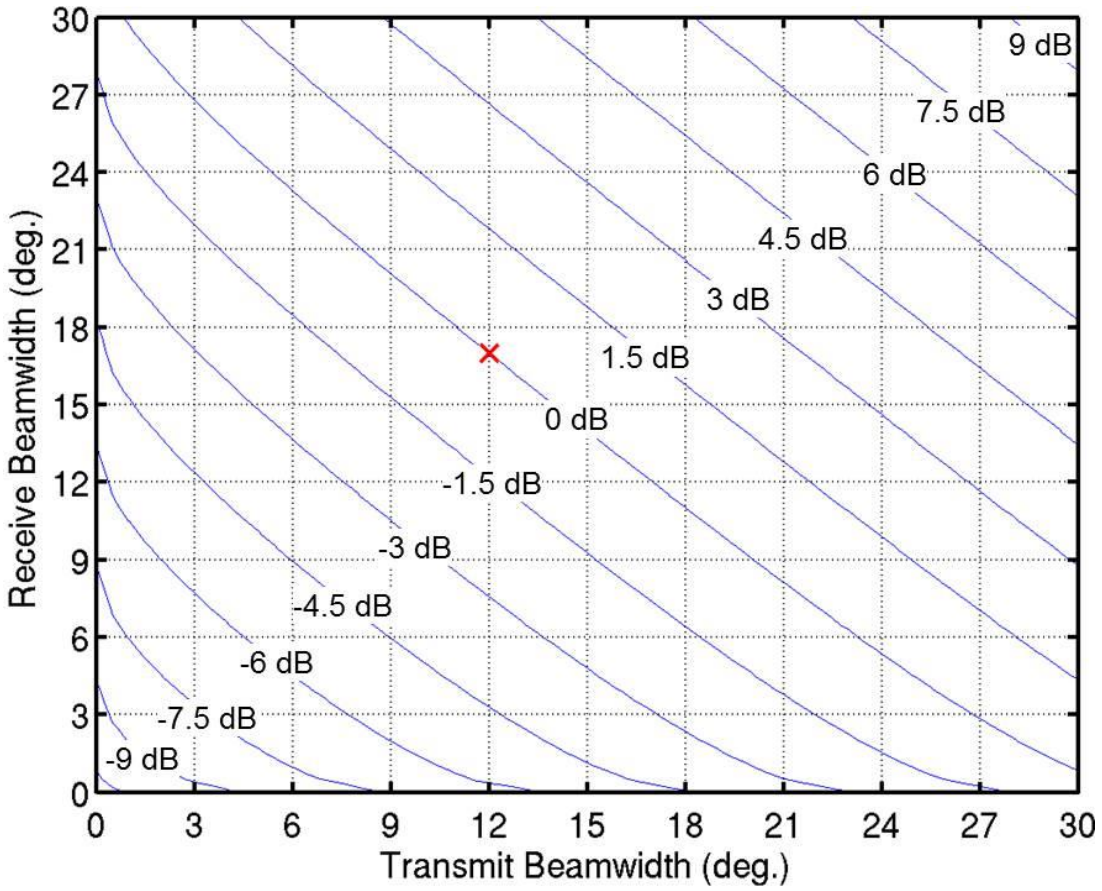

Figure 18) The antenna beamwidth correction for the outdoor Rice K-factor. The red x marks the beamwidth values at which the original curve fitting was performed.

2.1.1 Indoor Paths

Soma's model applies only to outdoor propagation. Rice K-factor dependence on indoor antenna gain is discussed in [Valenzuela,Hafezy,Chandra]. For indoor terminals use data from [Chandra], taken at selected frequencies in a concrete block building. The transmitter and receiver heights are 1.9 and 1.5 m above floor level. Only measurments taken with transmitter and receiver on the same floor were used. These measurements all had an LOS path, and the resulting values of K will be high when the indoor component of the propagation path is not LOS. The measured values are listed in Table 2. The Rice K-factor is clearly dependent on frequency. In order to use these results over the full frequency range, a staight line was fit to the data in dB

$$K_{med} = 11.7 - 0.00379 f_{MHz} \quad dB \tag{3.6}$$

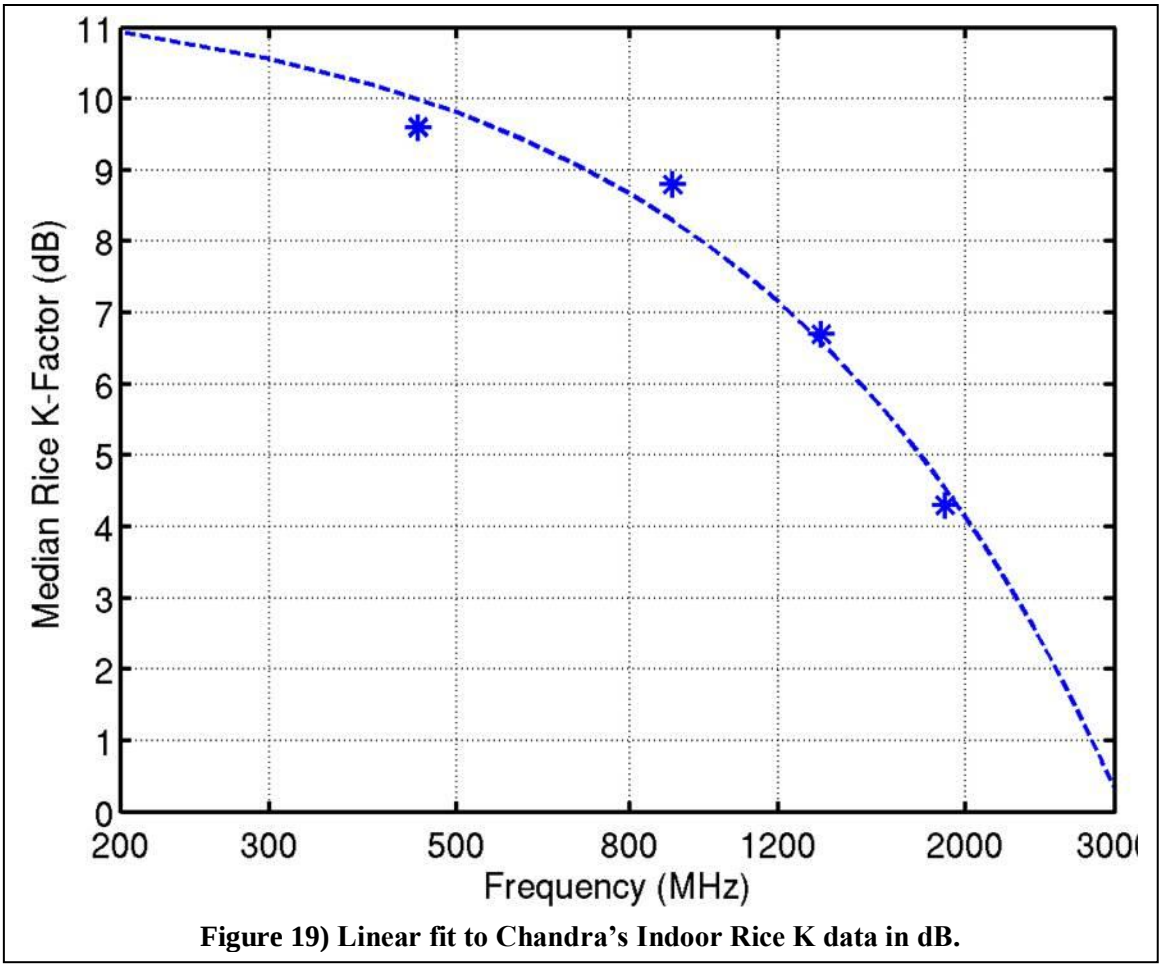

Figure 19) Linear fit to Chandra's Indoor Rice K data in dB.

Figure 19 shows the measured data and curve of eq. (3.6).

Table 2. Measured Rice K-Factor in Concrete Block Building

Frequency (MHz)	Mean K-Factor
450	9.6
900	8.8
1350	6.7
1890	4.3

The variable component of the Rice K-factor for indoor propagation was taken to be a log-normal random variable with standard deviation 4 dB.

2.2 The Total Path

When a propagation path includes an outdoor component and one or more indoor components (e.g., two indoor terminals in different buildings) K-factors are calculated seperately for each sub-path, and combined. It is more convenient to work with the ratio of specular to total power

$$\alpha = \frac{k}{k+1} \tag{3.7}$$

Each sub-path reduces the specular component of total power by a factor α_i calculated from the K-factor for that sub-path. The final ratio of specular to total power is then

$$\alpha = \prod_i \alpha_i \tag{3.8}$$

which is converted to an overall K-factor using

$$K = 10\log_{10}\left(\frac{\alpha}{1-\alpha}\right) \quad dB \tag{3.9}$$

The log-normally distributed K-factor is generated by adding a zero-mean gaussian random value to the median value in dB. Standard deviation does not depend on beamwidth [Greenstein] and is taken to equal 8 dB.

3 Shadow Loss Standard Deviation

Equation Chapter (Next) Section 1

The models for median path loss listed in Section 2, and discussed at greater length in Section 6 return a median value for the short-term average path loss. The realized short-term path loss is subject to slow fading, or shadowing, causing it to fluctuate about the median value. These fluctuations are modeled as log normally distributed. That is the loss in dB has a standard deviation with mean value equal to the median pathloss, and standard deviation found as described in this section.

Some of the pathloss models also return a value for shadowing standard deviation, others do not and shadowing standard deviation had to be found separately. When multiple pathloss models were used for a single path, for example a building penetration model followed by an outdoor propagation model, shadowing standard deviations from each model were combined as the RSS. Each model used is listed in Table 2. Some models are quite simple, for example building penetration models always assumes 4 dB shadowing standard deviation for each building.

3.1 Okumura-Sigma Model

This is the default model used for outdoor propagation, whenever the pathloss model did not return a shadowing standard deviation value. As such, it is described in some detail.

The measurements campaign [Okumura] that provided the numerical data on which the Hata model [Hata] is based, also has some data on the shadowing loss standard deviation, displayed in Figure 39 of [Okumura]. This figure shows two curves, one for an urban setting, and one that is claimed to be representative of either a suburban setting or a rural

setting with “rolling, hilly terrain’. Figure 20 shows data values read off Figure 39 of [Okumura], along with curves fit to that data. The curve fit to urban data is
Providing a mean squared error of 8.3x10^{-4}. The curve fit to suburban, or rural hilly data is

$$\sigma = 2.0 + (291 + f_{MHz})^{0,259} \tag{4.1}$$

for MSE 3.22×10^{-3}.

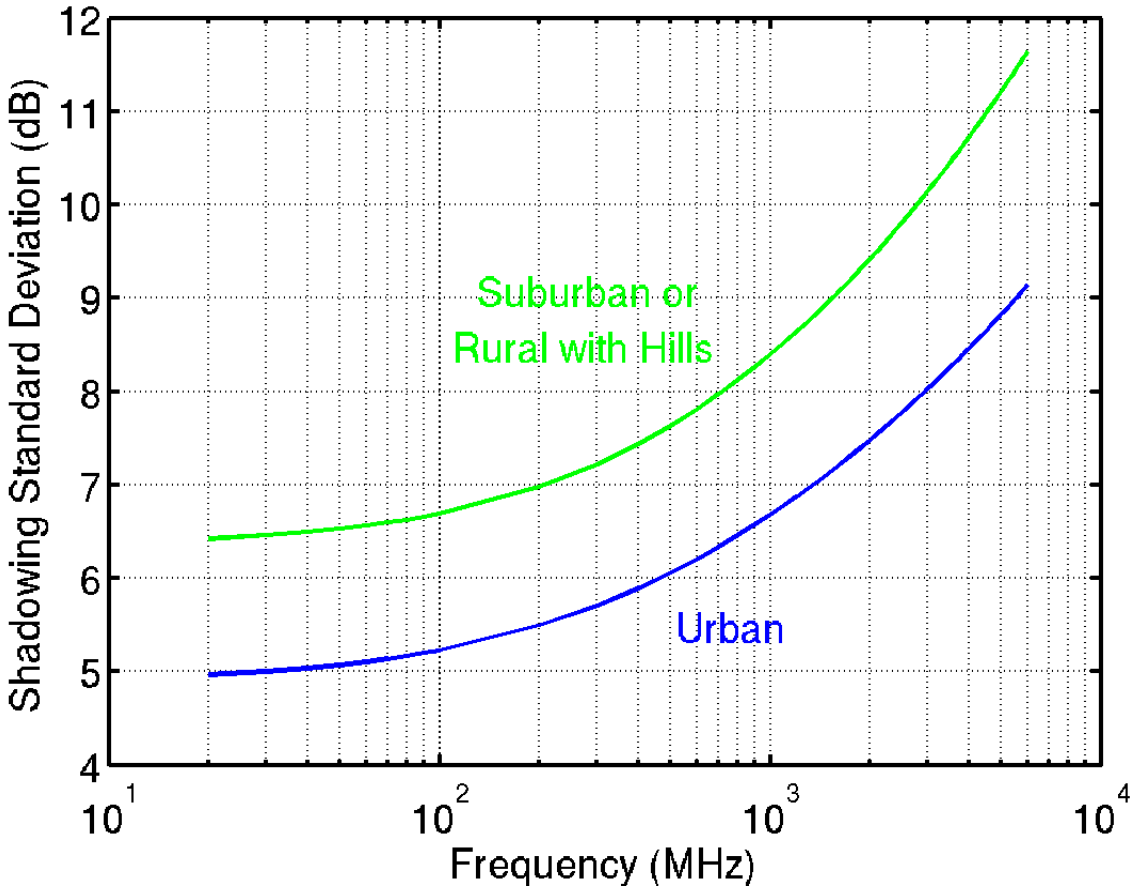

Figure 20) Shadowing standard deviation data from [okumura], with fitted curves.

The figure on which these results are based has support on the range 100 MHz to 3 GHz. The curves are approaching horizontal lines as frequency grow small, and it is expected that results are insensitive to frequency below 100 MHz, justifying extension of the fitted curves to lower frequencies. As frequency increases towards 3 GHz, curve slope increases, and so results become more sensitive to frequency. Figure 21 shows a plot of shadowing standard deviation returned by the Longley-Rice model, which is applicable in rural areas, or where buildings are not a significant cause of shadowing, but is based on data for a wider range of frequencies, and allows the user to select a parameter describing ground elevation variability. The Longley-Rice model is shown for elevation ranges (10^{th} percentile to 90^{th} percentile) of 1, 2, 5 and 10 meters. ….

Discuss standard deviation dependence on range and Rx/Tx height. Look in Hata. Also discussion in my log-normal/Pareto paper.

3.2 Other Shadow Loss Variation Models

3.2.1 The Longley Rice Model

The Longley-Rice model finds pathloss as a function of range, frequency, and various environment parameters, for a specified reliability value, where reliability is defined as the probability observed loss will not exceed the value returned by the model. The median path losses are found by setting reliability to 0.5. Path loss standard deviation is found by using the Longley-Rice model to predict the path loss with reliability 0.8413 and subtracting the median path loss from that result.

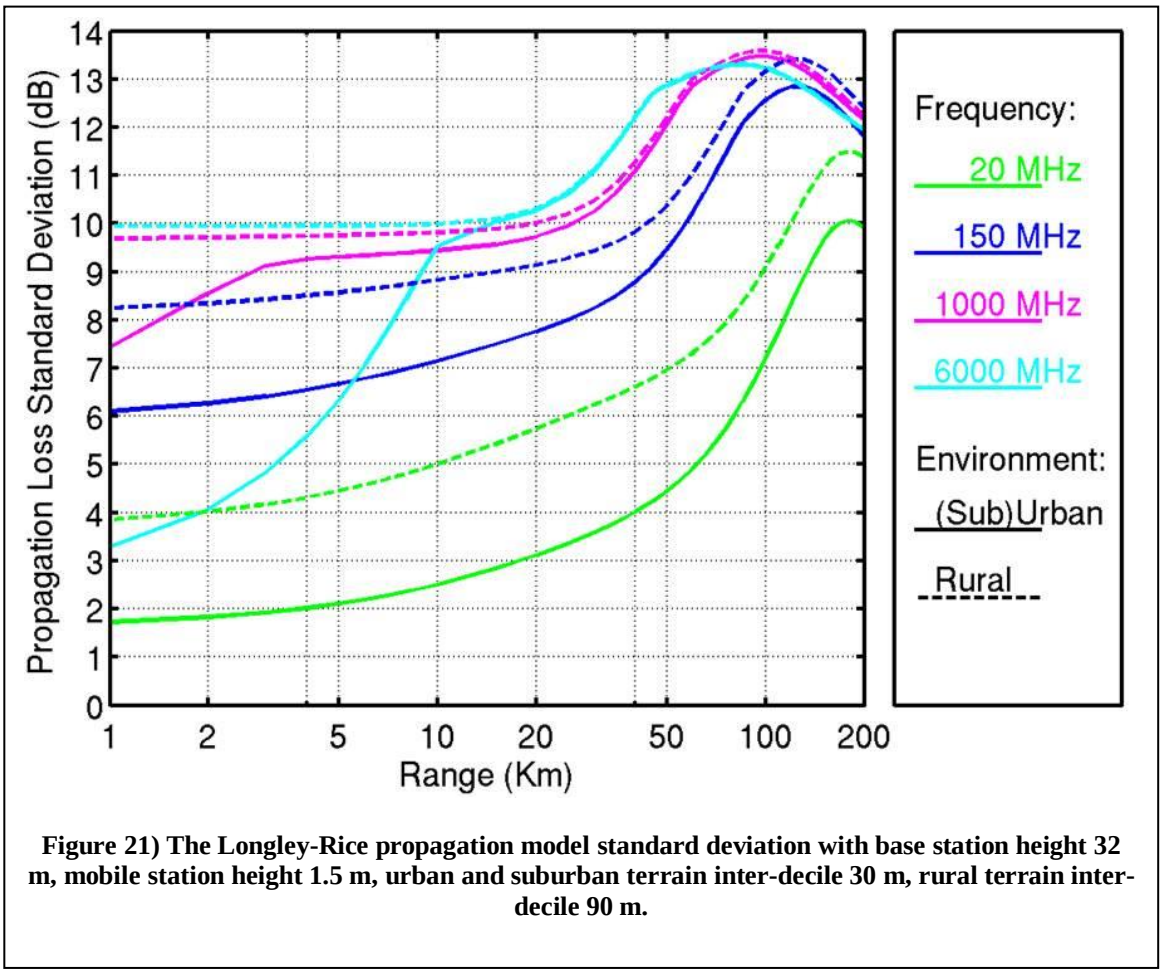

Figure 21) The Longley-Rice propagation model standard deviation with base station height 32 m, mobile station height 1.5 m, urban and suburban terrain inter-decile 30 m, rural terrain inter-decile 90 m.

Figure 21 is a plot of the pathloss standard deviation returned by the Longley-Rice model as a function of range, at different frequencies. Results are shown with terrain inter-decile 30m, used in urban and suburban settings, and inter-decile 90 m, used in rural settings. At shorter ranges where propagation is dominated by ground bounce and terrain shadowing, the 30 m results vary slowly with range. In this scenario the remote terminal disappears

over the horizon at range 25 km. Near that point the standard deviation begins to rise rapidly. At greater ranges where the dominant propagation mode is tropospheric scatter the standard deviation falls off. The exception to this overall trend is higher frequencies in a rural setting. The assumed greater terrain variation and poor diffraction at high frequencies combine to increase the standard deviation rapidly at shorter ranges.

3.2.2 The Cabot Model

The Cabot model is a simple model that finds propagation median loss and standard deviation in outdoor rural settings at ranges below 1 km, where range is too short for the Longley-Rice model, and none of the short-range urban or suburban models apply. This model finds propagation parameters by interpolating between the free space values at 10 m, and the Longley-Rice values at 1 km. Shadowing standard deviation is found using

$$\sigma = \sqrt{\frac{\log_{10} d_m - \log_{10} 10}{\log_{10} 1000 - \log_{10} 10}\ \sigma_{1000}} = \sqrt{\frac{\log_{10} d_m - 1}{29}\ \sigma_{1000}} \qquad (4.2)$$

Where d_m is the link range in meters, and σ_{1000} is the Longley-Rice shadowing standard deviation at 1 km range.

3.2.3 The Indoor Model

The indoor model assumed 4 dB shadowing standard deviation anytime the transmitter and receiver were in different rooms, including on different floors. When both antennas are in a single room the standard deviation is scaled according to

$$\sigma = 4 \times \min\left(1, \frac{r-1}{d_w - 1}\right) \quad \text{dB} \qquad (4.3)$$

Where r is the path length, and dw is the shortest distance from an antenna to one of the room walls. This results in a minimum shadowing standard deviation of 0 at 1 m (distances less than 1 m are not supported), with a maximum value of 4 dB at long ranges.

3.3 Shadowing Correlation

Accurate estimates of interference between pairs of communications links must include an estimate of the degree of correlation between shadowing losses experienced by two signal paths terminating at a common node. Figure 22 illustrates the problem. Signals emanating from the two transmitters in the upper part of this figure are both shadowed along their routes to the receiver in the lower part of the figure. Near the transmitters, the two paths are far apart and shadowing on one path is independent of shadowing on the other path. As the two paths converge at the receiver, an object shadowing one path will shadow the other path as well with increasing probability. Common obstructions on both paths results in correlated shadowing losses on the two paths.

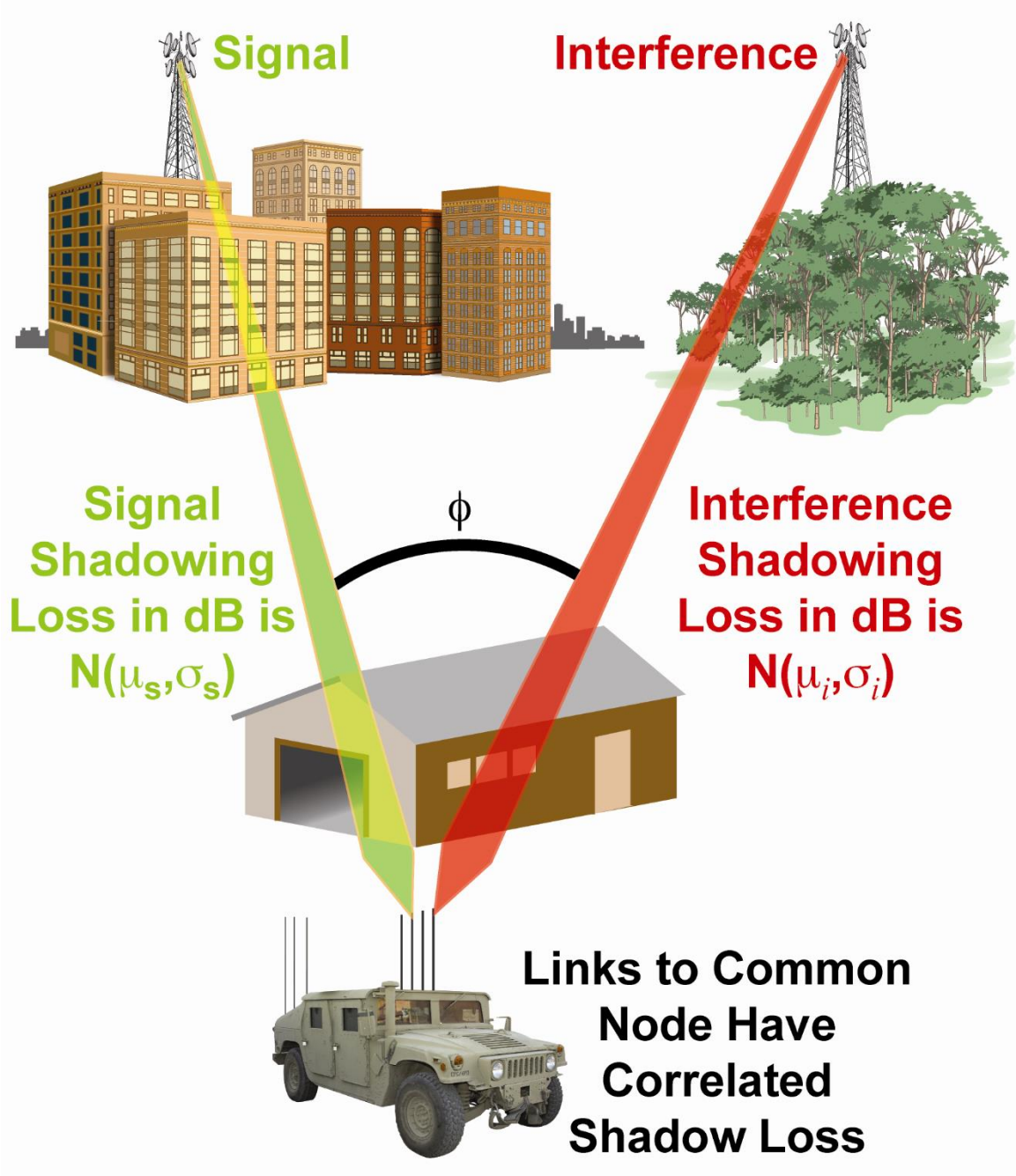

Figure 22) The origin of correlated shadowing loss on two paths with a common end-point.

The severity of interference between links is a function of the ratio of desired signal power to interfering signal power, or signal-to-interference ratio (SIR). The median value of SIR is $\mu_s - \mu_i$ dB, where μ_s and μ_i are the short-time-average signal and interference power median values in dB. The actual SIR is a random variable with a log-normal distribution, which varies about this median value. When signal and interference shadowing standard deviations are σ_s and σ_i, and shadowing correlation between the

two links is given by ρ, then SIR in dB will have a Gaussian distribution about the median value, with standard deviation

$$\sigma = \sqrt{\sigma_s^2 + \sigma_i^2 - 2\sigma_s\sigma_i\rho} \tag{4.4}$$

Figure 23 plots SIR CDF's for the case of a signal and interference with equal short-time-average mean power and different correlation coefficients. The y-axis has a Gaussian scale so the log-normally distributed ratios (normal when measured in dB) look linear. As expected with equal long-term mean power signals, the median value is always 0 dB. When shadowing loss on the signal and interference link are highly correlated, the resulting smaller SIR standard deviation produces a distribution with lower slope, i.e., the SIR is more likely to fall near its median value. As the two paths become less correlated, the distribution slope increases, showing that a particular instance of the SIR ratio is more likely to fall far from the median. This plot can be easily extended to the case where both links do not have the same short-time-average mean value by sliding the curves to the right by the difference between the desired signal and interference medians in dB. Thus, when the desired signal median is larger than the interference median, correlated shadowing reduces the probability of SIR below threshold. Conversely, if the desired signal median is smaller than the interference median, correlated shadowing increases the probability that SIR will fall below the threshold. So that a low power mobile transmitter, for which shadowing varies with time, sharing the channel with strong interference is more likely to be detected when signal and interference shadowing are uncorrelated.

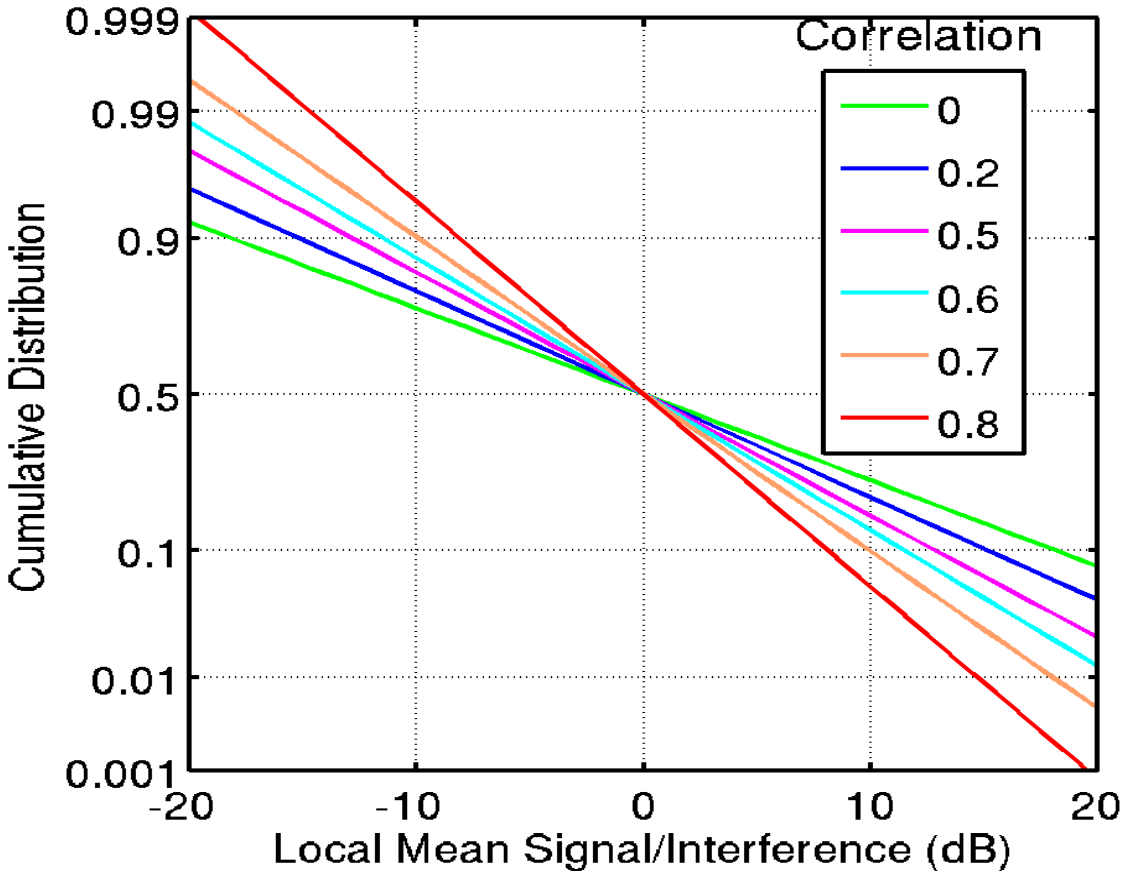

Figure 23) Cumulative distribution of SIR for equal mean-power signal and interference, parameterized by shadowing correlation coefficient.

The shadowing correlation statistics used in the llamacomm model are from [Graziano], in which a mobile receiver drove around the Washington Beltway, while measuring received power of 900 MHz signals from transmitters at three different remote sites.

Figure 24is a plot of the measured data from [Graziano] along with a bilinear approximation to that data. The approximation used is

$$\rho = \begin{cases} 0.75 - 0.004\Delta\Phi & |\Delta\Phi| \le 90^\circ \\ 0.004 & 90^\circ < |\Delta\Phi| \le 180^\circ \end{cases} \tag{4.5}$$

This model resulted in the smallest mean-square error of the several different curve types used to fit this data, including an exponential model, and a raised cosine model as suggested in [Fabio]. The correlation does not approach 1 as the link angular separation approaches 0 because it is assumed that even with identical azimuth angles the two links are not identical, e.g. the two remote nodes are at different ranges and elevations, so that some shadowing components are not common to both links.

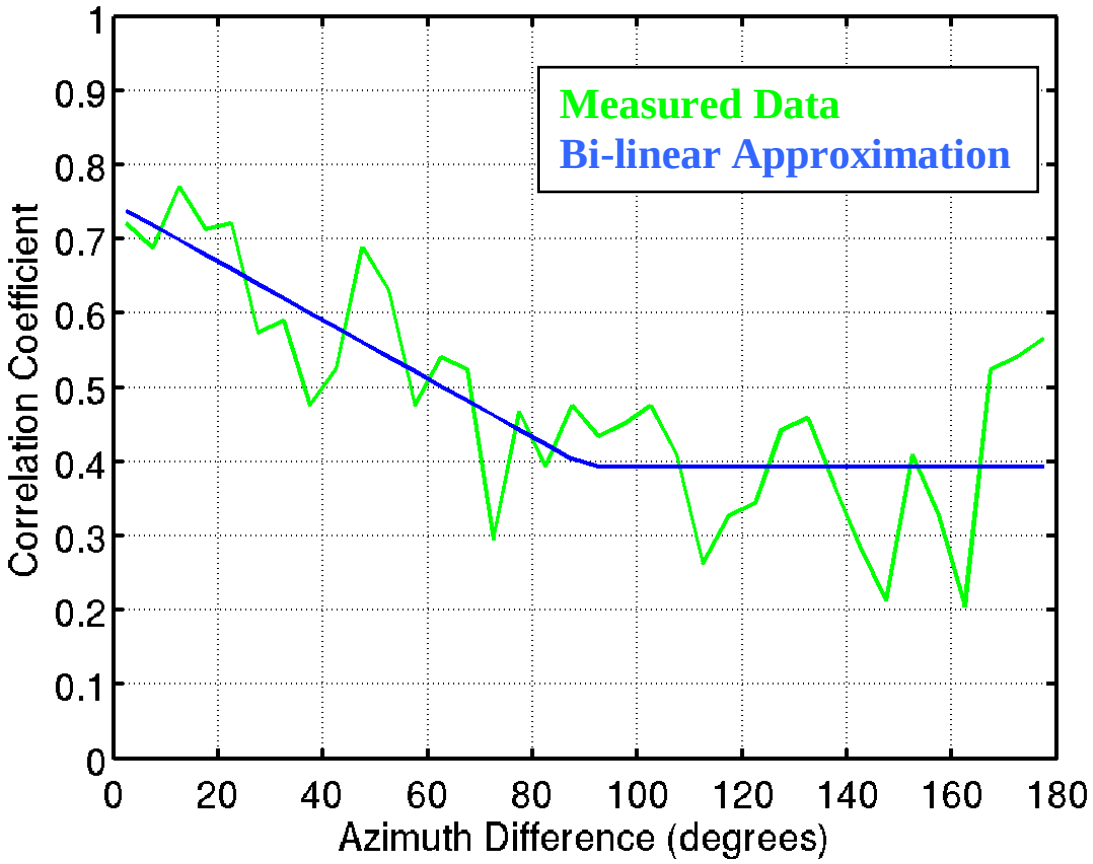

Figure 24) Shadowing correlation coefficient versus difference in transmitter azimuth angle at common receiver.

One possible explanation for this bi-linear function is that the constant correlation at greater angles represents the correlation due to similarity of the environment in all directions, caused by, for example, the tendency for buildings in a neighborhood to be similar in height. The linearly increasing correlation as angular separation declines represents the increasing likelihood that both radio links are blocked by a common obstruction.

The llamacomm simulation package uses the shadow-loss covariance matrix to generate an instance of shadow loss values during simulation. In order to do this, the simulated radio links are ordered in an arbitrary way, as illustrated in Figure 25a. This figure shows a collection of five nodes. Link 1, in green, is the communications link of interest, and links 2-6, in red, are interference to the communicating nodes. In general assume there are N links to be modeled. The covariance matrix R with elements ρ_{ij} can be filled in with ones one the main diagonal (i=j), and values given by eq. 4.5 for pairs of links that share a common end-point, such as links 1 and 2 in Figure 25a. Pairs of links without a common end-point also non-zero correlation. For example, links 2 and 4 are both correlated with link 1. A simple model of this relationship would be to set the shadowing loss on link 2 to

$$L_2 = \sigma_2 \left(\sqrt{1-\rho_{12}^2}\ \alpha_2 + \rho_{12} \left(L_1 - \mu_1 \right) / \sigma_1 \right) + \mu_2 \quad dB \tag{4.6}$$

and on link 4 to

$$L_4 = \sigma_4 \left(\sqrt{1-\rho_{14}}\ \alpha_4 + \rho_{14} \left(L_1 - \mu_1 \right) / \sigma_1 \right) + \mu_4 \quad dB \tag{4.7}$$

with α_i a unit-normal random variable which is independent of the loss on link 1, and L_1 the random shadowing loss term for link 1. The two resulting shadow loss terms will then have the desired means, standard deviations, and covariances with link 1. They will also have a non-zero covariance with each other

$$\rho_{24} = \frac{E\left\{ \left(L_2 - \mu_2 \right) \left(L_4 - \mu_4 \right) \right\}}{\sigma_2 \sigma_4} \quad = \quad \rho_{12}\rho_{14} \tag{4.8}$$

This approach is not generally applicable, however, as for example links 2 and 4 share a similar relationship with both links 6 and 3, and it is typically not possible to have $\rho_{24} = \rho_{12}\rho_{14}$, $\rho_{24} = \rho_{23}\rho_{34}$ and $\rho_{24} = \rho_{26}\rho_{46}$ at the same time.

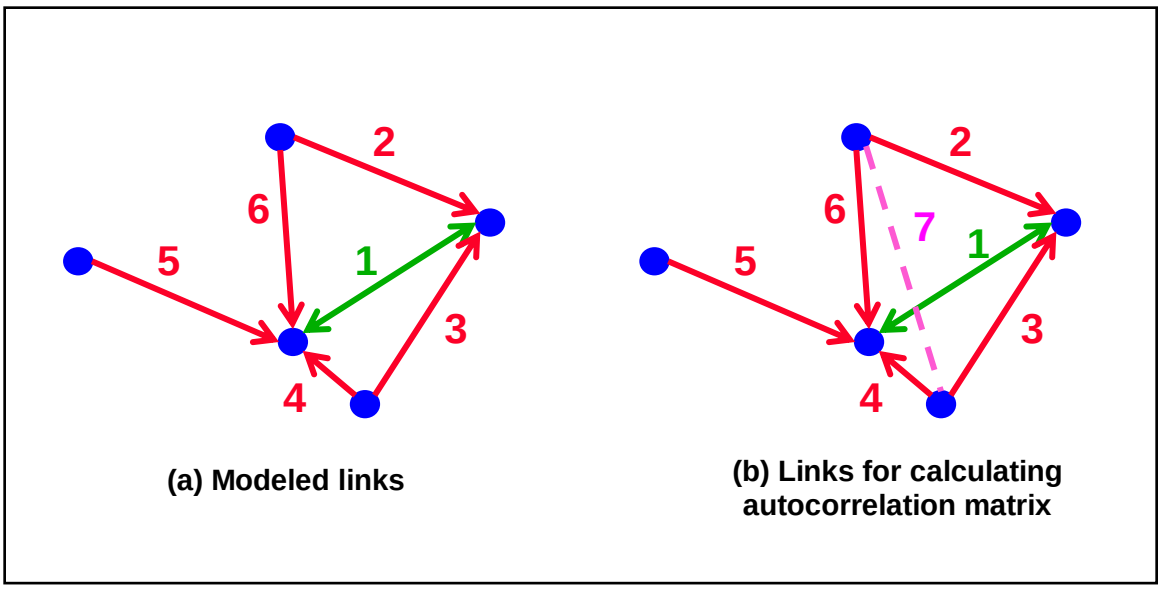

Figure 25) Shadowing autocorrelation approximation.

The autocorrelation between two links that do not share a common endpoint is approximated by the average of products of covariances between the two links of interest, and each of the possible four links connecting an end-point of one link to an end-point of the other. In the example here

$$\rho_{24} = \frac{\rho_{12}\rho_{14} + \rho_{13}\rho_{34} + \rho_{16}\rho_{64} + \rho_{17}\rho_{74}}{4} \tag{4.9}$$

Note that link 7 of this example is not a link being simulated. However, its covariance with links 2 and 6 is easily calculated in the same was as for those links that are being simulated, based on the azimuth differences between link paths.

When using this approximation it is possible that the resulting covariance matrix may not be positive definite. When that happens, the matrix must be diagonal-loaded to create a positive definite matrix

$$R' = \frac{R + \delta I}{1 + \delta} \tag{4.10}$$

The initial value of δ used is 0.05, then δ is incremented by 0.05 and the operation repeated until the covariance becomes positive definite.

4 Background Noise

Equation Chapter (Next) Section 1

External noise into a receiver is a combination of man-made external noise and thermal radiation from objects in-view of the antenna, e.g., the ground, buildings, etc. The external noise is modeled as white Gaussian noise, described by a man-made noise figure which gives noise density (power per Hertz) in dB relative to thermal noise at 290 Kelvins. The man-made noise figure depends on environment and frequency according to [ITU372]:

$$F_m = \begin{cases} 67.2 - 27.7\log_{10} f_{MHz} & \textit{rural area} \\ 72.5 - 27.7\log_{10} f_{MHz} & \textit{residential area} \\ 76.8 - 27.7\log_{10} f_{MHz} & \textit{business area,} \quad f_{MHz} \le 129 \\ 44.3 - 12.3\log_{10} f_{MHz} & \textit{business area,} \quad f_{MHz} > 129 \end{cases} \tag{5.1}$$

External thermal noise is represented by restricting the noise figure to a minimum value of 0 dB. Figure 26 shows the external noise figures used as a function of frequency.

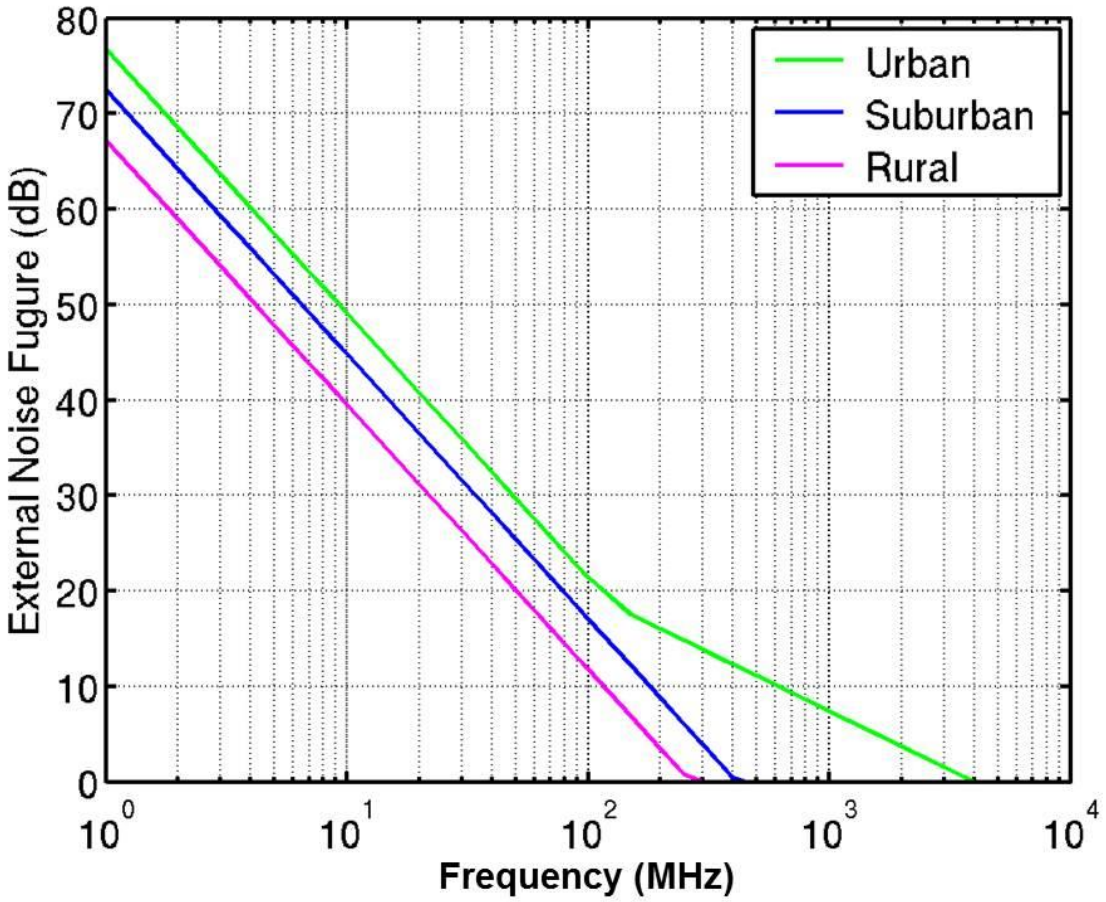

Figure 26) External noise model.

5 Outdoor Pathloss Models

Equation Chapter (Next) Section 1

Where possible, the Llamacomm propagation model was constructed by combining existing pathloss models. Most of these models are based on extensive measurement campaigns that would be costly and time consuming to reproduce. The following sections give a brief description of the various models used.

5.1 The Mean Two-Path Model

The mean two-path model is used at very short ranges where propagation is line-of-sight, but multipath reflections may be an issue. The slant-path in meters is given by

$$r_m = \sqrt{d_m^2 + (h_1 - h_2)^2} \quad \text{m} \tag{6.1}$$

Where d_m is the ground range and h_1 and h_2 are antenna heights above ground, all in meters. The range difference between the direct path and a single ground bounce path is

$$\Delta r = \sqrt{d_m^2 + (h_1 + h_2)^2} - r_m \tag{6.2}$$

And the path elevation angle at the reflection point is

$$\psi = \tan^{-1}\left(\frac{h_1 + h_2}{d_m}\right) \tag{6.3}$$

The reflection coefficient is found at the reflection point using [Parsons]

$$\rho = \begin{cases} \dfrac{(\varepsilon_r - jx)\sin\psi - \sqrt{(\varepsilon_r - jx) - \cos^2\psi}}{(\varepsilon_r - jx)\sin\psi + \sqrt{(\varepsilon_r - jx) - \cos^2\psi}} & \text{Vertical Polarization} \\ \dfrac{\sin\psi - \sqrt{(\varepsilon_r - jx) - \cos^2\psi}}{\sin\psi + \sqrt{(\varepsilon_r - jx) - \cos^2\psi}} & \text{Horizontal Polarization} \end{cases} \tag{6.4}$$

where

$$x = \frac{\sigma}{\omega\varepsilon_0} = \frac{18{,}000\sigma}{f_{MHz}} \tag{6.5}$$

is the normalized ground conductivity. Llamacomm uses ground electrical parameter values considered typical for average quality ground: $\varepsilon_r = 15$ for the relative dielectric constant; and $\sigma = 0.005$ Siemens for ground conductivity.

At short ranges loss is found directly. At longer ranges where destructive interference between the direct and ground bounce paths causes frequent nulls, loss is averaged over a small range of distances. The resulting loss calculation is

$$L = \begin{cases} 20\log_{10}\left(\dfrac{4\pi r_m}{\lambda}\right) - 10\log_{10}\left(\left|1 + \rho e^{-j2\pi\Delta r/\lambda}\right|^2\right) & \Delta r < \dfrac{\lambda}{4} \\ 20\log_{10}\left(\dfrac{4\pi r_m}{\lambda}\right) - 10\log_{10}\left(1 + |\rho|^2\right) & \Delta r < \dfrac{\lambda}{4} \end{cases} \tag{6.6}$$

where λ is wavelength in meters.

5.2 The Okumure-Hata Model

The Okumura-Hata model is based on an extensive set of measurements by Okumura [Okumura] of mobile radio propagation losses in Japan. The environments measured range from rural to densely built-up urban areas. All links measured had one antenna mounted above surrounding obstructions, and one antenna at street level. In the Okumura-Hata model these nodes are referred to as the base station (BS) and the mobile station (MS), respectively.

Hata subsequently fit curves to Okumura's data over a restricted region of the operating parameters [Hata]. Parameter ranges for the basic Hata model are listed in Table 4.

Table 4. Okumura-Hata Model Operating Parameter Range

Parameter	Minimum	Maximum
Frequency	150 MHz	1500 MHz
Range	1 km	10 km
BS Height	30 m	200 m
MS Height	1 m	10 m

The measured data were classified into four different environment types, listed in Table 5, each producing a slightly different curve fit.

Table 5 Okumura-Hata Model Environments

Environment	Description
Rural	Open, few or no buildings
Suburban	Not defined
Low-Density Urban	Moderately dense buildings less than 15 m average height
Urban	Moderately dense buildings more than 15 m averag height

All four environments begin with Hata's basic urban loss term

$$L_U = 69.55 + 26.16\log_{10}(f_{MHz}) - 13.82\log_{10}(h_{bm}) - ahm + \left[44.9 - 6.55\log_{10}(h_{bm})\right]\log_{10}(d_{km}) \quad (6.7)$$

where

- f_{MHz} is carrier frequency, in MHz
- h_{bm} is base station height above mean ground level, in meters
- d_{km} is the link ground range, in km and
- ahm is a building height correction factor that depends on the environment, carrier frequency, and mobile station height

$$ahm = \begin{cases} 8.29 \log_{10}\left(1.54 h_{mm}\right)^2 - 1.1 & \textit{Urban}, \quad f_{MHz} \le 200 \\ 3.2 \log_{10}\left(11.75 h_{mm}\right)^2 - 4.97 & \textit{Urban}, \quad f_{MHz} > 200 \\ \left(1.1 \log_{10}\left(f_{MHz}\right) - 0.7\right) h_{mm} - 1.56 \log_{10}\left(f_{MHz}\right) + 0.8 & \textit{Otherwise} \end{cases} \quad (6.8)$$

Where h_{mm} is the mobile station height above mean ground level, in meters. Eqs. (6.7) and (6.8) are sufficient to describe shadowing and range loss in an urban or low-density urban environment. Additional correction factors are required for the other two environments. The suburban correction factor is

$$K_r = 2 \log\left(\frac{f_{MHz}}{28}\right)^2 + 5.4 \quad (6.9)$$

The rural correction factor is

$$Q_r = 4.78 \log_{10}\left(f_{MHz}\right)^2 - 18.33 \log_{10}\left(f_{MHz}\right) + 40.94 \quad (6.10)$$

And the final propagation loss value returned by this model is

$$L_{Hata} = \begin{cases} L_U & \textit{Urban \& Low Density Urban} \\ L_U - K_r & \textit{Suburban} \\ L_U - Q_r & \textit{Rural} \end{cases} \quad (6.11)$$

In Llamacomm, this model is implemented by the function hata.m, with arguments range, frequency, mobile and base station height, and environment.

Figure 27 is a plot of the Okumura-Hata model pathloss versus range for different environments and frequencies. The two urban models are very close for the selected mobile station height of 1.5 m, and only the low-density urban pathloss is plotted.

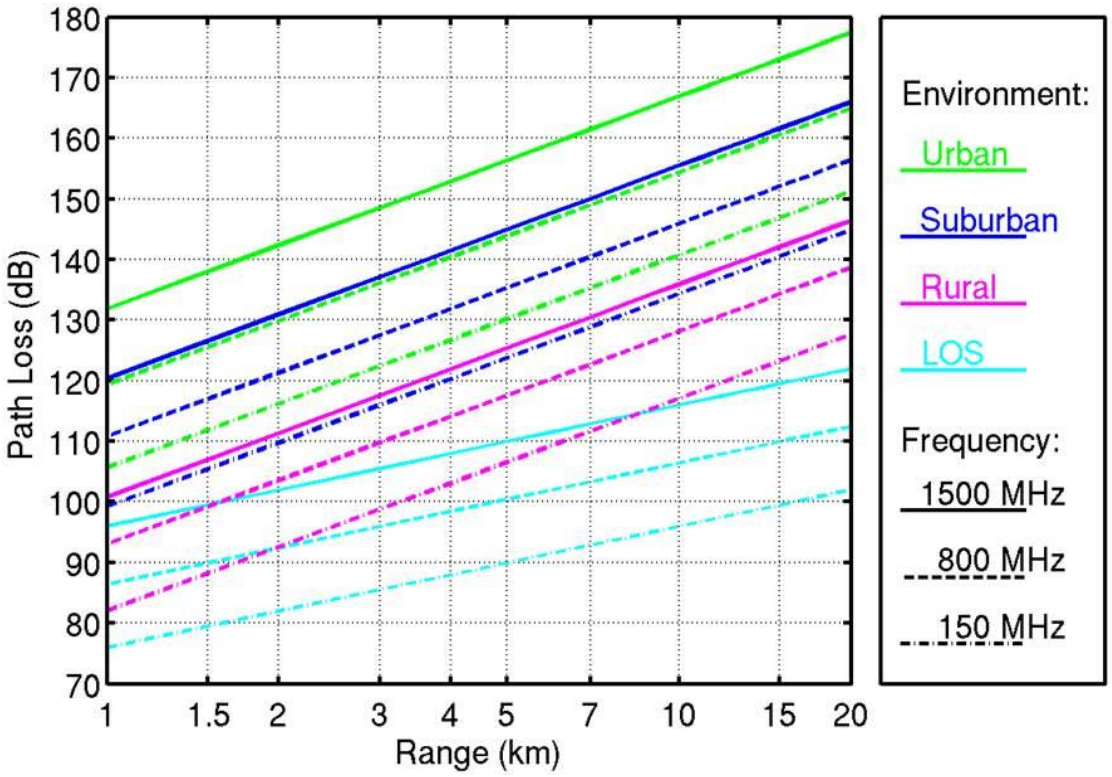

Figure 27) The Okumura-Hata propagation model, base station height 32 m, mobile station height 1.5 m.

5.3 Okumura-Hata Model with COST-231 Frequency Extensions

The COST-231 (COoperation europeenne dans le domain de la recherche Scientifique et Technique, action 231) committee developed an extension to the Okumura-Hata propagation model for operation at higher carrier frequencies [COST231]. As before, all measurements were taken with the base station antenna above surrounding obstructions, which the COST-231 committee defined as having no obstructions at or above antenna height within a distance of 100-200 m of the base station antenna. The parameter ranges supported by the extended model are listed in Table 6. The frequency range is from the maximum frequency of the original Hata model to 2 GHz, otherwise parameters are unchanged.

Table 5. Okumura-Hata Model with COST-231 Extensions, Operating Parameter Range

Parameter	Minimum	Maximum
Frequency	1500 MHz	2000 MHz
Range	1 km	20 km
BS Height	30 m	200 m
MS Height	1 m	10 m

The COST-231 measurements on which the model is based are classified into two categories, Urban and Dense urban. Category descriptions vary slightly from the basic Okumura-Hata model, and are described in Table 7. Based on their descriptions, the Hata-Cost231 Urban environment appears to be equivalent to the Okumura-Hata Low-Density Urban environment. And the Hata-Cost231 Dense Urban environment appears to be equivalent to, or more severe than the Okumura-Hata Urban environment. The Okumura-Hata suburban and rural corrections were retained in this implementation of the model to allow for non-urban settings.

Table 7. Okumura-Hata Model with COST-231 Extensions, Environments

Environment	Description
Rural	Open, few or no buildings
Suburban	Not defined
Urban	Small city or suburb with lots of trees
Dense Urban	Urban center

The extended-frequency-range version of the basic propagation loss in urban settings is

$$\begin{aligned} L_{LU} \quad = \quad & 46.3 + 33.9\log_{10}\left(f_{MHz}\right) - 13.82\log_{10}\left(h_{bm}\right) - \\ & ahm + \left[44.9 - 6.55\log_{10}\left(h_{bm}\right)\right]\log_{10}\left(d_{km}\right) \end{aligned} \tag{6.12}$$

where

- f_{MHz} is carrier frequency, in MHz
- h_{bm} is base station height above mean ground level, in meters
- d_{km} is the link ground range, in km, and
- ahm is a building height correction factor that depends on the environment, carrier frequency, and mobile station height

The building height correction factor is given by

$$ahm = \left(1.1\log_{10}\left(f_{MHz}\right) - 0.7\right)h_{mm} - \left(1.56\log_{10}\left(f_{MHz}\right) - 0.8\right) \tag{6.13}$$

This version of the model adds a 3 dB correction factor for operation in the dense urban environment. The Hata correction factors have been retained for the suburban setting

$$K_r = 2\left(\log_{10}\left(\frac{f_{MHz}}{28}\right)\right)^2 + 5.4 \tag{6.14}$$

and the rural setting

$$Q_r = 4.78\left(\log_{10}\left(f_{MHz}\right)\right)^2 - 18.33\log_{10}\left(f_{MHz}\right) + 40.94 \tag{6.15}$$

The resulting total loss is

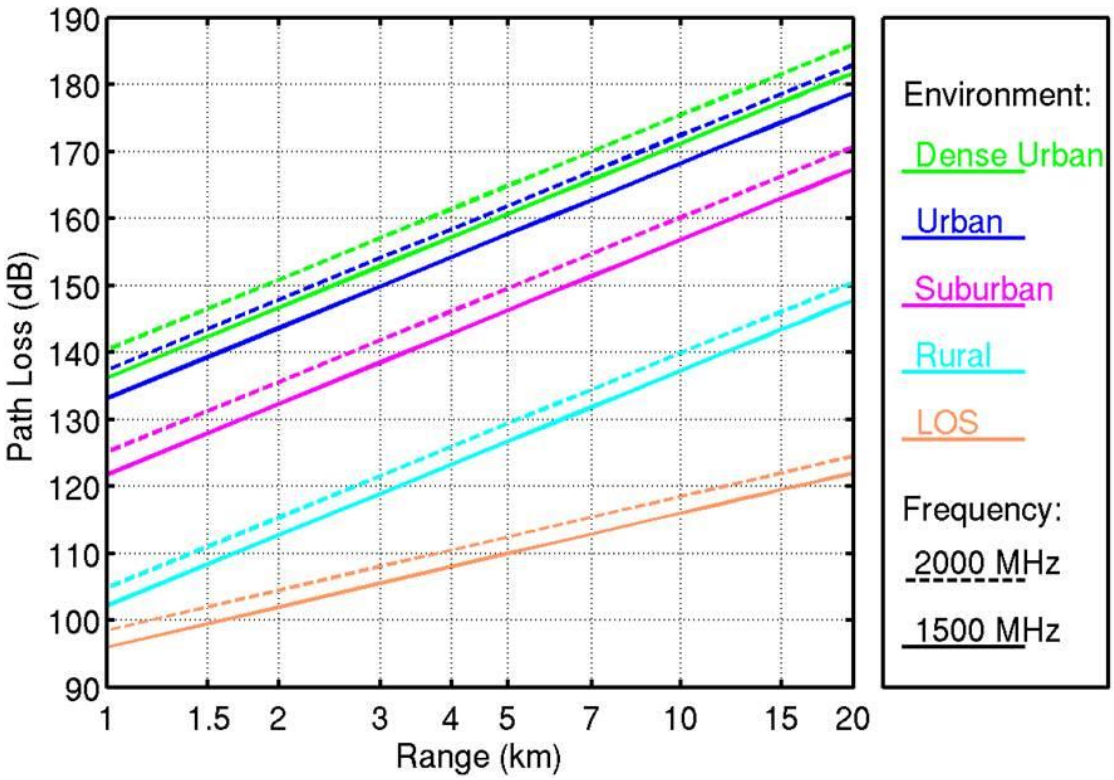

Figure 28) The Okumura-Hata propagation model with the COST-231 frequency extension, base station height 32 m, mobile station height 1.5 m.

$$L_{Hata-Cost} = \begin{cases} L_{LU} + 3 & Dense\,Urban \\ L_{LU} & Urban \\ L_{LU} - K_r & Suburban \\ L_{LU} - Q_r & Rural \end{cases} \tag{6.16}$$

In Llamacomm, this model is implemented by the function hata_cost.m, with arguments range, frequency, mobile and base station height, and environment.

Figure 28 is a plot of the Okumura-Hata model with the COST-231 frequency extension. Observe that the 1500 MHz curve is slightly higher than that of the original Okumura-Hata model.

5.4 Cost-231 Walfisch-Ikegami Model

A useful model for range dependent shadowing loss in urban and dense suburban settings is the COST-231 Walfisch-Ikegami model [Cost-231], sometimes referred to as the COST-231 model. This model is useful when buildings are close together and both antennas are below roof height, e.g. an urban micro-cell. Unlike the Okumura-Hata model, or the extended Hata-Cost231 model, it provides support at ranges as low as 20 m.

This model is based on semi-analytic models described in [Walfisch,Ikegami]. It is nearly as accurate as the Okumura-Hata model in situations where both are applicable, but does not perform well when the higher terminal is close to roof height [Low]. This are actually two COST-231 Walfisch-Ikegami models, a line-of-sight model for street-level propagation in urban canyons, and a non-line-of-sight model that assumes propagation over roof tops. Only the non-line-of-sight model is used here.

The COST-231 Walfisch-Ikegami model has been tested and found reasonably accurate over parameter ranges in Table8 [COST-231,Low]. In particular it works well when the "settled field distance" $d_s<1$ [COST-231]

$$d_s = \frac{\lambda\left(d_{km}/1000\right)^2}{\left(h_{bm}-h_{rm}\right)^2} \tag{6.17}$$

Where

- d_{km} is link range in km
- λ is the wavelength in m
- h_{bm} is base station antenna height in m
- h_{rm} is the average roof height in m

Table8. COST-231 Walfisch-Ikegami Operating Parameter Range

Parameter	Minimum	Maximum
Frequency	800 MHz	2000 MHz
Range	20 m	5 km
BS Height	4 m	50 m
MS Height	1 m	3 m

Input parameter for the COST-231 Walfisch-Ikegami model are listed in Table 9. The input parameters b_m, w_m, and φ_{deg}, which describe building and street locations relative to the link, are set to the recommended default values listed in Table when used in the Llamacomm model. The suburban environment is recommended for use in both suburban setting with many trees, and in medium size cities, or outside the city center.

Table 9. Walfisch-Ikegami Model Input Parameters

Parameter	Units	Description	Default
d_{km}	km	range between terminals	N/A
f_{MHz}	MHz	frequency	N/A
h_{bm}	m	base station antenna height	N/A
h_{mm}	m	mobile station antenna height	N/A
h_{rm}	m	average roof height	N/A
b_m	m	distance between buildings	35
w_m	m	street width	$b_m/2$
$\phi_{\deg}$	degrees	angle between street and line connecting terminals	45

env	N/A	environment flag: 0=suburban, 1=metro center	1

Typical values for average roof height are 3 times the number of floors, plus an extra 3 m if the roof slopes. The distance between buildings in an urban setting is typically 20 to 50 m. φ_{deg} varies from 0 to 90 degrees, where 90 degrees is the worst case.

Using the COST-231 Walfisch-Ikegami model, the median loss in dB due to range and shadowing is written as

$$L_{CWI} = \begin{cases} L_0 + L_{rts} + L_{msd} & L_{rts} + L_{msd} > 0 \\ L_0 & \textit{otherwise} \end{cases} \tag{6.18}$$

where L_0 is the free space loss

$$L_0 = 32.4 + 20\log_{10} d_{km} + 20\log_{10} f_{MHz} \tag{6.19}$$

L_{rts} describes ``rooftop to street screening''

$$L_{rts} = \max\left(0,\ -16.9 - 10\log_{10} w_m + 10\log_{10} f_{MHz} + 20\log_{10}\left(h_{rm} - h_{mm}\right) + L_{ori}\right) \tag{6.20}$$

which depends on street orientation with respect to the propagation path as

$$L_{ori} = \begin{cases} -10 + 0.354\phi_{\text{deg}} & \left|\phi_{\text{deg}}\right| < 35° \\ 2.5 + 0.075\left(\phi_{\text{deg}} - 35\right) & 35° \le \left|\phi_{\text{deg}}\right| \le 55° \\ 4.0 - 0.114\left(\phi_{\text{deg}} - 55\right) & 55° \le \left|\phi_{\text{deg}}\right| \le 90° \end{cases} \tag{6.21}$$

The final term is due to ``multi-screen diffraction'', and is given by

$$L_{msd} = L_{bsh} + k_a + k_d \log_{10} d_{km} + k_f \log_{10} f_{MHz} - 9.0\log_{10} b_m \tag{6.22}$$

which has a range-independent base station height term

$$L_{bsh} = \begin{cases} -18.0\log_{10}\left(1 + h_{bm} - h_{rm}\right) & h_{bm} > h_{rm} \\ 0 & \textit{otherwise} \end{cases} \tag{6.23}$$

and two range-dependent base station height terms

$$k_a = \begin{cases} 54.0 & h_{bm} > h_{rm} \\ 54.0 - 0.8(h_{bm} - h_{rm}) & h_{bm} \le h_{rm} \quad \& \quad d_{km} \ge 0.5 \\ 54.0 - 0.8(h_{bm} - h_{rm}) & h_{bm} \le h_{rm} \quad \& \quad d_{km} < 0.5 \end{cases} \tag{6.24}$$

as well as

$$k_d = \begin{cases} 18.0 & h_{bm} > h_{rm} \\ 18.0 - 15.0\dfrac{h_{bm} - h_{rm}}{h_{rm}} & h_{bm} \le h_{rm} \end{cases} \tag{6.25}$$

and an environment-specific frequency term

$$k_f = \begin{cases} -4.0 + 0.7\left(\frac{f_{MHz}}{925} - 1\right) & env = 0 \\ -4.0 + 1.5\left(\frac{f_{MHz}}{925} - 1\right) & env = 1 \end{cases} \tag{6.26}$$

Figure 29 shows a plot of the Walfisch-Ikegami model in urban and suburban settings. The Walfisch-Ikegami line-of-sight model is also shown for comparison. Not that this LOS model includes the effects of multipath in a setting with many reflectors, and is not the free space model used in the previous two sections for line-of-sight propagation.

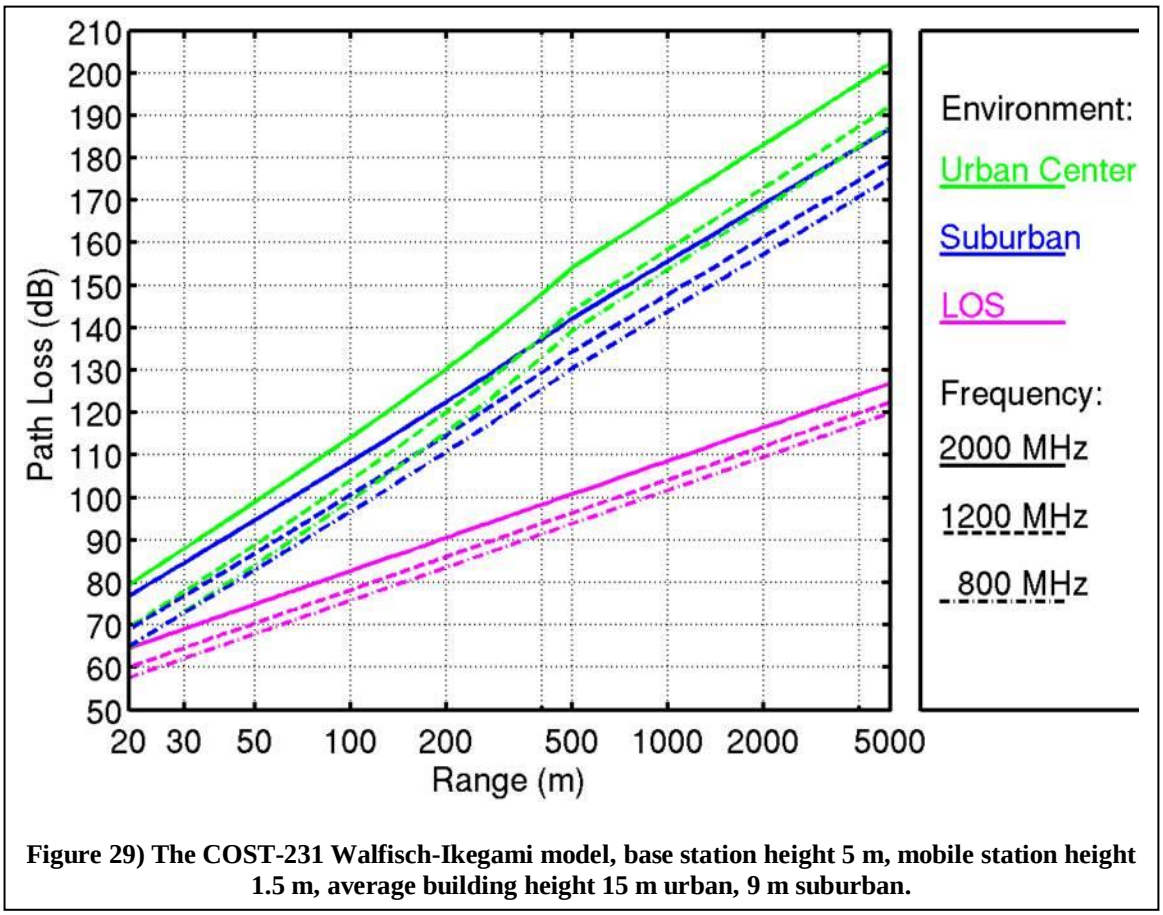

Figure 29) The COST-231 Walfisch-Ikegami model, base station height 5 m, mobile station height 1.5 m, average building height 15 m urban, 9 m suburban.

5.5 The Longley-Rice Area Coverage Model

The Longley-Rice Area-Coverage model [Hufford], formally known as the ITS Irregular Terrain Model, is based on an extensive series of measurements performed by the National Telecommunications and Information Administration (NTIA) Institute for Telecommunication Studies (ITS). It includes the effects of ground reflection, diffraction over terrain obstacles and over the horizon, and atmospheric refraction (atmospheric

scattering). It does not include propagation losses due to buildings, and is best for rural settings when used without the correction factors described in subsequent sections. The measurements on which it is based were taken in arid regions where trees are sparsely distributed, and it does not accurately reflect loss due to foliage. The model does not include ionospheric reflections, another source if inaccuracy at frequencies below 50 MHz.

The different sources of propagation loss (or transmission in the case of atmospheric scattering over the horizon) were modeled analytically, then combined with empirically determined weights. The resulting model is complex, and will not be reprinted here, but is available at [NTIA] along with documentation. The original Fortran code available at [NTIA] was converted to Matlab, to simplify integration into the Llamacomm model.

Parameter ranges supported by the Longley-Rice model are listed in Table10. The right column of this table shows the default values used by Llamacomm. Those listed as variable are extracted from the node or environment objects, as applicable. Terrain irregularity is the interdecile[4] ground elevation along a typical radio path in the coverage area. The default value used is typical of flat regions such as the great plains of the central US. The ground electrical parameters used are typical values for average quality soil. The siting variable is specified separately for each node. Both nodes are set to Random siting, which means the terminal is equally likely to be anywhere in the coverage region without regard to ground elevation. The mode setting determines how the specified reliability and confidence levels are incorporated into the calculations. Longley-Rice uses reliability to indicate the variation in propagation loss that would be expected to occur over the ensemble of radio links under study, and confidence describes other sources of variability that determine how likely a particular setting is to conform to the model used. For example, a 50% reliability level means 50% of links in the region modeled are predicted to have lower propagation loss than the returned value. A 50% percent confidence level means 50% of regions modeled with the particular set of parameters selected will perform as well as or better than the modeled propagation-loss and reliability indicate. The mode setting determines whether variability from different sources contributes to reliability or confidence. The mobile mode was selected to model fixed but unknown location targets because it includes both time variability (due to tropospheric scattering) and location variability as factors contributing to reliability. Both confidence and reliability were set to 50% to return propagation loss median values. Other values of reliability are used as described below to calculate the shadowing loss standard deviation.

Table 10. Longley-Rice Area Coverage Parameters

Parameter	Supported Range	Value Used
Frequency	20 MHz – 20 GHz	Variable
Ground Range	1 – 2000 km	Variable
Antenna Heights	0.5 m – 3 km	Variable
Polarization	Vertical,	Variable

[4] Difference between the 90th and 10th percentile values.

	Horizontal	
Mean Ground Elevation	No Limits Given	0 m
Terrain Irregularity	No Limits Given	30 m urban, suburban 90 m rural
Ground Relative Permittivity	No Limits Given	15
Ground Conductivity	No Limits Given	0.005 Siemens/m
Climate	Equatorial Continental Subtropical Maritime Subtropical Desert Continental Temperate Maritime Temperate Over Land Maritime Temperate Over Sea	Continental Temperate
Siting Criteria	Random Careful Very Careful	Random Random
Mode	Single Use Fixed Mobile Broadcast	Mobile
Reliability	0.1 – 99.9%	50%
Confidence Level	0.1 – 99.9%	50%

The Longley-Rice model calculates excess propagation loss. The realization used in LLamacomm has been modified by adding in the free space loss, to get total median loss.

The Longley-Rice model is not intended to model air-to-ground propagation, but is considered reliable for broadcast channels with transmitters elevated up to 3 km above the surrounding mean ground level. However, when a ground-to-air link elevation angle exceeds 10 degrees, the predicted median loss may be larger than it should be.

Figure 30 is a plot of Longley-Rice plus free space path loss versus range. Free space loss is also plotted alone for comparison. Both vertical and horizontal polarization results are shown. At higher frequencies vertically and horizontally polarized signals experience virtually identical path loss. At 150 MHz, horizontally polarized signals suffer about 3 dB greater path loss, and at 20 MHz the difference is about 10 dB. The slope of path loss curves plotted against the log of range varies as the loss mechanism changes, from ground-bounce at very short ranges, to diffraction over hills, then over the horizon. The most noticeable change occurs at very long ranges when the dominant transmission path changes from diffraction over the horizon to tropospheric scatter.

5.5.1 The Longley-Rice Urban Correction Factor

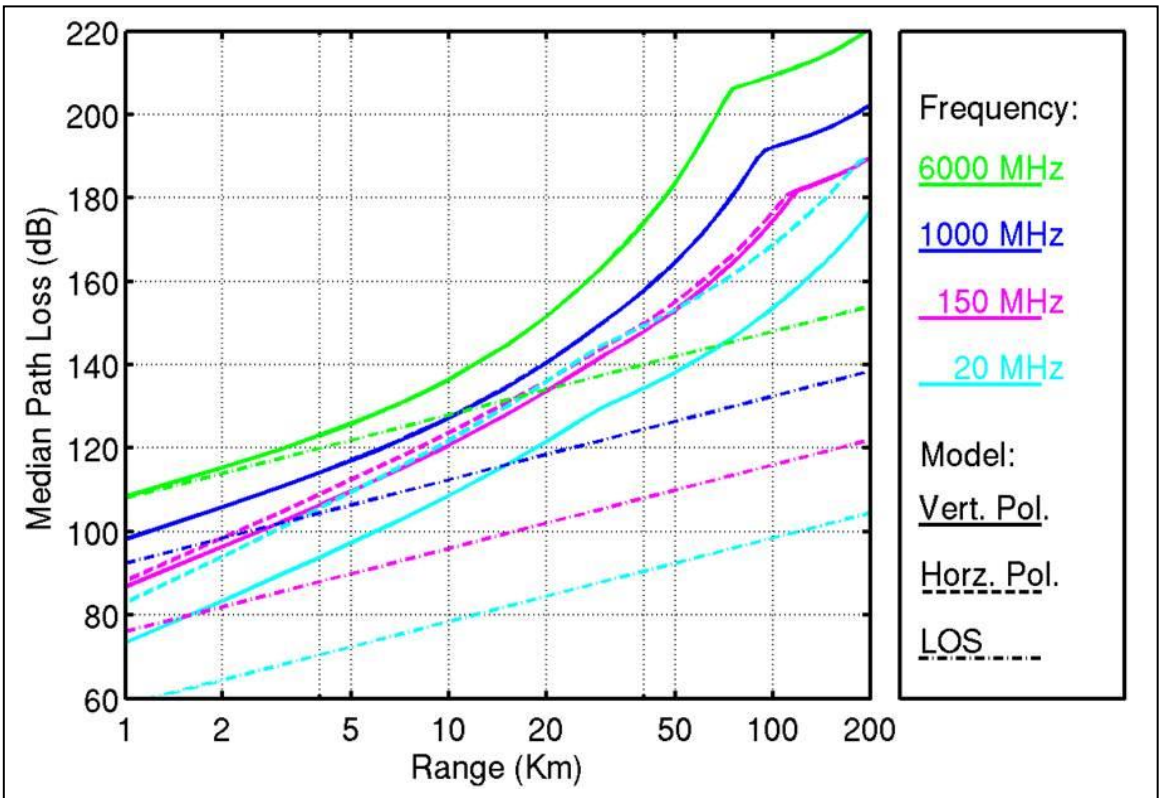

Figure 30) The Longley-Rice propagation model with base station height 32 m, mobile station height 1.5 m, terrain inter-decile 30 m.

The Longley-Rice model was originally developed in open areas, where the probability of shadowing due to buildings and other man-made structures is low. A correction factor for Urban areas was developed by Longley [Longley], by comparing Longley-Rice median loss values with those produced by Okumura [okumura]. The comparison was mode over frequencies ranging from 100 MHz to 3 GHz, distances of 10 – 100 km, antenna heights of 200 m and 3 m. and "rather smooth" terrain. Other antenna height values were also tested, and it was found that the urban correction was insensitive to terminal height for heights up to 600 m. The resulting correction factor is

$$L_U = 16.5 + 15\log_{10}(f_{MHz}) - 0.12 d_{km} \quad dB \tag{6.27}$$

Where f_{MHz} is the frequency in MHz, and d_{km} is link range in km. Longley [Longley] reports that this expression matches the calculated urban correction values to within 1 dB for all frequencies out to a range of 70 km, and out to 100 km for frequencies below 500 MHz. Above 500 MHz, at ranges beyond 70 km the correction tends to over-estimate urban propagation loss.

Figure 31 is a plot of the Longley-Rice model with the urban correction factor. The Hata model [Hata] is shown for comparison. The Longley-Rice urban correction factor and the Hata model were both fit to data collected by Okumura [Okumura]. The red dashed lines at 10 and 100 km show the minimum and maximum ranges at which Longley's fit to Okumura's data was carried out. The Hata model, fit to a maximum range of 20 km, is

shown for comparison. In the overlapping region between 10 and 20 km the two models

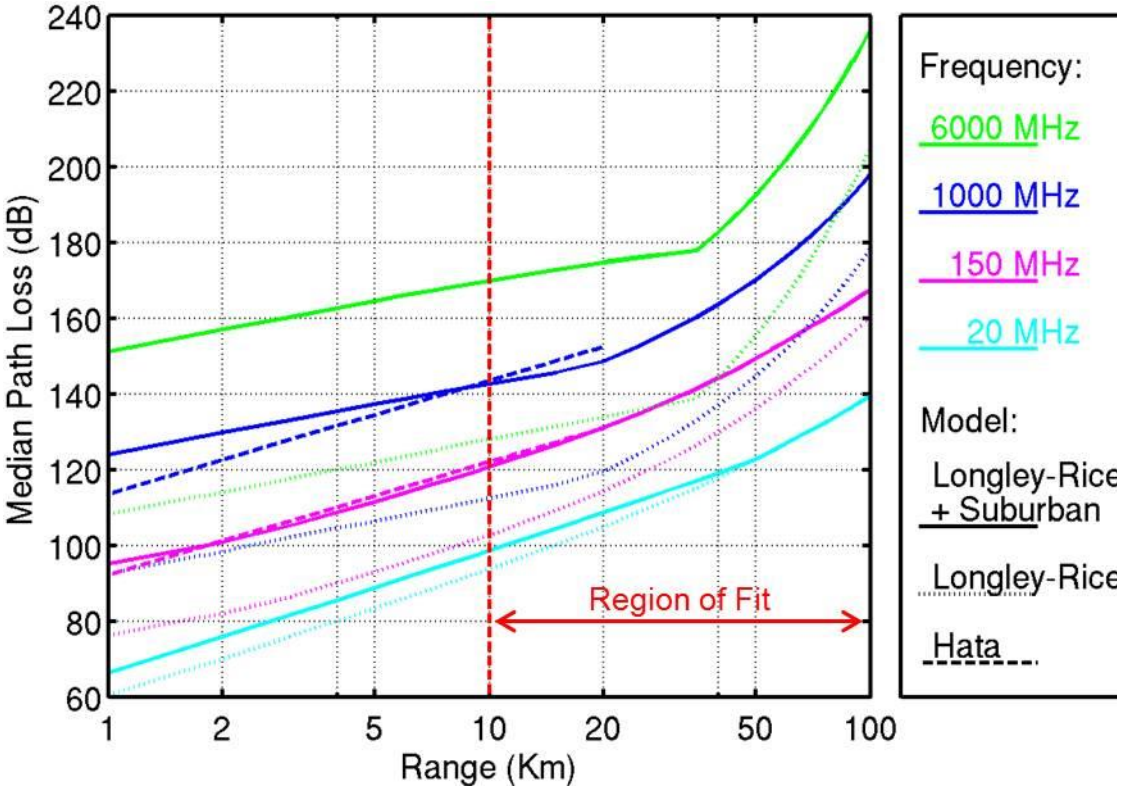

Figure 31) The Longley-Rice propagation model with urban correction, base station height 200 m, mobile station height 3 m. The Hata model shown for comparison was computed for the same antenna heights in a dense urban setting.

are close, though perhaps not as close as indicated by Longley. Some of the difference may be due to errors in Hata's fit to Okumura's data.

5.5.2 The Longley-Rice Suburban Correction Factor

A correction factor for use with the Longley-Rice area coverage model in Suburban environments was developed as follows. The median propagation loss predicted by the Longley-Rice model was compared with the loss predicted by the Okumura-Hata model for frequency range 100 MHz to 2 GHz, and distances 1 to 20 km. At frequencies above 1.5 GHz the COST-231 frequency extension was included. Antenna heights used were 200 m and 3 m. As for the urban correction, results were found to be insensitive to antenna height. Error magnitudes observed range from 5 to 17 dB as range, frequency, and antenna height vary. For a given range value, the correction was found to be reasonably well approximated by a linear fit in the log-frequency

$$L_S = a + b\log_{10}\left(\frac{f_{MHz}}{100}\right) \tag{6.28}$$

(6.28)Where f_{MHz} is the frequency in MHz. The parameters a and b are approximated as bi-linear functions of range:

$$a = \begin{cases} 7.472 + 1.193 d_{km} & d_{km} < 4 \\ 12.976 - 0.130 d_{km} & d_{km} \geq 4 \end{cases} \tag{6.29}$$

and

$$b = \begin{cases} 1.440 + 0.570 d_{km} & d_{km} < 9 \\ 6.719 - 0.053 d_{km} & d_{km} \geq 9 \end{cases} \tag{6.30}$$

Figure 32 is a plot of the error magnitude when using eqs. (6.28)-(6.30). Excluding a region in the upper-right corner, the error is seen to be below 2 dB. Peak values in the upper right corner are approximately 3.3 dB, and the average error magnitude is 0.8 dB. The means-squared error is 1.1 dB. The horizontal line at 1.5 GHz shows where the COST frequency extension is first used.

Figure 33 shows the Longley-Rice model with suburban correction path loss as a function of range.

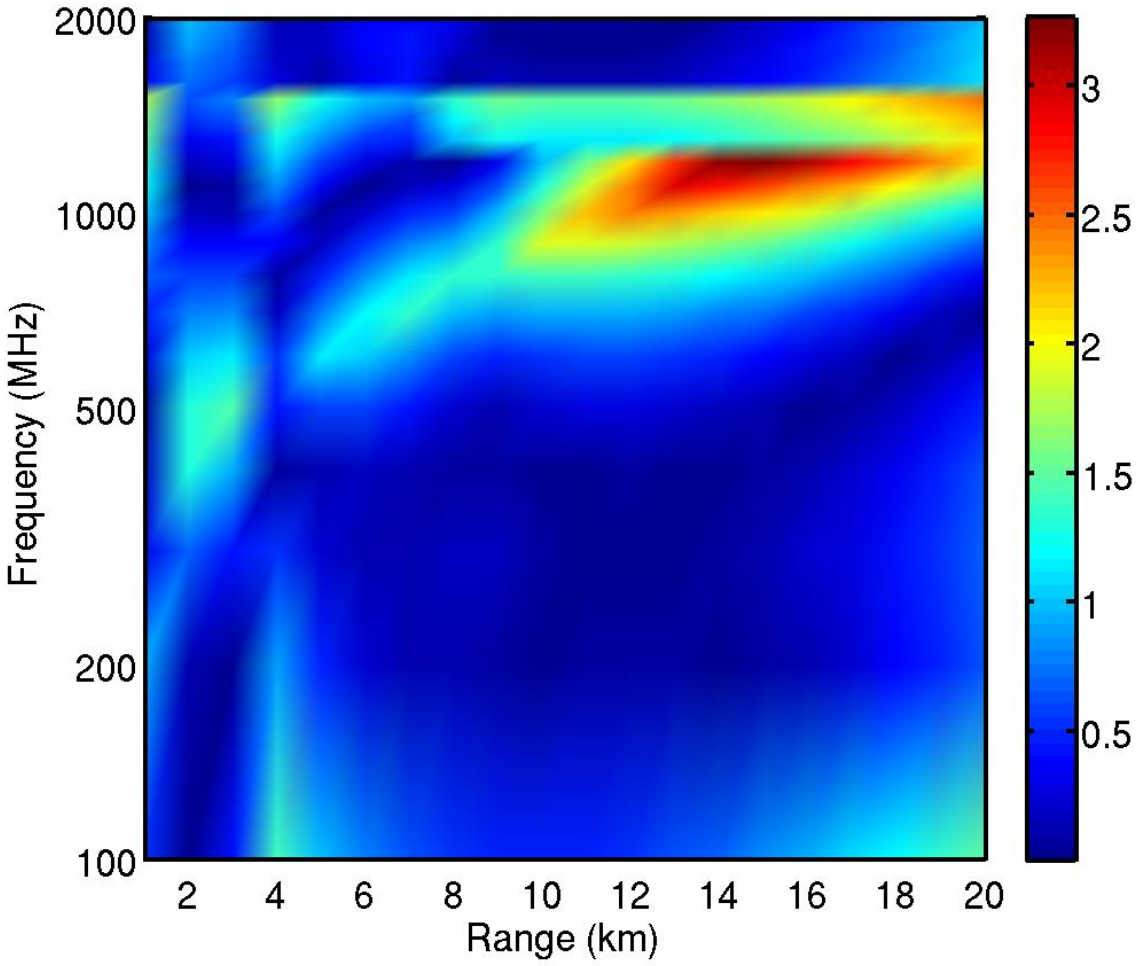

Figure 32) Longley-Rice suburban correction factor numerical approximation error magnitude, terminal heights 200 m and 3 m.

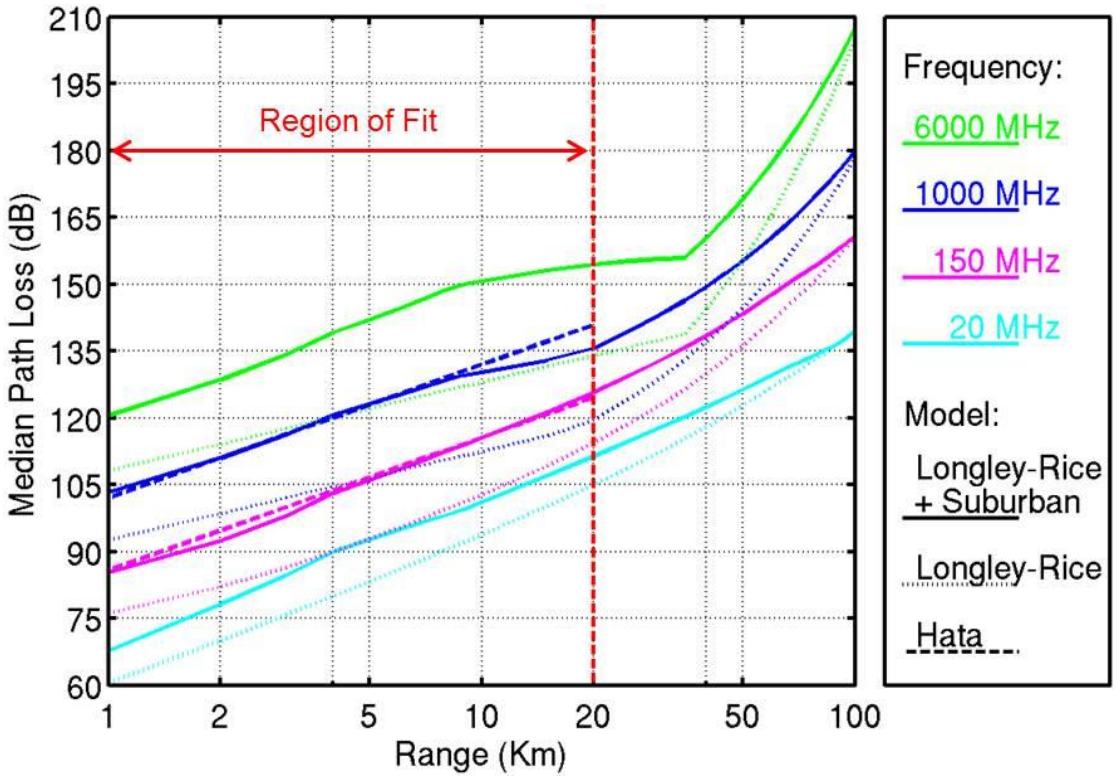

Figure 33). The Longley-Rice propagation model with suburban correction, base station height 200 m, mobile station height 3 m. The Hata model shown for comparison was computed for the same antenna heights in a suburban setting.

5.6 Hybrid Models

Although the different models used are generally consistent, within the accuracy to be expected from statistical propagation models, there are discontinuities at sets of parameters values, e.g. range and frequency, where Llamacomm transitions from one model to another. Discontinuities may interfere with attempts to optimize performance by searching over network parameters. In order to prevent problems the Llamacomm model has been smoothed at some transitions. There are also cases where a gap between models has been filled in by interpolating between applicable models on either side of the gap. Cases of smoothing and interpolating are described here.

5.6.1 Longley-Rice Rural Approximations at Range below 1 km (The Cabot Model)

The Cabot model is a simple model that finds propagation median loss and standard deviation in outdoor rural settings at ranges below 1 km, where range is too short for the Longley-Rice model, and none of the short-range urban or suburban models apply. This model finds propagation parameters by interpolating between the free space values at 10 m, and the Longley-Rice values at 1 km.

If both nodes are above 1,000 m altitude, propagation is modeled as line-of-sight. Otherwise the model interpolates between LOS loss at 10 m, and Longley-Rice loss at 1 km, using the standard environment parameters for rural settings, e.g. terrain inter-decile 90 m. For path slant-range r in meters, the range-loss is approximated as

$$L = L_{10} + \left(\log_{10} r - \log_{10}(10)\right)\frac{L_{1000} - L_{10}}{\log_{10}(1000) - \log_{10}(10)} = L_{10} + \left(\log_{10} r - 1\right)\frac{L_{1000} - L_{10}}{29} \quad (6.31)$$

Where L_{10} is LOS loss at 10 m, and L_{1000} is Longley-Rice loss at 1 km.

5.6.2 Air to Ground Models

Propagation models used in Llamecom are intended for ground-to-ground communication and typically have a maximum assumed antenna height. In cases where an airborne node is desired, the airborne node exceeds the supported height. Air-to-ground signals experience free-space propagation over most of their range, but are subject to blockage and other effects near the ground.

Llamacomm deals with those effects by defining a pseudo-node situated along the ground to airborne path at a location where both the pseudo-node to ground terminal ground range and the pseudo-node height are in the range supported by the applicable ground-to-ground propagation model, and one is at its maximum allowed value. Total path loss is the sum of the free space loss between the ground and airborne nodes plus excess path loss between the ground and pseudo-node.

5.6.3 Roof Height Transition Models

A hybrid model is used in urban and suburban outdoor settings when the higher of the two antennas is just above roof height and the lower antenna is below roof height, to smooth the transition in propagation loss as the higher antenna exceeds roof height. A variable Δh = 10 m was defined to be the width of the transition region, a value of Δh = 10 m was used. Pathloss is calculated using two different models which are appropriate for the setting and link parameters: L_b is the pathloss in dB for the model that supports links with two antennas below roof height; and L_a is pathloss for a model supporting one antenna below roof height and one above. The total path loss is a weighted sum of those two loss values in dB

$$L = \frac{\left(h_h - h_r\right)L_a\left(h_h, h_l, h_r\right) + \left(h_r + \Delta h - h_h\right)L_b\left(h_h, h_l, h_r\right)}{\Delta h} \quad \text{dB} \qquad (6.32)$$

Where h_h and h_l are the higher and lower antenna heights, respectively, and h_r is mean roof height.

6 Building Penetration Models

Equation Chapter (Next) Section 1

Building penetration loss characterizes the reduction in signal power that occurs when one terminal is inside a building, and the other is outside, relative to an otherwise identical radio link in which the building is not present. Building penetration also results in an increase in the shadowing standard deviation.

No single building penetration loss model was identified that covers or comes close to covering the desired range of link parameters. As a result, the model used here is a combination of various published results. The main result used is the COST-231 building penetration model [COST-231], which gives building penetration loss at the European mobile phone frequencies, 900 MHz and 1800 MHz.
It includes two distinct cases, a "line-of-sight" (LOS) case in which the outdoor terminal has a line-of-sight view of the building that contains the indoor terminal, and a non-line-of-sight (NLOS) case, in which there is no LOS path from the external terminal to the building. This model is attractive because it explicitly models link geometry, particularly the position of the internal terminal in the building, and for the LOS case the angle between the direct radio path and the building façade. The disadvantage of the COST-231 model is that it covers only a small subset of the required frequency range. A frequency correction factor for use with the COST-231 building penetration model is developed here, based on a collection of measurement results published by different authors.

6.1 COST-231 Building Penetration Model: LOS to Building

The COST-231 LOS building penetration model [COST-231] estimates pathloss for a signal at 900 MHz when one antenna is inside a commercial building such as an office building, or apartment building, and the other is outside, but has a line-of-sight path to the building. The parameters used in this model are defined with respect to the "building penetration point", the spot on the building's exterior wall that is closest to the interior antenna. A line drawn from the interior antenna to the penetration point is perpendicular to the wall. The model geometry is illustrated in Figure 34. Model parameters are:

- Frequency f_{MHz} = 900 MHz,
- Outdoor range r in meters, from 1 to 500 m. Note that r is slant range from the outdoor antenna to the building penetration point, and includes the effects of height difference between the two antennas as well as horizontal displacement
- Indoor range dd in meters, measured from the indoor terminal to the penetration point
- Grazing angle θ, the angle between the direct path from the exterior antenna to the penetration point and the wall on which the penetration point is located. This angle can equal 90^o only if both antennas are at the same height above ground
- Number of interior walls, n, blocking the path from the penetration point to the interior antenna

.

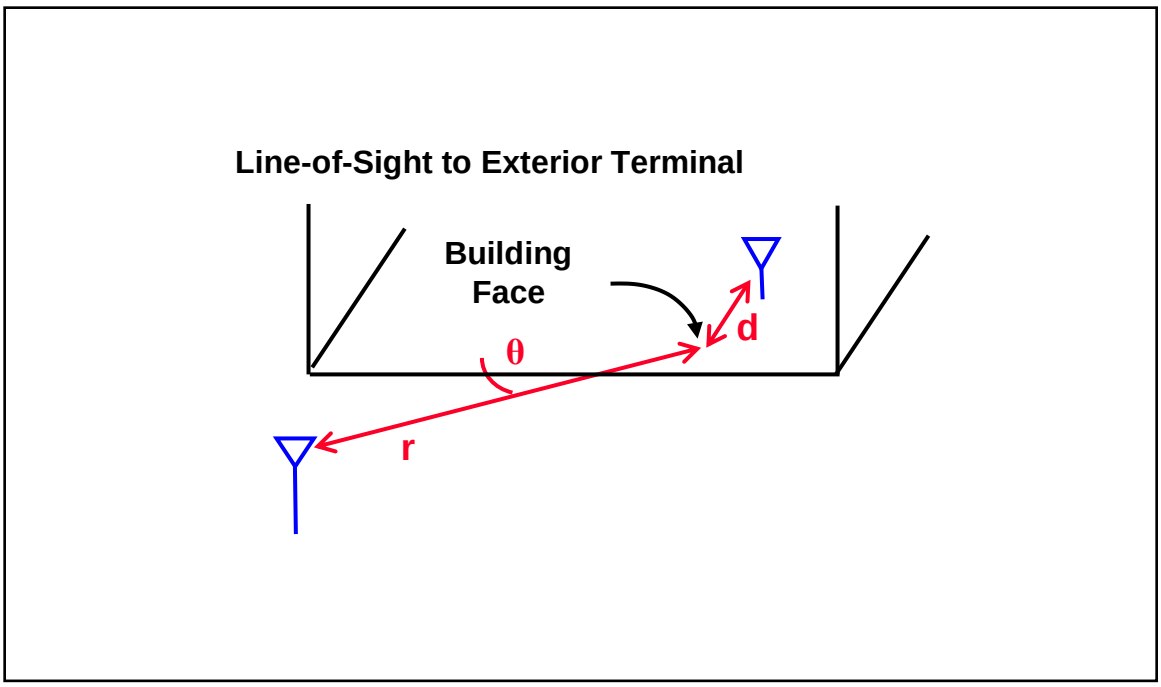

Figure 34) COST-231 line-of-sight (LOS) building penetration model geometry.

Using these parameters, the COST-231 model for LOS median building penetration loss at 900 MHz is

$$\begin{aligned} L = \quad & -27.6 + 20\log_{10}(f_{MHz}) + 20\log_{10}(r+d) + \\ & W_e + W_{ge}(1-\sin\theta)^2 + \\ & \max\left(nW_i, \alpha(d-2)(1-\sin\theta)^2\right) \quad dB \end{aligned} \tag{7.1}$$

The value of constants use in this model are:

- W_e = 7 dB. exterior wall penetration loss at 90º grazing angle, range 4-10 dB, the value used here is for concrete walls with normal sized windows
- W_{ge} = 20 dB, additional exterior wall penetration loss at 0º grazing angle
- W_i = 7 dB, interior wall penetration loss, range 4-10 dB, the value used here is for concrete walls
- α = 0.6 dB/m, propagation loss per m along interior hallways

The first line of this expression is the line-of-sight propagation loss along a path from the external antenna to the penetration point, and from there to the interior antenna. Consequently, this model stands alone, providing both building penetration loss and range loss. The assumption of LOS propagation from the external terminal to the building over short ranges (0.5 km or less) makes this term relatively invariant to other environment parameters, although results are expected to be somewhat pessimistic on open areas.

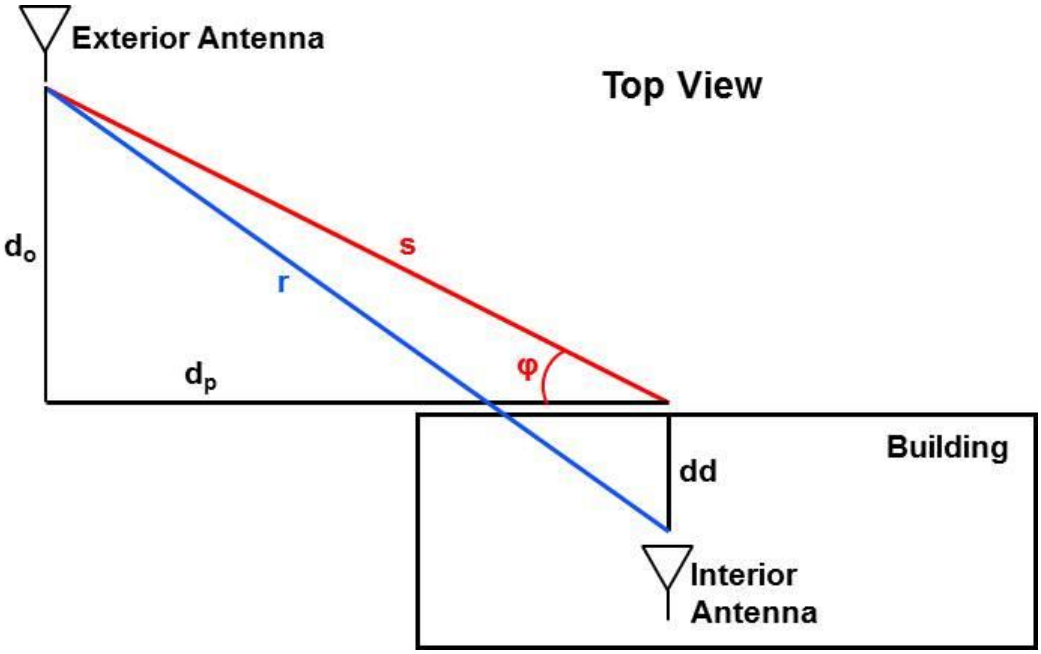

Figure 35. LOS building penetration model, top-view (two-dimensional) geometry.

The second line of this equation models penetration loss through the exterior wall, assumed to be 7 dB for a path striking the wall perpendicularly, with a correction term for other grazing angles. The third line is excess loss from the penetration point to the interior antenna, due either to losses resulting from interior walls along the signal path, or losses incurred while propagating down a hallway. Although the model has been broken down conceptually into these three components, the parameter values were selected to give a best fit of the entire model to measured data, and do not necessarily work well outside the complete model [COST-231].

Figure 35 shows the LOS building penetration model geometry as seen from directly overhead, i.e., differences in antenna height are not accounted for yet. The initial known parameters are

- r, the ground range between antennas, in m
- dd, ground range from the penetration point to indoor node, in m
- φ, angle between the building face and a line from the penetration point to the outdoor node, in degrees
- h_{1m}, antenna 1 height above ground, m (either antenna can be antenna 1, as long as the ordering is used consistently)
- h_{2m}, antenna 2 height above ground, m (either antenna can be antenna 2, as long as the ordering is used consistently)
- n_{wall}, number of interior walls between penetration point and interior antenna

Parameters needed to call the LOS building penetration model include two additional ranges,

- do, perpendicular ground range from the outdoor antenna to the building face, in m
- dp, parallel ground range from the outdoor antenna to the penetration point

These last two distances are found using the law of cosines to obtain the ground range s between the outdoor antenna and the penetration point

$$s = \frac{-a_1 + \sqrt{a_1^2 - 4a_0}}{2}$$
$$a_0 = dd^2 - r^2 \qquad (7.2)$$
$$a_1 = -2s \cdot dd \cos(\varphi + \pi/2)$$

Then the required ranges are found simply as

$$d_o = s \cdot \sin\varphi$$
$$d_p = s \cdot \cos\varphi \qquad (7.3)$$

When the LOS building penetration model is used, the resulting loss term is the median, assumed to have a standard deviation of 4 dB, as suggested in [COST-231].

One suggested aspect of the COST-231 model that has not been implemented in Llamacomm is the urban-canyon option, in which the actual position of the exterior antenna is replaced with a virtual position halfway between buildings on either side of the street. This is supposed to incorporate the effect of strong multipath reflections that occur when the exterior antenna is bounded on all sides by nearby tall buildings.

Plots?

6.2 COST-231 Building Penetration Model: NLOS to Building

Under COST-231, a separate model is used when the external antenna does not have a LOS path the the building. In this case, the model is used in conjunction with an appropriate NLOS pathloss model between the external antenna and a point outside the building, at the penetration point, and 2 m above ground level. The COST-231 NLOS building loss is added to the external NLOS pathloss to estimate the total mean propagation loss. As for the LOS case, this model was developed from measurements of large masonry office and apartment buildings, mostly poured concrete, and presumably with metal reinforcement bars (rebar) embedded in the walls.

Model parameters are:

- Frequency f_{MHz} = 900 MHz,
- Indoor range d in meters, measured from the indoor terminal to the penetration point
- Indoor antenna height above outdoor ground level h_m in meters
- Number of interior walls, n, blocking the path from the penetration point to the interior antenna

The penetration point is defined as for the LOS case. The model is

$$L = L_e + W_e + W_{ge} + \max(nW_i, \alpha d) - G_h(h_m - 2) \qquad (7.4)$$

Where L_e is the external pathloss generated by an appropriate model.
The ability to select different models to generate L_e allows the model to be used in a wider range of environments, and over greater ranges than the LOS building penetration model.

Constant values used in this model are:

- W_e = 7 dB. exterior wall penetration loss at 90º grazing angle, range 4-10 dB, the value used here is for concrete walls with normal sized windows
- W_{ge} = 4 dB, additional exterior wall penetration loss experienced due to the non-specular nature of the exterior signal, which arrives along multiple paths at different angles to the exterior wall. Range 3-5 dB at 900 MHz. Note that both the definition and value of W_{ge} differ from those for the LOS model.
- W_i = 7 dB, interior wall penetration loss, range 4-10 dB, the value used here is for concrete walls
- α = 0.6 dB/m, propagation loss per meter along interior hallways
- G_h = 1.4 dB/m, height gain

In [COST-231] the standard deviation for this model is claimed fall on the range 4-6 dB. Llamacomm uses a standard deviation of 4 dB, which combines with the outdoor path loss standard deviation using a RSS law.

6.3 COST-231 Building Penetration Model Frequency Correction

Ideally, a single set of measurements would be used to derive the building penetration model as a function of both terminal position and frequency. Unfortunately at this time no study has been identified that provides all the needed information, and the Llamacomm model uses the COST-231 models described above for 900 MHz propagation, because it allows the model to reflect interior and exterior terminal locations, along with a frequency correction described here.

A large number of measurements of building penetration loss at different frequencies have been reported [Aguirre,Davidson,de Toledo,Ferreira,Gahleitner,Hoppe,Okamoto,Rice,Siwiak,Tanis,Turkmani]. Unfortunately, there is considerable variation not only in frequency, setting, and type of building, but also in the definition of measured values such as outdoor loss, and building penetration loss. In order to reduce the effect of inconsistencies between data collected by different authors, only results that present measurements in the same setting(s) at two or more different frequencies were considered, and the parameter extracted from each study was the change in loss due to frequency.

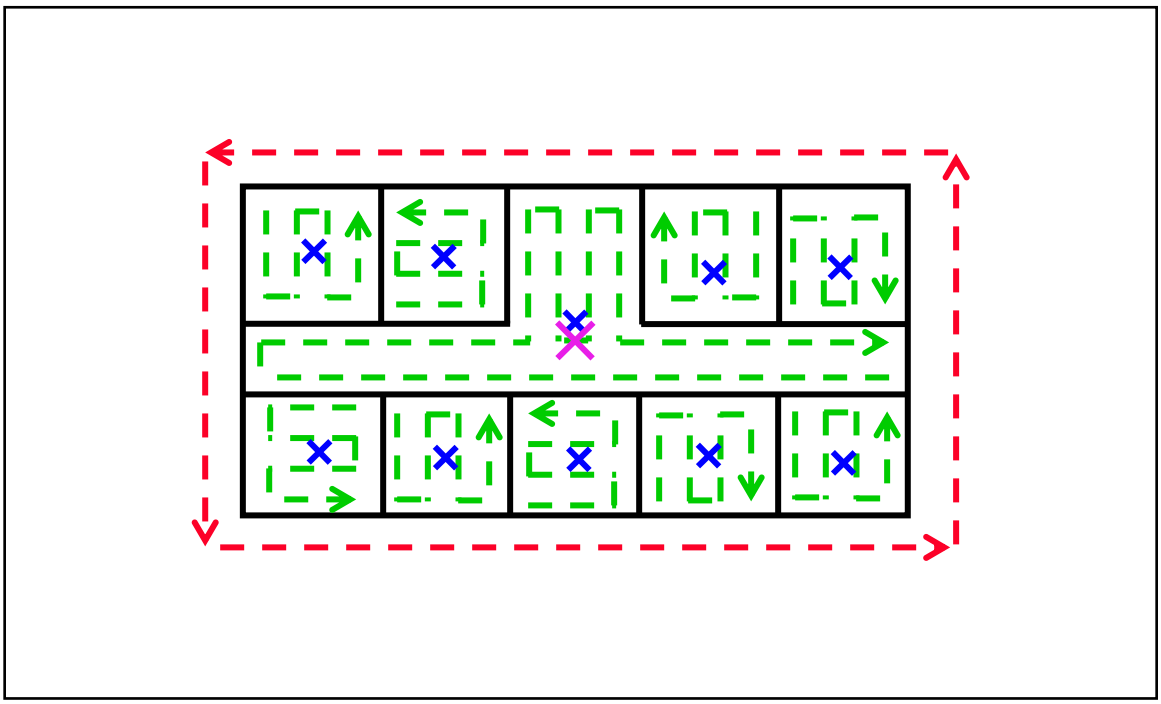

Figure 36) Example building penetration loss measurement routes.

Typically, a building penetration study compares two measurements. Received power is measured outside the building "at the closest possible approach", as indicated in Figure 36 by the red dashed-line, and along a path on the ground floor of the building which should provide a representative set of set of values, as indicated by the green dashed-line in Figure 36. For each set of measurements, power is averaged over short sub-paths, typically on the order of ten wavelengths to eliminate effects of multipath fading. The difference between the median value of all outdoor short-time-averages and the median value of all indoor short-time-averages is used as an estimate of building penetration loss. Table 11 summarizes the studies used here, with a brief description of the setting (outdoor transmitter location, building type, and building location) and measurements used by each. Note that exterior measurement locations include measurements around all four walls, around three walls, along on wall, closest to the wall, or along both sides of the street, along a balcony running around the building, etc. Similarly indoor measurements include full coverage of ground floor, in the outside corners only, along hallways only, in rooms with windows only, and other "representative" sets of locations.

All building used were medium to large masonry or steel frame buildings. There was considerable variability in the number and size of windows. It is believed, though not perfectly clear, that none of the buildings had windows with metalized reflective coatings. Most buildings were located in built-up urban areas, although a few were in suburban office park type settings, with parking lots all around.

Table 11. Differences between building penetration loss measurement programs conducted by different authors

Reference	Exterior Transmitter	Exterior Power Measurement	Interior Measurement	Buildings	Setting
Aguirre	5 m high, within 200 m range, NLOS.	Zig-zag pattern next to unobstructed exterior wall closest to transmitter	Zig-zag pattern in each exterior corner of ground floor	15-50 stories. 1) glass & steel frame, 2) stone 3) concrete	Downtown Denver, busy streets all around
Davidson	55 m high, 1900-4350 m range	measurements around outside 3 walls closest to transmitter	measurements along S- or U-patterns in interior rooms or halls or ground floor	"Medium size" office building, Mostly glass	Schaumburg, IL, parking lots all around
deToledo	40 m high, 180 to 350 m range, partial LOS	"Mean signal strength in the streets immediately outside"	Average of measurements in each room of ground floor	4-7 floors, steel frame/glass or reinforced concrete	University of Liverpool, freestanding in dense campus
Ferreira	Commercial GSM, DCS-1800, and UMTS Tx's, 200 m – 2 km range	Mean signal along accessible building facades, measured on both sides of street.	Median of rooms on all floors, at various distances from outside wall	"representative buildings", half taller than 6 stories	Lisbon and Porto, Portugal, some buildings abut neighbors, others are free-standing
Gahleitner	40 m high, 250 m range, partial LOS	Mean signal level on all four sides	Mean signal level on specific floor	~30 m high office buildings, brick and/or concrete, large windows	Downtown Vienna, densely built-up
Hoppe	40 m high, 80 m range, partial LOS[2]	Median on balcony outside building	Mostly corridors, some room measurements[3]	Concrete, low-rise with balconies	University of Stuttgart, parking lots, low buildings
Okamoto	80 m high, 180 m to	Mean on all four sides of	rooms with windows,	2-12 floor, reinforced	Yokohame, urban area,

	1.3 km range	building	usually large	concrete buildings	10 – 42 m between buildings
Rice	137 m high NYC mobile telephone tower, ca. 1959, 0.3-3 km range	Median in streets around building[1]	Median of measurements on ground floor	Brick or reinforced concrete	Downtown New York City
Siwiak	unknown	Signal levels on street	Signal levels on ground floor	Large downtown office buildings and malls	Urban
Siwiak	unknown	Signal levels on street	Signal levels on ground floor	Mid-size office and small apartment buildings	Urban
Tanis	38 – 136 m high, Partial LOS	"as parallel as possible to the inside runs"	hallways near the building center on ground floor	9 story hotel, 1 & 2 story malls	Suburban Philadelphia, freestanding, surrounded by trees
Turkmani	25 m high, 235-290 m range, partial LOS	"representative signal strength" at street level	Mean signal for ground floor, all rooms and corridors	4, 7 story buildings	University of Liverpool, modern buildings in campus setting

1) Rice defines "building loss" as difference between median measured in-building power, and median street power at building range, and "local building loss" as difference between median measured in-building power, and measured median power in street outside building. Results used here are "local building loss".
2) Only data taken at different frequencies from same location (data sets T2,T3) are used.
3) Hoppe is not clear how outside and inside measurements are compared, e.g. outside median minus median median, parallel paths, etc.

Figure 37 is a plot showing the published building penetration loss measurements at multiple frequencies. This plot is an elaboration of one originally published in [Davidson]. Each curve is color coded, and labeled with the name of the first author for the publication in which it is found. The original plot, published in 1997, was used to

argue that penetration loss declines with frequency. The argument in support of this effect is that although the amount of signal power absorbed by walls increases with frequency, the majority of power that enters a building gets in through windows, and as frequency increases the width of the first Fresnel zone where the propagation signal enters through the window becomes smaller, reducing loss as the signal passes through the window [Stavrou]. However, most of the added curves, for frequencies at or above 900 MHz show increased loss as frequency goes up. The pair of curves labeled Siwiak, from [SiwiakBook], are shown as dashed lines because the original data is not publicly available [SiwiakPrivate]. These curves are appealing because they cover nearly the full range of frequencies of interest, and because they provide results broken down by building size. They are based on a set of measurements carried out by employees of Motorola Corporation, and not published in the open literature other than two plots appearing in [SiwiakBook].. Siwiak's curves take a middle course, showing penetration loss falls with frequency up to 900 MHz, then flattens out. This observation would be consistent with the Fresnel zone argument, as at frequencies above 900 MHz the wavelength is less than 0.33 m, typically smaller than the window size for a commercial building, and geometric optics models depending mostly on the fraction of the exterior wall penetrated by windows become more accurate. Curves showing loss increasing with frequency can be attributed to either increased signal absorption, possibly by window glass and more likely by interior walls, or increased diffraction loss when signals do not arrive perpendicular to the building face, and must bend around the window edge to enter the building.

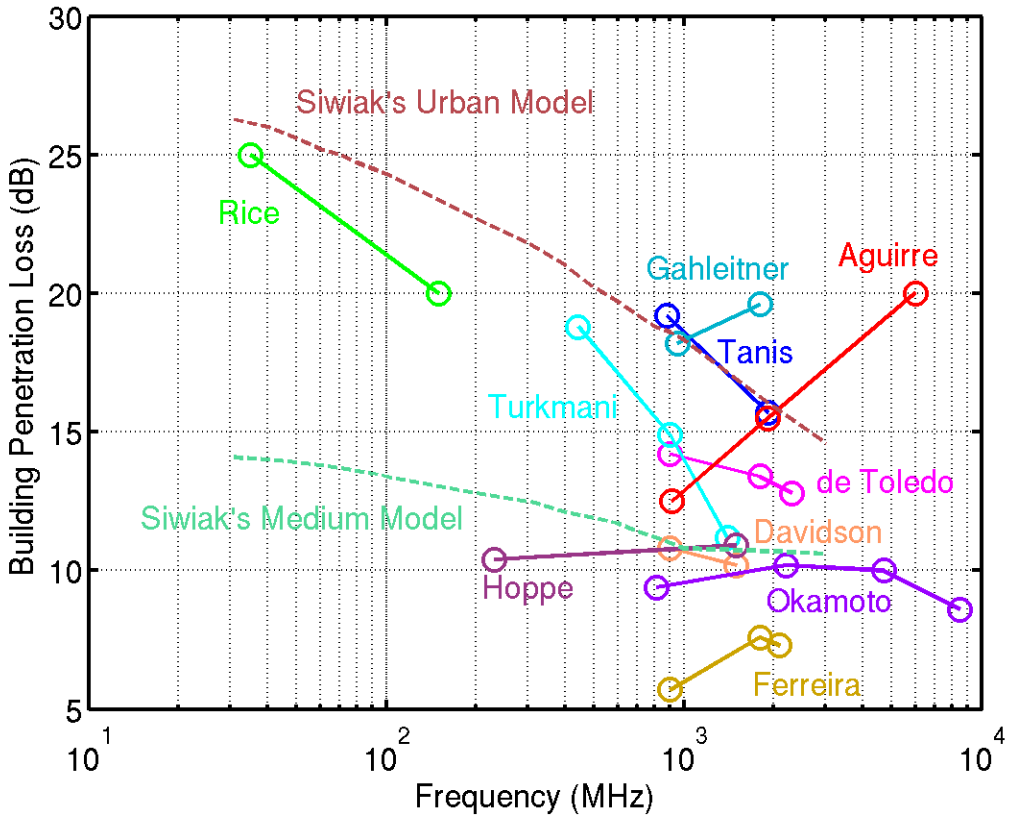

Figure 37) Measured building penetration loss versus frequency in masonry buildings, from various studies.

To combine this data with the COST-231 building penetration loss models, the slope of loss in dB versus frequency was averaged. It was assumed that the COST-231 penetration loss estimate at 900 MHz was accurate, and a correction term for other frequencies was found by integrating the mean slope from 900 MHz to the frequency of interest. Figure 38 shows the resulting frequency correction curve, along with a piecewise linear approximation that is used by Llamacomm.

$$L_f = \begin{cases} 15.5 - 5.26\log_{10}(f_{MHz}) & 30 \le f_{MHz} \le 900 \\ 1.5 - 0.53\log_{10}(f_{MHz}) & 900 \le f_{MHz} \le 3000 \\ 16.3 + 4.58\log_{10}(f_{MHz}) & 3000 \le f_{MHz} \le 6000 \end{cases} \quad (7.5)$$

The piecewise linear approximation is within 1 dB of the integral at all frequencies, and typically within a few tenths of a dB.

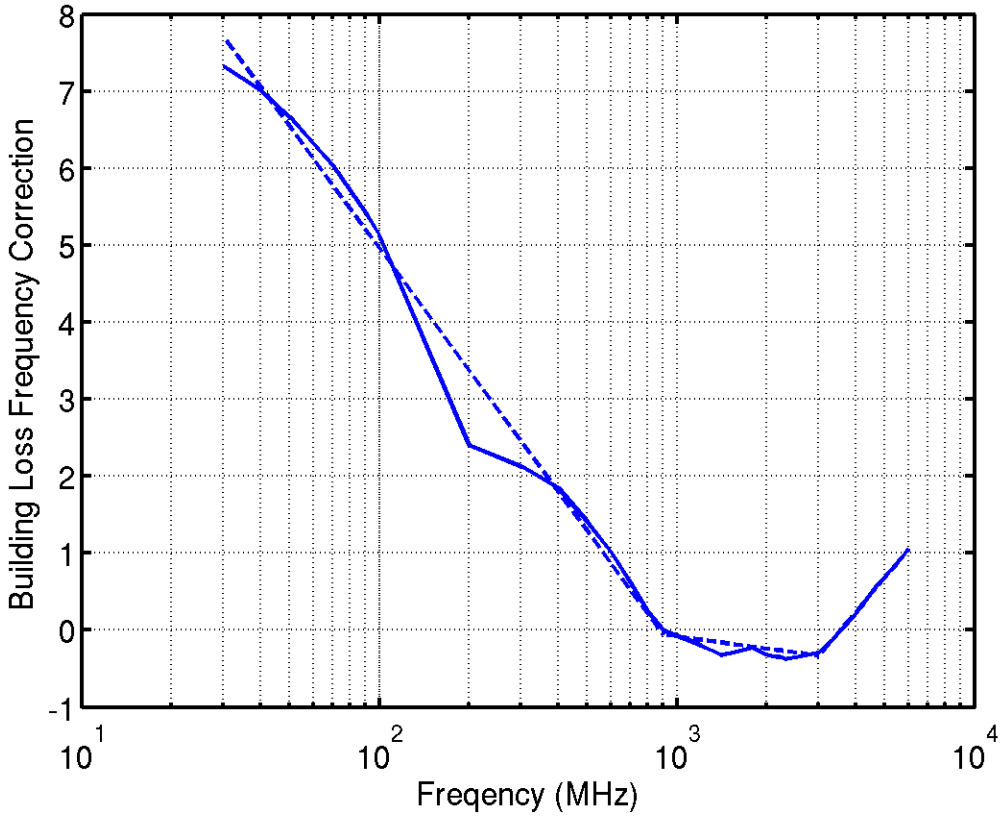

Figure 38) Building penetration model frequency correction for masonry buildings.

This correction is applied to the two COST-231 building penetration models as follows. The LOS model includes a range loss term calculated at 900 MHz, with must be replaced with range loss at the frequency of interest

$$L = L(900) - 20\log_{10}(900) + 20\log_{10}(f_{MHz}) + L_f(f_{MHz}) \tag{7.6}$$

where L(900) is the previously calculated pathloss with building penetration at 900 MHz, and L_f is the frequency correction. The NLOS model with frequency correction is

$$L = L_e(f_{MHz}) + (L(900) - L_e(900)) + L_f(f_{MHz}) \tag{7.7}$$

where $L_e(f_{MHz})$ is the exterior pathloss term calculated at the specified frequency.

This correction applies to the first floor, and so the possibility exists that the height gain terms in eqs. () and () may have to be modified as well. However, this term has been studied repeatedly [Davidon,de Toledo,Rice,Tanis] and found to show little variation with frequency.

What about standard deviation?

Note: US Army measurements kind of confirm, didn't use because buildings too different, show graphs.

Houses: not too different, but not enough data for separate curve. Show plot (Figure 39), along with COST-231+3 dB gain, plus frequency correction

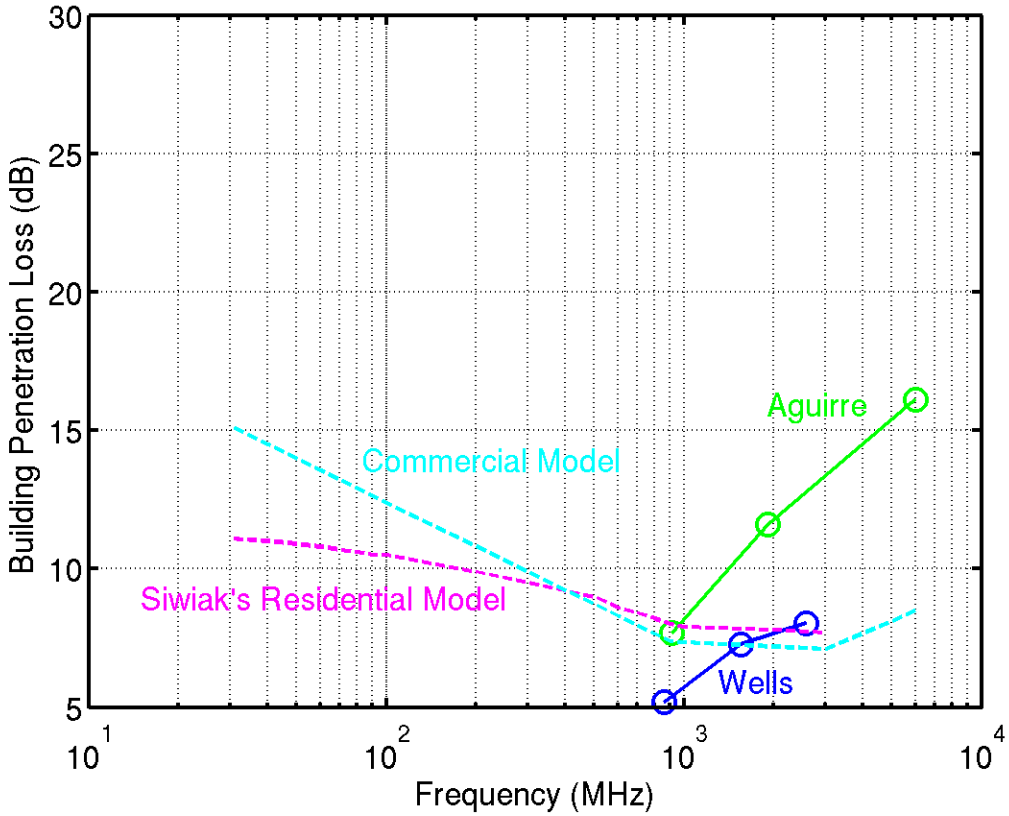

Figure 39) Measured building penetration loss versus frequency in wood frame buildings, from various studies.

All results were found using vertically polarized signals. Paper by Turney suggest there may be differences, but to little data. Other paper in folder says no difference (Wells, in houses at 860 MHz, Price, no difference at 35 – 150 MHz

In practice, penetration loss will vary greatly from building to
Building, depending on a large number of factors such as building material and construction, how close other buildings are both next door, and street width, and how much furniture is inside the building. This model represents an average value for building penetration loss over a variety of buildings, but one case that is not covered by this model is the presence of metalized windows. Many modern office buildings have coated glass to block infra-red radiation. Some coatings are plastic and have little effect on propagation, but others are metallic, and have been found to increase propagation losses by 20 dB or more.

6.4 The Rural Building Penetration Model Correction

In rural environments, Llamacomm assumes there are two penetration points, on the two exterior walls closest to the interior antenna. ….

7 Indoor Propagation Models

Equation Chapter (Next) Section 1

Results from a many different experiments were combined to provide an indoor propagation model over the frequency range of interest. In all cases incorporated here, the measurement data was used to create a model of the form

$$L_{med} = L_{LOS}(1) + 10a\log_{10}(d_m) \tag{8.1}$$

where L_{med} is the median propagation loss in dB, $L_{LOS}(1)$ is the theoretical (Friis equation e.g. [Parsons]) LOS loss at 1 m, in dB, and d_m is link range in meters. Values for parameter *a* are available at different frequencies, and different building types, as summarized in Table 12 for the case where the link is LOS (transmitter and receiver in same room) and Table for NLOS propagation.

Insufficient data for residences and metal interior walls.

Table 12. Line-of-sight indoor propagation range-loss parameter for office buildings.

Frequency	a	sigma	Reference
450 MHz	1.39	2.0	[Affandi]
450 MHz	1.79	n/a	[Chandra]
900 MHz	1.72	n/a	[Chandra]
900 MHz	2.10	1.41	[Affandi]
910 MHz	1.6	2.5	[Ganesh]
1300 MHz	1.84	4.9	[Rappaport92]
1350 MHz	0.44	n/a	[Chandra]
1500 MHz	1.7	n/a	[Saleh87]
1800 MHz	1.6	n/a	[Ju]
1800 MHz	2.00	1.87	[Affandi]
1890 MHz	1.55	3.5	[Pappadakis]
1890 MHz	2.22	n/a	[Chandra]
2250 MHz	1.5	n/a	[Nobles]
2400 MHz	1.4	4.42	[Lim]
2400 MHz	1.9	n/a	[Janssen]
2400 MHz	1.9	n/a	[Giannopaulos]
2400 MHz	2.30	2.07	[Affandi]
4000 MHz	1.84	4.8	[Rappaport92]
4750 MHz	2.0	n/a	[Janssen]
5200 MHz	1.3	2.2	[Medbo]
5250 MHz	1.7	n/a	[Nobles]
5300 MHz	1.7	2.74	[Lim]

5800 MHz	2.64	2.26	[Affandi]

Table 13. Non-line-of-sight indoor propagation range-loss parameter for office buildings with open floor plan.

Frequency	a	sigma	Reference
915 MHz	2.4	9.6	[Rappaport94]
915 MHz	2.8	14.2	[Rappaport94]
1900 MHz	2.6	14.1	[Rappaport94]
1900 MHz	3.8	12.7	[Rappaport94]
5200 MHz	3.1	2.9	[Medbo]

Table 14. Non-line-of-sight indoor propagation range-loss parameter for office buildings with concrete interior walls

Frequency	a	sigma	Reference
450 MHz	2.56	3.15	[Affandi]
900 MHz	2.40	2.66	[Affandi]
941 MHz	3.9	n/a	[Alexander]
1700 MHz	6.0	7.2	[Karlsson]
1800 MHz	3.08	4.28	[Affandi]
1800 MHz	4.5	8.7	[Phaiboon]
1800 MHz	6.0	n/a	[Ju]
2400 MHz	3.04	4.44	[Affandi]
2400 MHz	3.75	5.09	[Lim]
2400 MHz	3.9	n/a	[Giannopoulou]
5200 MHz	5.1	2.1	[Medbo]
5200 MHz	7	3.9	[Medbo]
5300 MHz	4.85	5.18	[Lim]
5800 MHz	2.80	3.31	[Affandi]

Table 15. Non-line-of-sight indoor propagation range-loss parameters for office buildings with plasterboard interior walls.

Frequency	a	sigma	Reference
850 MHz	3	n/a	[Rappaport94]
910 MHz	3.3	5.7	[Ganesh]
941 MHz	2.8	n/a	[Alexander]
941 MHz	3.7	n/a	[Alexander]
941 MHz	5.3	n/a	[Alexander]
941 MHz	6.2	n/a	[Alexander]

1300 MHz	3.43	14.1	[Rappaport92]
1500 MHz	3	n/a	[Saleh87]
1890 MHz	3.76	4.1	[Papadakis]
2250 MHz	2.5	n/a	[Nobles]
2400 MHz	3.3	n/a	[Jansson]
4000 MHz	2.77	16.0	[Rappaport92]
4750 MHz	3.8	n/a	[Janssen]
5200 MHz	4.1	2.7	[Medbo]
5250 MHz	2.8	n/a	[Nobles]

Figure 40 is a scatter plot of the data in Table with curves fit to them, to approximate range-loss parameter as a function of frequency. The curves were found by fitting polynomials of different order (1, 2, or 3) to the data, using either frequency or the log of frequency as the free variable. The points colored red in Tables 12 - 15were treated as outliers. In general, the best fit produced was a second order polynomial in linear frequency, results of which are shown in the figure. Coefficients for each case are listed inTable 16. These coefficients are used to find the indoor propagation range-loss coefficient according to the equation

$$a = b_0 + b_1 f_{MHz} + b_2 f_{MHz}^2 \tag{8.2}$$

For the case with LOS propagation, the mean-squared error when using a constant range-loss coefficient was only 6% higher than the MSE using the second order polynomial fit, so that case was forced to be constant, i.e., b_1, $b_2 = 0$. It is interesting to observe in Figure 41 that at low frequencies a higher path loss is observed for plasterboard walls than for concrete walls. Possibly this reflects the fact that plasterboard in modern office buildings is supported internally by metal studs, spaced about 18 inches (45 cm) apart. The frequency at which the two curves cross is near 650 MHz, where the wavelength (46 cm) equals stud spacing. In contrast, many of the buildings listed as having concrete interior walls had walls made of concrete blocks with no metal reinforcement. Or it could just be wrong.

Table 16. Coefficients for finding indoor propagation range-loss coefficient as a function of frequency.

Environment	b_0	b_1	b_2
LOS	1.80	0	0
NLOS, Open-Plan	2.661	-9.954×10^{-5}	3.536×10^{-8}
NLOS, Concrete Walls	2.593	9.490×10^{-4}	-7.254×10^{-8}
NLOS, Plasterboard Walls	3.213	-3.064×10^{-5}	1.258×10^{-8}

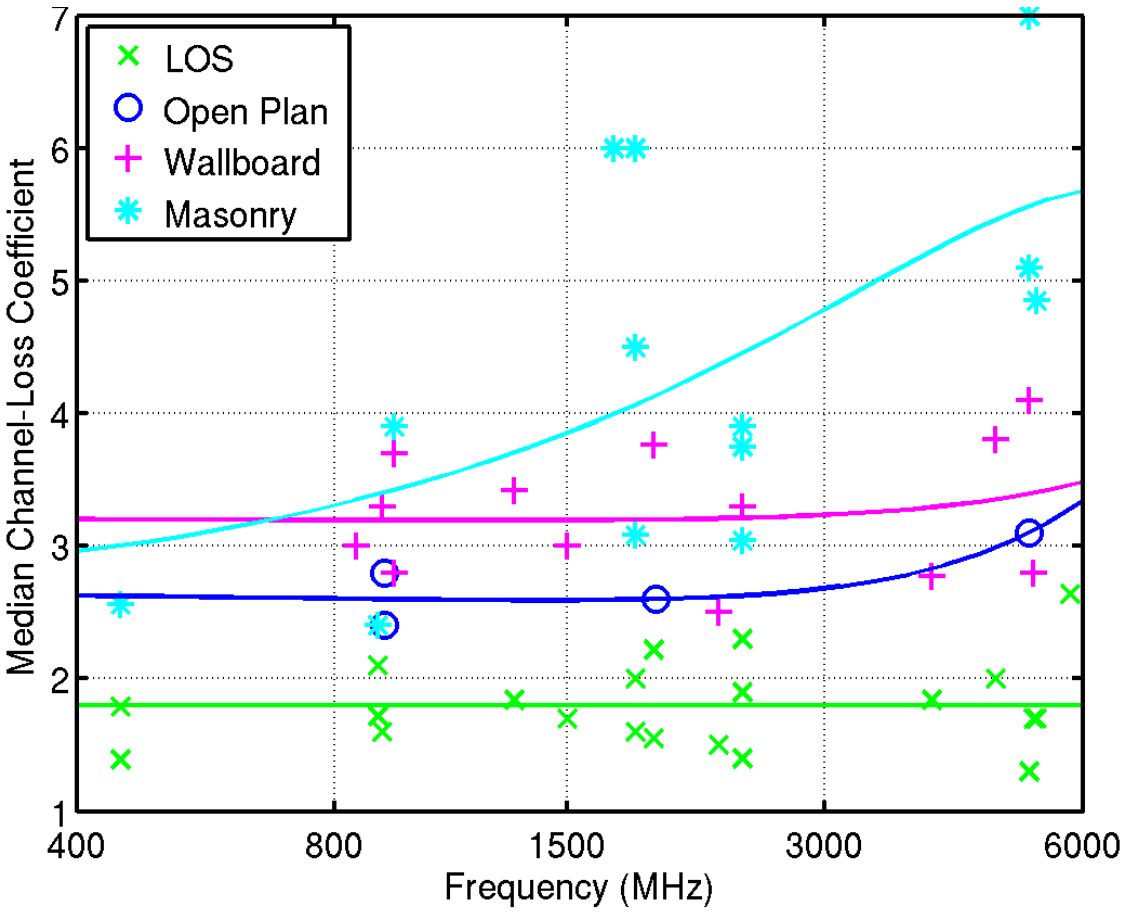

Figure 40) Indoor propagation loss coefficient a for different frequencies and environments.

These results assume the transmitter and receiver are on the same floor. When they are on different floors, an additional loss term must be included. The model currently adds 20 dB of loss per floor separation between the two nodes. This value comes from [cost231], and is based on measurements at 900 MHz and 2400 MHz in concrete office buildings.

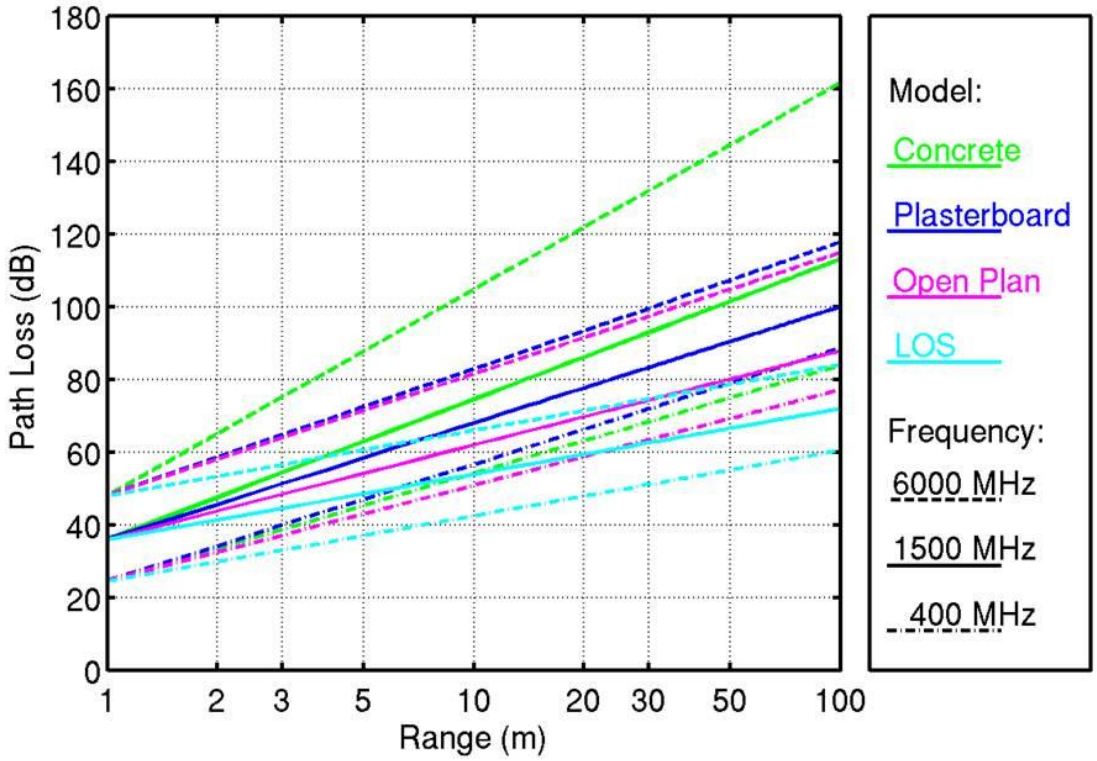

Figure 41) The same-floor indoor propagation models as a function of range, for different frequencies, and in different environments.

LLamacomm uses a function called indoor_concrete, which assumes all buildings have concrete interior walls, to calculate path loss on indoor links. Input parameters are horizontal range between antennas, frequency, antenna heights, and the distance from one antenna to the nearest wall..The horizontal range between antennas is compared to distance to the nearest wall to determine if there are intervening walls on the signal path, and the difference in antenna heights to determine if antennas are on different floors of the building. Note that antenna heights must both be measured from a common reference level, e.g. ground level, not height above the floor on which the antenna sits, unless both antennas are on the same floor.

For radios in the same room, eq. 8.1 is used with the Line-of-sight parameter values. For radios on the same floor but in different rooms, eq. 8.1 is used with the Non-Line-of-Sight parameters for concrete wall. When radios are on different floors the indoor propagation loss model used is

$$L_{med} = L_{los}(r_m, f_{MHz}) + 15n_f + 7n_w \quad \text{dB} \qquad (8.3)$$

Where
L_{los} is the free space loss function in dB
r_m is the slant range between antennas, in meters
n_f is the number of building floors between antennas
n_w is the number of building walls between antennas
Building geometry is estimated using

$$n_f = \max\left(1, round\left(\frac{|h_2 - h_1|}{3}\right)\right) \quad (8.4)$$

Where h_1 and h_2 are antenna heights measured from a common reference in meters, and

$$n_w = round\left(\frac{d_m}{7}\right) \quad (8.5)$$

Where d_m is the horizontal range between antennas in meters.

Plot indoor concrete here, with different number of floors and walls

8 Delay Spread

9 Bibliography

[Affandi] A. Affandi, G. El Zein, J. Caterne, "Investigation on Frequency Dependence of Indoor Radio Propagation Parameters," Proc. IEEE Veh. Tech. Conf., 1999.

[Aguirre] Sergio Aguirre, Lynette H. Loew, Yeh Lo, "Radio Propagation Into Buildings at 912, 1920, and 5990 MHz Using Microcells," Proc. 3rd Intl. Conf. Universal Personal Communications, San Diega, CA, Sept. 29 – Oct. 1, 1994, pp 129-134.

[Alexander] S. E. Alexander, "Characterizing Buildings for Propagation at 900 MHz," IEE Electronic Letters, 1983, Vol. 19, pp 860.

[CRC] William H. Beyer (ed.), *CRC Standard Mathematical Tables*, 25th Ed., CRC Press, West Palm Beach, FL, 1978.

[Chandra] Ashok Chandra, Ambuj Kumar, P. Chandra, Comparative Study of Path Losses From Propagation Measurements at 450 MHz, 900 MHz, 1.35 GHz and 1.89 GHz in the Corridors of a Multifloor Laboratory-cum-Office Building, Proc. IEEE Veh. Tech. Conf., Vol. 4, Sept. 19-22, 1999, pp 2272-2276.

[COST-231] COST 231 Final Report, *Digital Mobile Radio Towards Future Generation Systems*, COST Telecom Secretariat, Brussels (available online at http://www.lx.it.pt/cost231/final_report.htm).

[Davidson] Allen Davidson, Casey Hill, "Measurement of Building Penetration into Medium Buildings at 900 and 1500 MHz," IEEE Trans. Veh. Tech., Vol. 46, No. 1, Feb. 1997, pp 161-168.

[De Toledo92] De Toledo, Turkmani, "Propagation Into and Within Buildings at 900, 1800, and 2300 MHz," Proc. IEEE Veh. Tech. Conf., May 10-13, 1992, Vol. 2, pp 633-636.

[De Toledo98] De Toledo, Turkmani, “Estimating Coverage of Radio Transmission Into and Within Buildings at 900, 1800, and 2300 MHz,” IEEE Personal Comm. Magazine, April 1998.

[Fabio] Fabio, Graziosi, Marco, Pratesi, Marina Ruggieri, Fortunato, Santucci, “A Multicell Model of Handover Initiation in Mobile Cellular Networks,” IEEE Trans. Vehicular Technology, Vol. 48, No. 3, May 1999, pp 802-814.

[Ferreira] Lucio Ferreira, Martijn Kuipers, Carlos Rodrigues, Luis M. Correia, “Characterisation of Signal Penetration into Buildings for GSM and UMTS,” 3rd Intl. Symp. Wireless Communication Systems, Valencia, Sept. 6-8 2006, pp 63-67.

[Gahleitner] Rainer Gahleitner, Ernst Bonek, “Radio Wave Penetration into Urban Buildings in Small Cells and Microcells,” Trans. IEEE Vehicular Tech. Conf., Stockholm, July 1994, pp 887-8.
[Giannapoulou] K.Giannapoulou, A. Katsareli, D. Dres, D. Vouyioukas, P. Constantinou, “Measurement for 2.4 GHz Spread Spectrum System in Modern Office Buildings,” Proc. 10th Mediterranean Electrotechnical Conf., 2000.

[Ganesh] R. Ganesh, K. Pahlavan, “Statistical Characterization of a Partitioned Indoor Radio Channel,” Proc. Intl. Conf. Comm., 1992, pp 1252-1256.

[Glazunov] Andres Alayon Glazunov, Henrik Asplund, Jan-Erik Berg,
{\em Statistical analysis of measured short-term impulse response functions at 1.88 GHz radio channels in Stockholm with corresponding channel model,} Proc. IEEE Veh. Tech. Conf., Vol. 1, Sept. 19-22, pp 107-111.

[Graziano] Victor Graziano, “Propagation Correlations at 900 MHz,” IEEE Trans. Vehicular Technology, Vol. VT-27, No. 4, Nov. 1978, pp 182-189.

[Greenstein] Larry J. Greenstein, Saeed Ghassemzadeh, Vinko Erceg, David G. Michelson, Ricean K-Factors in Narrowband Fixed
Wireless Channels, Proc. 2nd Intl. Conf. on Wireless, Personal Multimedia Communications, Amsterdam, 1999.

[Hafezi] P. Hafezi, M. Beach, A. Nix, Y. Sun, Exploiting the
Spatial Domain for High Bit Rate Indoor Communications, IEE Colloquium Ant. and Prop. for Future Mobile Comm., 1998.

[Hata] Masaharu Hata, ``Empirical Formula for Propagation Loss
in Land Mobile Radio Services," IEEE Trans. Vehicular Technology,
Vol. VT-29, No. 3, 1980, pp 317-325.

[Hawbaker] D. A. Hawbaker, T. S. Rappaport, ”Indoor Radiowave Propagation Measurements at 1.3 GHz and 4.0 GHz,” IEE Electronic Letters, Vol. 26, No. 21, Oct. 11, 1990, pp 1800-1802.

[Hoppe] R. Hoppe, G Wolfle, F. M. Landstorfer, “Measurement of Building Penetration Loss and Propagation Models for Radio Transmission into Buildings,” Trans. IEEE Vehicular Tech. Conf., Vol. 4, Amsterdam, Sept. 19-22, 1999, pp 2298-2302.

[Hufford] G. A. Hufford, A. G. Longley, W. A. Kissick, {\em A Guide to the Use of the ITS Irregular Terrain Model in the Area Prediction Mode,} NTIA Report 82-100, U.S. Dept. of Commerce, National Telecommunications and Information Administration, Boulder, CO, 1982.

[IEEE802.16] IEEE 802.16 Broadband Wireless Access Working Group, *Channel Models for Fixed Wireless Application*, IEEE 802.16.3c-01/29r2, [July 5, 2001.

[Ikegami] F. Ikegami, S. Yoshida, T. Takeuchi, M. Umehira, ``Propagation Factors Controlling Mean Field Strengths on Urban Streets," IEEE Trans. on Antennas and Propagation, Vol. AP-32, No. 8, Aug. 1984, pp 822-829.

[ITU378] ITU R-P.378-8 man-made noise

[Jensson] G. J. M. Jensson, R. Prasad, ”Propagation Measurements in an Indoor Radio Environment at 2.4 GHz, 4.75 GHz and 11.5 GHz,” Trans. IEEE Veh. Tech. Conf., 1992, pp 617-620.

[Ju] K. M. Ju, C. C. Chiang, H. S. Liaw, S. L. Her, ”Radio Propagation in Office Buildings at 1.8 GHz,” IEEE, 1996.

[Karlsson] Peter Karlsson, “Investigation of Radio Propagation and Macroscopic Diversity in Indoor Microcell at 1700 MHz,” IEEE, 1990.

[JBKeller] J. B. Keller, ``Geometrical Theory of Diffraction," J. Opt. Soc. Am., 1962, pp 116-130.

[Lim] J.-W. Lim, Y.-S. Shin, J.-G. Yuok, “Experimental Performance Analysis of IEEE 802.11 a/b Operating at 2.4 and 5.3 GHz,” Proc. 10th Asia Pacific Conf. on Comm., and 5th Intl. Symp. On Multi-Dimensional Mobile Comm., 2004, pp 133-136.

[Longley] A. G. Longley, {\em Radio Propagation in Urban Areas,} OT Report 78-144, US Dept. of Commerce, National Telecommunications and Information Administration, Boulder, CO, 1978.

[Low] Karl Low, ``Comparison of Urban Propagation Models With CW-Measurements," IEEE Vehicular Technology Conf., 1992, pp 936-942.

[NTIA] National Telecommunications and Information Administration, U. S. Dept. of Commerce, *Irregular Terrain Model (ITM) (Longley-Rice) (20 MHz – 20 GHz)*, http://www.its.bldrdoc.gov/resources/radio-propagation-software/itm/itm.aspx, last accessed 8 Oct., 2015.

[McDonell] T. Edward McDonell, "5 GHz Indoor Channel Characterization Measurements and Models," Proc. IEE Colloquium on Antennas and Propagation for Future Mobile Communications, 1998.

[Marchand] P. R. Hirschler-Marchang, *Penetration Losses in Construction Materials and Buildings*, Lincoln Laboratory Project Report TrACC-1, Oct. 28, 2005.

[Medbo] J. Medbo, J-E Berg, "Simple and Accurate Path Loss Modeling at 5 GHz in Indoor Environments with Corridors," Proc. IEEE Veh. Tech. Conf., 2000.

[Nobles] P. Nobles, D. Ashworth, F. Halsall, "Indoor Radiowave Propagation Measurements at Frequencies up to 20 GHz," Proc. IEEE Veh. Tech. Conf., June 8-10, 1994, pp 873-877.

[Okamoto] Hideaki Okamoto, Koshiro Kitao, Shinichi Ichitsubo, "Outdoor-to-Indoor Propagation Loss Prediction in 800-MHz to 8-GHz Band for Urban Area," Submitted to IEEE Trans. Vehicular Technology, 2007.

[Okumura] Y. Okumura, E.Ohmori, T. Kwano, K. Fukuda, ``Field Strength and its Variability in VHF and UHF Land-Mobile Radio Service," Review of the ECL, Vol. 16, 1968, pp 825-873.

[Papadakis] N. Papadakis, A. C. Kanetas, E. Angelou, M. Maraitis, P. Constantinou, "Indoor Mobile Radio Channel Measurements and Characterization for DECT Picocells," Proc. Intl. Conf. Telecommunications, June, 1988.

[Parsons] J. D. Parsons, *The Mobile Radio Propagation Channel*, Pentech Press, London, 1992.

[Phaibuou] S. Phaibuou, "An Empirically Based Path Loss Model for Indoor Wireless Channels in Laboratory Building," Proc. IEEE TENCON, 2002, pp 1020-1023.

[Rappaport92] T. Rappaport, D. A. Hawbaker, "Wide-Band Microwave Propagation Parameters Using Circular and Linear Polarized Antennas for Indoor Wireless Channels," IEEE Trans. Comm., Vol. 40, No. 2, Feb. 1992, pp ?.

[Rappaport94] T. Rappaport, Sandip Sandhu, "Radio Wave Propagation for Emerging Wireless Personal-Communications Systems," IEEE Ant. And Prop. Magazine, Vol. 36, No. 5, Oct. 1994, pp 14-24,

[Rice] L. P. Rice, "Radio Transmission into Buildings at 35 and 150 mc," Bell System Technical Journal, Vol. 38, NO. 1, Jan 1959, pp 197-210.

[Saleh] A. A. M. Saleh, R. A. Valenzuela, "A Statistical Model for Indoor Multipath Propagation," IEEE J. Spec. Areas. Comm., Vol. SAC-5, No. 2, Feb. 1987, pp 128-137.

[Siwiak] Kazimierz Siwiak, Yasaman Bahreini, *Radiowave Propagation and Antennas for Personal Communications, 3rd. ed*., Artech House, Boston, 2007.

[Siwiak_b] Kazimierz Siwiak, private communication, March 3, 2008.

[Soma] P. Soma, D. S. Baum, V. Erceg, R. Krishnamoorthy, A. J. Paulraj, Analysis and Modeling of Multiple-Input Multiple-Output (MIMO) Radio Channel Based on Outdoor Measurements Conducted at 2.5 GHz for Fixed BWA Applications, Proc. IEEE Intl. Conf. Comm., Vol. I, April 28 - May 2, 2002, pp 272-276.

[Stavrou] S. Stavrou, S. R. Saunders, "Factors Influencing Outdoor to Indoor Radio Wave Propagation," Proc. Intl. Conf. Antennas and Propagation, Vol 2., March 31 – April 3, 2003, pp 581-585.

[Stone] W. C. Stone, *Electromagnetic Signal Attenuation in Construction Materials*, NISTR 6055, Report No. 3, October 1997, Building and Fire Research Laboratory, NIST Gaithersburg Mariland, 20899

[Tanis] William J. Tanis, Glenn J. Pilato, "Building Penetration Characteristics of 880 MHz, and 1922 MHz Radio Waves," Trans. IEEE Veh. Tech. Conf., May 18-20, 1993, pp 206-209.

[Turkmani88] A. M. D. Turkmani, J. D. Parsons, D. G. Lewis, "Measurement of Building Penetration Loss on Radio Signals at 441, 900 and 1400 MHz," J. Int. Electronic and Radio Engineers, Vol. 58, No. 6 (supplement) ppS169-S174, Sept.-Dec. 1988.

[Turkmani91] A. M. D. Turkmani, A. F. de Toledo, "Radio Propagation at 1800 MHz Into and Within Multistory Buildings," IEE Proc. I, Vol. 138, No. 6, Dec. 1991, pp 577-583.

[Turkmani93] A. M. D. Turkmani, A. F. De Toledo, "Modelling of Radio Transmissions into and Within Multistory Buildings at 900, 1800, and 2300 MHz," IEE Proc. I, Vol. 140, No. 6, Dec. 1993, p 462-470.

[Valenzuela] Reinaldo A. Valenzuela, Dmitry Chizhik, Jonathan Ling, {\em Measurements and Predicted Correlation Between Local Average Power and Small Scale Fading In Indoor Wireless Communication Channels,} Proc. IEEE Veh. Tech. Conf., Vol. 3, May 18-21, 1998, pp 2104-2108.

[VanRees] Jan Van Rees, “Cochannel Measurements for Interference Limited Small-Cell Planning, Archiv. Elek. Ubertrag., 1988, pp 316-320.

[Walfisch] J. Walfisch, H. L. Bertoni, ``A theoretical Model of UHF Propagation in Urban Environments," IEEE Trans. on Antennas and Propagation, Vol. AP-36, No. 12, Dec. 1988, pp 1788-1796.

[Wells] Paul I. Wells, “The Attenuation of UHF Radio Signals by Houses,” IEEE Trans. Vehicular Tech., Vol VT-26, No. 4, Nov. 1977, pp 358-362.